# A STRUCTURAL AND KINETIC STUDY INTO THE ROLE OF THE QUATERNARY SHIFT IN *BACILLUS STEAROTHERMOPHILUS* PHOSPHOFRUCTOKINASE

A Dissertation

by

ROCKANN ELIZABETH MOSSER

Submitted to the Office of Graduate Studies of
Texas A&M University
in partial fulfillment of the requirements for the degree of

DOCTOR OF PHILOSOPHY

August 2010

Major Subject: Biochemistry

# A STRUCTURAL AND KINETIC STUDY INTO THE ROLE OF THE QUATERNARY SHIFT IN *BACILLUS STEAROTHERMOPHILUS* PHOSPHOFRUCTOKINASE

A Dissertation

by

ROCKANN ELIZABETH MOSSER

Submitted to the Office of Graduate Studies of
Texas A&M University
in partial fulfillment of the requirements for the degree of

DOCTOR OF PHILOSOPHY

Approved by:

| | |
|---|---|
| Chair of Committee, | Gregory D. Reinhart |
| Committee Members, | James C. Hu |
| | John M. Scholtz |
| | Ryland F. Young |
| Head of Department, | Gregory D. Reinhart |

August 2010

Major Subject: Biochemistry

# ABSTRACT

A Structural and Kinetic Study into the Role of the Quaternary Shift in *Bacillus stearothermophilus* Phosphofructokinase.

(August 2010)

Rockann Elizabeth Mosser, B.S., The University of Texas at Austin

Chair of Advisory Committee: Dr. Gregory D. Reinhart

*Bacillus stearothermophilus* phosphofructokinase (BsPFK) is a homotetramer that is allosterically inhibited by phosphoenolpyruvate (PEP), which binds along one dimer-dimer interface. The substrate, fructose-6-phosphate (F6P), binds along the other dimer-dimer interface. The different functional forms BsPFK can take when in the presence of F6P and PEP can be described by the following diproportionation equilibrium:

$$XE + EA \leftrightarrow XEA + E$$

where XE is the enzyme bound to PEP, EA is the enzyme bound to F6P, E represents the apo enzyme, and XEA is the ternary complex formed when both substrate and inhibitor are bound. Currently in the Protein Data Bank (PDB) there are two relevant forms of wild-type BsPFK, the EA form and the X'E form, which represents the enzyme bound to the PEP analog, phosphoglycolate (PGA). When comparing the EA and the X'E structures, a 7° rotation about the substrate-binding interface is observed and is termed the quaternary shift. The current study uses methyl TROSY NMR to examine the

different liganded states of BsPFK, and for the first time structural data for the XEA species is shown. In addition, crystallography was used to obtain the first apo structure of BsPFK. To distinguish between changes associated with the quaternary shift and those associated with the intra-subunit tertiary changes, the variant D12A BsPFK was studied using kinetics, crystallography, and NMR. Crystal structures of apo and PEP bound forms of D12A BsPFK both indicate a shifted structure similar to the X'E form of wild-type. Kinetic studies of D12A BsPFK, when compared to wild-type, show a 50-fold diminished F6P binding affinity, 100-fold enhanced binding affinity, and a similar coupling constant. A conserved hydrogen bond between D12 and T156 takes place across the substrate binding interface in the EA form of BsPFK. The variant T156A BsPFK shows similar binding, coupling, and structural characteristics to D12A BsPFK. PEP still inhibits these variants of BsPFK despite the fact that the enzymes are in the quaternary shifted position prior to PEP binding. Therefore the quaternary shift of BsPFK primarily perturbs ligand binding but does not directly contribute to heterotropic allosteric inhibition.

# DEDICATION

To my parents: Rocky and Dawn Mosser. You've created an oasis in our home, a place where I know I will always be welcomed, loved, and protected. I know it is not the place that possesses these qualities; it is you, because I feel this way whenever I'm with you two. It is truly amazing to have you both in my life and I try to never take either one of you for granted, though I know I do. Knowing I will always have you on my team, no matter what I do, is empowering and gives me the courage to follow through. You taught me through your actions and your words everything I know about being a respectable, intelligent, and considerate person. Because of this and all that you have given me, I humbly dedicate this dissertation to my parents.

# ACKNOWLEDGEMENTS

I would like to thank my advisor, Dr. Gregory D. Reinhart, for his guidance, support, and his ability to motivate and support me. Also, I want to thank Dr. Hu, Dr. Scholtz, and Dr. Young for serving on my committee and providing great advice and support throughout my graduate career. I want to thank Dr. Raushel for subbing on my prelim committee and Dr. Igumenova for subbing on my oral dissertation committee. Also, I want to thank Dr. Igumenova and her lab for their extensive help and guidance with the NMR project discussed in Chapter IV. I want to thank Dr. Sacchettini, Dr. Reddy, and Dr. Bruning for their work and advice with the crystal structures discussed in Chapters II and III.

I want to thank my lab mates, both past and present, for stimulating discussions, hilarious jokes, and awesome T-shirts. Thank you to the friends I've made over the last 6 years; I seriously doubt I would have made it through graduate school without you. I've never in my life had such a diverse and dependable group of friends, and I truly hope I never lose touch with any of you. Also, I want to thank Mom for asking about and listening to ramblings about my work, and convincing me with her enthusiasm that she wanted to hear more. I want to thank Dad(dy) for slipping me money when I least expected it and making some of the most awesome stew ever known to man every time I went home. I want to thank Clif for the late night telephone calls, for introducing me to Devil Driver, and for being the kind of brother that makes his sister feel incredibly special. I want to thank Chi Toe for just being. And finally, I want to thank God.

# NOMENCLATURE

| | |
|---|---|
| BCA | Bicinchoninic Acid |
| BsPFK | Phosphofructokinase from *Bacillus stearothermophilus* |
| DTT | Dithiothreitol |
| EcPFK | Phosphofructokinase from *Escherichia coli* |
| EDTA | Ethylenediamine Tetraacetic Acid |
| EPPS | N- [2-Hydroxyethyl] Piperazine-N'-3-Propanesulfonic Acid |
| F16BP | Fructose-1, 6-Bisphosphate |
| F6P | Fructose-6-Phosphate |
| LB | Lysogeny Broth |
| LbPFK | Phosphofructokinase from *Lactobacillus delbrueckii* |
| MOPS | 3-[N-Morpholino] Propanesulfonic acid |
| NADH | Nicotinamide Adenine Dinucleotide, reduced form |
| PAGE | Polyacrylamide Gel Electrophoresis |
| PEP | Phosphoenolpyruvate |
| PDB | Protein Data Bank |
| PFK | Phosphofructokinase |
| PGA | Phospoglycolate |
| SDS | Sodium Dodecyl Sulfate |
| Tris | Tris [Hyroxymethyl] Aminomethane |
| $K_{ia}^{\circ}$ | Dissociation constant for A in the absence of effector |
| $K_{ia}^{\infty}$ | Dissociation constant for A in the saturating presence of effector |

| | |
|---|---|
| $K_{ix}^{\circ}$ | Dissociation constant for X in the absence of substrate |
| $K_{ix}^{\infty}$ | Dissociation constant for X in the saturating presence of substrate |
| ε | Extinction coefficient |
| [A] | Concentration of substrate |
| [E] | Concentration of enzyme |
| [ES] | Concentration of enzyme substrate complex |
| ΔG | Coupling free energy of entire reaction |
| $\delta$G | Coupling free energy of individual components |
| $Q_{ax}$ | Coupling constant between substrate and effector |
| [S] | Concentration of substrate |
| v | Initial velocity |
| $V_{max}$ | Maximal velocity |
| [X] | Concentration of effector |

TABLE OF CONTENTS

CHAPTER Page

# LIST OF FIGURES

FIGURE Page

# LIST OF TABLES

# CHAPTER I

# INTRODUCTION: A HISTORY OF OUR UNDERSTANDING OF ALLOSTERIC ENZYMES

This review attempts to follow the development of discoveries and ideas that have led us to our current understanding of allosteric enzymes. The most apparent theme realized while researching this article is the fact that every concept, every experiment, and every theory relies on a previously established concept, experiment, or theory, and it is through the written word that scientists are able to pass their research on to the current and next generations. The foundations of the modern scientific method can be traced to a treatise written in 1637 by Rene Descartes (*1*). Descartes enlightened the scientific community to the advantages of treating science as a method, and soon after, the first scientific publications started to appear. The advent of scientific publications during the mid to late 17$^{th}$ century propagated the emergence of modern science, a body of work that grew exponentially. In 1700, only 35 years after the first scientific publication appeared, there were 30 scientific journals in existence, and in 1800 several hundred existed. Today, there is an estimated 15,000 journals world-wide with a staggering one to two million articles published every year (*2*). With this in mind, a thorough and complete discourse of allosteric enzymes cannot be made without examining the beginnings of our understanding of proteins, enzymes, and kinetics.

---

This dissertation follows the style of *Biochemistry*.

**The Discovery of Protein and Catalysis**

The very first description of a protein can be traced back to a communication of Iacopo B. Beccari made in 1745, where he separated and identified gluten and starch from wheat flour. Beccari classified gluten as being an animal substance, and starch as being a vegetable substance. He theorized that gluten was an animal component of the plant which animals used as building blocks for their tissues (*3, 4*). In 1774, Hilaire M. Rouelle named the glutinous material Beccari had discovered "vegeto-animal matter" when he realized that the substance was not confined to flour and had a lot in common with casein from milk (*5, 6*). Later, in 1789, Giovanni V. M. Fabbroni wrote a memoir connecting the action of fermentation with the "vegeto-animal matter" (*7*). In his memoir, Fabbroni describes, "the material which decomposes sugar in vinous effervescence is the vegeto-animal substance." (*6, 7*).

The "vegeto-animal matter" was later given the name "protein" around the year 1838. The Dutch scientist, Gerhardus J. Mulder, and the Swedish chemist, Jöns Jacob Berzelius, wrote numerous letters to each other concerning the nature of the "vegeto-animal matter" (*8*). Mulder, under the advisement of Berzelius, analyzed the "vegeto-animal" substance present in blood, silk, egg whites, and plants and realized that all of the materials contained carbon, hydrogen, nitrogen, and oxygen in the same ratio: $C_{400}$, $H_{620}$, $N_{100}$, $O_{120}$. He also found a very small percentage of phosphorous and sulfur in all of the samples (*9*). Berzelius was impressed with the quantity of oxygen present in the material and wrote a letter to Mulder where he said:

> The name protein that I propose to you for the organic oxide of fibrin and albumin I wish to derive from πρωτείοσ [primarius] because it appears to be the primary or principal substance of animal nutrition which the plants prepare for the herbivores, and which these then supply to the carnivores (*10*).

Mulder wrote two papers, one in 1838 and one in 1839, where he presented his findings along with the proposal of the new name for the "vegeto-animal material" (*9, 11*). Since Mulder was the first to publish the word "protein", he is often incorrectly credited with deriving the word.

One of the first descriptions of the action of an enzyme was published in 1810 by Louis Planche. In this paper, Planche describes an intense blue color that occurred when he added a small piece of horseradish root to a tincture of guaiacum (*12*) (guaiacum is a flowering plant that was often used to treat syphilis). Later, in 1820, Planche followed up on his previous observations by proving that the color change was not due to light or air exposure, as was previously hypothesized, but rather was a property of a substance in horseradish root (*13*). As a result, Planche is credited with being the first to discover horseradish peroxidase, and, more importantly, to provide the first description of an enzyme in the literature.

One of the first papers to describe an enzyme isolate was written by a pair of French chemists in 1833. Anselme Payen and Jean F. Persoz isolated a water-soluble, amorphous substance from malt barley that broke down starch into dextrose and maltose (*14*). They were interested in using this substance, which they named diastase (meaning

to separate), for use in the sugar and starch industries. Many subsequent papers used the word "diastase" or the suffix –ase to describe the component that was responsible for what we now know is enzyme action. Therefore, it appears to be happenstance that the suffix –ase was adopted as the suffix used for naming enzymes.

By the early 1800's, it was known that digestion was caused by something in addition to hydrochloric acid. In 1834, Johannes Müller studied the report given by Payen and Persoz and concluded that the unknown component of digestion may be related to diastase. With the help of his assistant, Theodor Schwann, he was able to confirm the presence of a catalytic component in gastric fluid that facilitated digestion. Schwann concluded, "the digestive principle is characterized as an individual substance, to which I have given the name pepsin." (*15*).

Catalysis was a very novel concept for Schwann and Müller to use in their paper. In fact, the words "catalytic" and "catalysis" were coined by Berzelius earlier in the same year that Schwann's paper was published. Berzelius stated, "The catalytic force appears to consist intrinsically in this: that bodies through their mere presence, and not through their affinity, may awaken affinities slumbering at this temperature." (*6, 16*). Berzelius defined catalysis through the use of several examples, one of which was diastase. Even though his definition of catalysis was not accurate; he is the first to recognize the process. He concluded that there are "thousands of catalytic processes" that occur in plants and animals, and he predicted that some day in the future we will understand the "catalytic force" in the body (*16*).

**Fermentation**

Enzyme action was an unknown and unfathomable concept in the early 19th century. It is to extensive research mostly on fermentation, but also digestion and putrefaction, that we owe the majority of our understanding of enzyme action. Therefore, a comprehensive description of how the concept of enzymes evolved must include a review on fermentation. Since fruits ferment naturally, mankind was manipulating the fermentative process long before recorded history began. The study of fermentation lead to some of the most formidable disagreements between scientists of the 19th century, and fueled some amazingly intuitive research into the foundations of enzymology.

As stated previously, Fabbroni may have been the first to postulate that it was the action of "glutens" with sugars that caused fermentation to occur (*7*). Unlike Fabbroni, who was very specific as to the nature of what caused fermentation, Louis J. Thenard was more cautious in his remarks. Thenard knew that yeasts were needed for fermentation to occur, although he didn't know how. He asked in his 1803 paper "What is the nature of this body? How does it act on the sugar?" (*6, 17*). He described the fermentative agent as a "ferment" and performed several tests he used to show that the ferment was of animal nature.

During the 1830's, as a testament to the controversial nature of the subject, there was an explosion of papers over whether or not fermentation (and presumably digestion and putrefaction) was a purely chemical mechanism or if it was a mixture of biological and chemical processes. With the emergence of microscopes that could magnify over

400 times, the microscopic world of the yeast cell was being uncovered. Papers written between 1837 and 1838 by Charles Cagniard-Latour, Theodor Schwann, and Friedrich T. Kützing supported the view that fermentation was a biological process that was caused by a living organism. Cagniard-Latour studied yeast using a microscope and a micrometer, which allowed him to measure the "globules". He concluded that yeast were able to reproduce themselves, which meant they were living, but they did not move on their own, which meant they belonged to the plant kingdom (*18*). Schwann suspected that the ferment was living, so he tried several types of poisons on the yeasts. He surmised (which was supported by Professor Franz F. Meyen, a German botanist and plant physiologist) that the yeast ferment was a fungus and not a plant due to the lack of green pigment (*19*). In the same paper, Schwann stated,

> Wine fermentation must be a decomposition that occurs when the sugar-fungus uses sugar and nitrogenous substances for growth, during which, those elements not so used are preferentially converted to alcohol.(*19, 20*).

Independently, Kützing made similar observations to those of Cagniard-Latour and Schwann and he knowingly published his redundant findings. Kützing felt that his paper had a few facts about ferments that were not discussed previously and he concluded that yeasts were not chemical compounds, but organic bodies or organisms (*6, 21*).

Among the most vocal opponents to the concept of yeast being a living organism were Jöns Berzelius, Justus von Liebig, and Friedrich Wöhler. These chemists were probably the most influential chemists of their day, and the fact that they opposed so

vehemently the research findings of Cagniard-Latour, Schwann, and Kützing slowed the advancement of microbiology. On the other hand, enzymology owes its emergence to the interpretation of fermentation as being a purely catalytic chemical force. The debate over whether or not yeasts/ferments were alive grew to ridiculous, if not humorous proportions. Liebig and Wöhler went so far as to publish an anonymous skit in their journal that ridiculed the microscopic findings of Cagniard-Latour, Schwann, and Kützing. The parody was titled, "The riddle of alcoholic fermentation solved" and related yeast to a distilling apparatus, where the yeast ate sugar and excreted alcohol from an anus and carbonic acid from its genitals (*20, 22*). Liebig wrote in his 1839 paper that ferments were internally unstable and transferred this instability to the sugar being fermented. He also believed that yeast were not alive, but were non-crystalline globular solids that precipitated from the solution undergoing fermentation (*23*). Berzelius believed that fermentation was a purely chemical phenomenon that occurred via catalysis and that yeasts were no more alive than a precipitate of alumina (*24*). He attacked Schwann's work by saying "his [Schwann's] experiments were worthless and his conclusions exhibited a frivolity which had long been banished from science." (*20, 25*). Almost twenty years later, in 1858, Moritz Traube entered the fray when he wrote that ferments were "definite chemical compounds arising from the reaction of protein substances with water". Traube did not think yeasts were alive, but he believed that ferments were proteins, which made him one of the first to relate fermentation to proteins (*6, 26*).

The question over whether or not fermentation was achieved by a living organism was finally laid to rest in 1861 by Louis Pasteur. Pasteur performed experiments that proved yeast were in fact cellular life. Pasteur proved that yeasts behaved like plants in the presence of oxygen and like ferments in the absence of oxygen (*6, 27*). With this question finally answered, another controversy soon became evident in the literature. The question was if processes such as fermentation occurred in the presence or absence of living organisms. The two major contributors to the argument were Pasteur and Pierre Berthelot, both of whom openly attacked the other's work. Pasteur believed in the vital force of living organisms. Vital force, or vitalism, is the belief that living entities have some fluid or spirit in them that makes them alive, and thusly different from inanimate things. Pasteur held firm to the idea that fermentation (and other reactions such as putrefaction and digestion) could only be achieved inside living organisms, and that the chemical reactions that are carried out inside living cells could not be separated from the living nature of the organism. Berthelot, on the other hand, believed that actions such as fermentation could occur outside of a living being.

A public debate that occurred between Pasteur and Berthelot revolved around the actions of what Berthelot named invertase. The invertase that Berthelot used was composed of a crude yeast lysate which hydrolyzed sucrose into a mixture of fructose and glucose (aka inverted sugar). Invertase got its name because the conversion of sucrose into inverted sugar manifests itself by an inversion of polarized light. In 1869, Pasteur argued that the formation of inverted sugar was "only an incidental phenomenon" that occurred due to the production of succinic acid. Succinic acid is

produced during fermentation; and Pasteur knew that acids inverted sucrose; therefore, Pasteur argued that it was the succinic acid and not invertase that inverted sucrose (*20, 28*). During the same year, Berthelot published the results of the following experiments. Berthelot prepared a cell free extract of invertase, and proceeded to set up three solutions, all of which contained a fixed amount of sucrose. To solution A he added succinic acid, in an amount that far exceeded that which is normally produced by yeast cells during fermentation. To solution B he added his preparation of invertase, and to solution C he added invertase and sodium bicarbonate. He showed that solution A produced a minute amount of inverted sugar, while both solutions B and C (which contained the invertase) produced substantial amounts of inverted sugar. Berthelot concluded "It is not to succinic acid that one must attribute the inversion which follows the yeast's action…These facts prove that beer yeast inverts cane sugar by its own action and independently of the acidity of the solution."(*20, 29*). Berthelot believed that it was the excreted "ferments" of cells that caused enzyme action, and that the cell itself did not necessarily act on the sugar (in the case of fermentation). Pasteur was not convinced by Berthelot's experiments and rebutted immediately with another paper which argued over semantics rather than the science, as he felt that his definition of a ferment was fundamentally different from Berthelot's definition (*20, 30*).

At this time, whole yeast cells and yeast extracts were often called "ferments", interchangeably. More specifically, ferments that performed enzyme action within cells were called formed or organized ferments, and ferments that acted in the absence of cellular life were called unformed or unorganized ferments. The word "enzyme" was

introduced in 1876 by Wilhelm Kühne in an attempt to differentiate between the two types of ferments. He suggested that the term "ferment" would be used to describe the organized ferments and the term "enzyme" would describe the chemical component that performed catalysis and functioned outside of the living cell (*31, 32*). "Enzyme" is a Greek word meaning "in yeast" or "in leaven", and is meant to reflect that fermentation is a process performed by a component that is found in yeast (*6*).

**Zymase and Oxidase**

The controversy headed up by Pasteur and Berthelot was finally laid to rest by the experiments of Eduard Buchner in 1897. Buchner had been working for years on a method of obtaining the cellular components of the yeast cell without damaging them. Finally, he was able to extract the "yeast juice" from the cells through a method that combined grinding and pressing the cells. Buchner added sugar to the extract in an effort to preserve it, and he recognized the ensuing fermentation that took place (*6*). In his publication he described how to prepare a cell free yeast extract capable of fermentation (*33*). Buchner wrote:

> Up to now, the following conclusions have to be drawn for the theory of fermentation. First, it is proved that to bring about the fermentation process, such a complicated apparatus as represented by the yeast cell is not required. It is considered that the bearer of the fermenting action of the press juice is more truly a dissolved substance, doubtless a protein; this will be designated as zymase (*6, 33*).

He believed that zymase was a single molecule that converted sugar into alcohol and carbon dioxide. Buchner did not think that zymase was an enzyme since it was a wide held belief, at that time, that enzymes were capable of performing only simple reactions. In fact, all known enzymes at the time were hydrolytic agents; therefore, all enzyme actions were assumed to partake in hydrolysis.

The discovery of zymase was a critical turning point in our understanding of enzymes, even though the fundamental comprehension of zymase was wrong. A new concept was evolving that regarded enzymes as functional catalysts that could reside both inside and outside of living cells. A new understanding of enzymes was emerging that owed its beginnings to the findings of Buchner and the realization that enzymes carried out reactions other than hydrolysis, such as oxidation and synthesis.

Gabriel Bertrand discovered the first oxidase in 1895 when he was trying to understand how the black lacquer finish, used by the ancient Chinese furniture makers, worked (*34*). He studied the latex from the Vietnamese lac tree and found that in order to get a good black finish; the latex had to be maintained in a very humid environment. Bertrand hypothesized that oxidation was occurring and that a water soluble enzyme may be involved. He was expecting a hydrolytic enzyme to be the culprit; however, he found that the enzyme in the latex, which he named "laccase", actually caused uptake of oxygen by several substrates (*34, 35*). A few years later, in 1897, Bertrand showed that the activity of laccase depended on the presence of the manganese ion (*36*). The manganese ion was not a substrate, but a cofactor; therefore, Bertrand was the first to discover enzyme cofactors. In 1906, Arthur Harden and William J. Young expanded on

Buchner's and Bertrand's discovery. Harden and Young dialyzed yeast extract; thereby separating the yeast extract into a dialysate and a residue. They found that the dialysate contained a substance that promoted fermentation, even when the dialysate was boiled (*37*). In a subsequent paper, Harden and Young described the component of the yeast extract as a "coferment" (aka coenzyme), and showed that the coferment did not restore fermentation to the inactivated residue of the yeast extract (*38*).

**Enzyme Kinetics**

At this time, the definition of a catalyst was ambiguous. Wilhelm Ostwald, a professor of Chemistry at Leipzig University, spent much of his time devoted to understanding catalysis, chemical equilibrium and rates of reaction. In addition to teaching a number of future high profile scientists, including Svante Arrhenius, Jacobus H. van't Hoff, and Walther Nernst, he correctly defined a catalyst as a component that increased the velocity of a chemical reaction while remaining unchanged itself (*39*). In addition, the catalyst must increase the velocity of a reversible reaction in both forward and reverse directions. Berzelius may have coined the term "catalyst", but it is Ostwald's definition of catalysis that we use today.

Another contribution to the notion that enzymes behaved like catalysts came from Arthur Croft Hill (*35*). In 1898, while studying the hydrolysis of maltose into two molecules of glucose by maltase, he found that exposing maltase to high concentrations of glucose caused the production of a significant amount of maltose (*40*). At the time of A. C. Hill's experiments, hydrolysis was known to be a reversible reaction. Hill's

experiments showed that maltase catalyzed the reverse reaction thus helping to further the concept that enzymes are catalysts and that enzymes are capable of various types of reactions, including synthesis.

The concept that enzymes act as catalysts initiated the desire to understand how the enzyme action worked. From this desire sprung the beginnings of enzyme kinetics which can be traced to a paper written in 1890 by Cornelius O'Sullivan and Frederick W. Tompson. They reported the results of an extensive study of invertase that examined the consequences of numerous variables such as quantity of enzyme and substrate, temperature, acidity, and alkalinity on the rate of inversion. They concluded that the enzyme followed the law of mass action, and the few instances when it did not were due to the differences in experimental conditions (*41*). This conclusion was important, although highly disputed, because for the first time the actions of an enzyme were being compared to a chemical reaction that takes place without a living organism. In other words, if the chemical laws were the same for the living and non-living worlds, then the validity of enzymes containing a 'vital force' was called into question. In addition, they showed that invertase combined with sucrose could withstand a temperature 25° higher than invertase alone. They explained this result by stating, "We are of [the] opinion that when invertase hydrolyses cane-sugar, combination takes place between the two substances, and the invertase remains in combination with the invert-sugar." (*41*). This is probably the first mention of the enzyme forming a complex with the substrate.

Just four years after O'Sullivan and Tompson published their paper, Emil Fischer proposed what may have been the first theory of enzyme action, which is extraordinary

given the fact that the fundamental nature of enzymes was still unknown. Fischer was initially interested in the stereochemistry of sugars, an interest that eventually evolved into a quest to understand the fermentability of different sugars. Fischer and his colleague H. Thierfelder obtained twelve different species of yeast and looked at how each species reacted with different sugars (*42*). He found that the yeast's behavior varied greatly depending on the sugar, and hypothesized that the yeast cells possess chemical agents with a configuration that allows them to react with sugars of a similar configuration (*6, 43*). To test this hypothesis, Fischer proceeded to conduct experiments where he showed that invertase reacted with the α-glucoside but not the β-glucoside, and that emulsin reacted with the β-glucoside but not the α-glucoside (*43*). Fischer discovered that enzymes were selective in the substrate they bound. He explained this selectivity of enzymes with the following statement, "To use a metaphor, I would say that enzyme and glucoside must fit together like lock and key in order to exert a chemical effect on each other." (*20, 43*).

In 1904, a student of Fischer's, Edward F. Armstrong, provided proof in support of Fischer's findings that the enzyme forms a complex with the substrate (*44, 45*). Armstrong did experiments similar to Fischer's invertase/emulsin glucoside experiments where he measured the rate of hydrolysis of four hexases after the addition of different hexoses and hexosides. He found that the only hexoses that inhibited the corresponding enzyme are those that are derived from the same (*45*). He also showed evidence of product inhibition which was more proof that enzymes underwent reversible reactions (*45*).

O'Sullivan and Tompson's 1890 paper provided evidence that the enzyme reacts with sucrose much the same way that acid reacts with sucrose and invertase follows the law of mass action (*41*). This observation was met with opposition from Adrian Brown, Victor Henri, and Emil Duclaux. Brown expressed concern with how O'Sullivan and Tompson prepared their invertase, stating that the amount of acid they used for purification "varied in every experiment in a most remarkable manner" (*46*). Brown believed that the enzyme O'Sullivan and Tompson used was compromised. Also, Brown and Duclaux criticized O'Sullivan and Tompson for basing their conclusion on a logarithmic curve that represented the activity of invertase. O'Sullivan and Tompson reported, based on this curve, that invertase compared quite nicely to a logarithmic curve representing mass action (*41*). O'Sullivan and Tompson used the following equation:

$$v = {}^{1}\!/_{t} \log \frac{1}{1-{}^{[P]}\!/_{[S]_\circ}} \qquad (1\text{-}1)$$

where v is the rate or velocity of the reaction, t is the time, [P] is the concentration of the enzyme, and $[S]_o$ is the initial substrate concentration. The above equation follows the law of mass action if the velocity of the reaction remains constant. However, Henri and Brown independently reported that the velocity of invertase was not constant, but steadily increased (*46, 47*). Duclaux reported that there was a difference between the action of acids and the action of invertase (*48*). The work of Henri, Brown, and Duclaux clearly showed that invertase did not follow mass action.

Brown showed in his paper, aptly titled "Enzyme Action," that the rate of invertase depended on a time factor that accompanied molecular combination. Brown

theorized that an enzyme-substrate complex must exist before the substrate was changed. Also, Brown described in detail product inhibition and introduced the concept that enzymes had a maximal rate of reaction, or maximal velocity ($V_{max}$) (*46*). Unfortunately, Brown used the generic rate equation (Equation 1-1) used by O'Sullivan and Tompson to describe the actions of invertase, which posed numerous problems. Brown was criticized for assuming that the enzyme-substrate complex had a fixed lifetime and for using an equation to describe a rate that did not take into account the changing substrate concentration (*49*). In addition, Brown's equation did not factor in the affinity of the enzyme for the substrate or the $V_{max}$. Henri wrote a paper in 1902, the same year as Brown's paper and like Brown, proposed a transient enzyme-substrate; however, unlike Brown, Henri's rate equation included terms for both the substrate concentration ([S]) and $V_{max}$, shown here in Equation 1-2 (*47*):

$$v = \frac{V_{max}[S]}{1+m[S]+n[P]} \qquad (1\text{-}2)$$

where m and n represent independent variables and [P] represents the enzyme concentration.

Søren P. L. Sørensen was interested in determining methods that would measure hydrogen ion concentrations. In 1909, he wrote a substantial paper which introduced the importance of hydrogen ion concentration and emphasized the impact this had on enzyme processes. He invented the concept of pH and demonstrated the importance pH had on enzyme activity. His experiments effectively proved that pH was a factor that was just as important as temperature to enzyme activity (*6, 50*).

Henri's equation (Equation 1-2] and Sørensen's findings were used by Leonor Michaelis and Maud Menten to derive their enzymatic rate equation, often referred to as the Michaelis-Menten-Henri equation (M-M equation). This was the first equation that included terms for the substrate concentration ([S]), $V_{max}$, and substrate affinity ($K_m$), shown below in Equation 1-3 (*51*):

$$v = \frac{V_{max}[S]}{[S]+K_m} \tag{1-3}$$

The introduction of this rate equation often overshadows the other very significant observations Michaelis and Menten made in their 1913 paper. They conducted experiments where a pH optimum for invertase was determined and were the first to propose the usage of buffers for enzyme storage and assays. Michaelis and Menton also showed that they could prevent complications that arose from product inhibition by measuring the initial enzymatic rate upon substrate addition (*51*).

Michaelis-Menten kinetics represents the simplest case of enzyme kinetics, or single-substrate kinetics, shown here:

$$E + S \underset{k_2}{\overset{k_1}{\rightleftharpoons}} ES \xrightarrow{k_3} E + P$$

where E, S, and P represent the enzyme, substrate, and product, respectively, and k represents the rate constants. Michaelis and Menten assumed the rapid equilibrium approximation where $k_3$ is much smaller than $k_2$ in deriving their substrate affinity constant ($K_m$). This meant that the $K_m$ is approximately the same as the dissociation constant for the substrate ($K_d$) where $K_d$ equals $k_2/k_1$. In 1914, a year after Michaelis and Menten published their paper, Donald D. Van Slyke and his assistant, G. E. Cullen, independently developed an equation that was very similar to that of Michaelis and

Menten (*52*). Van Slyke and Cullen were working with urease, whereas Michaelis and Menten were working with invertase; therefore, the assumptions that Van Slyke and Cullen made about the kinetics of urease were different from invertase. Van Slyke-Cullen kinetics is the opposite extreme of Michaelis-Menten kinetics in that $k_3$ is much greater than $k_2$. George E. Briggs and John B. S. Haldane proposed a more general version of the Michaelis-Menten equation in 1925 where $k_1$, $k_2$, and $k_3$ are all comparable to each other; therefore, the $K_m$ would equal $(k_3+k_2)/k_1$ (*53*) which is also called the quasi-steady state approximation. Interestingly, biochemistry textbooks today introduce the Michaelis-Menten-Briggs-Haldane version of the Michaelis-Menten equation, even though it is not what Michaelis and Menten originally intended.

**Hemoglobin**

While Henri, Brown, Michaelis, Menten, and others were busy defining an equation which described enzyme action, Archibald V. Hill was deriving an equation that described the binding actions of a known protein, hemoglobin. In 1910 Archibald Vivian Hill published a short paper titled "The possible effects of the aggregation of the molecules of hemoglobin on its dissociation curves" (*54*). Hill noticed that experimental results for the oxygen saturation curve of hemoglobin varied greatly depending on the preparation of the protein. At the time, researchers knew that hemoglobin was a multimer; but did not know the oligomeric state of the protein. Hill wanted to derive an equation that would describe hemoglobin's response to oxygen, no matter the oligomeric state of the protein. He proposed three equations that accurately described the binding of

oxygen to hemoglobin. The equation that became known as the Hill equation was his equation B, or Equation 1-4 shown here:

$$y = 100\frac{Kx^n}{1+Kx^n} \quad (1\text{-}4)$$

where y is the percentage of hemoglobin saturation with oxygen, x is the partial pressure of oxygen, K is the equilibrium constant, and n represents the number of molecules of hemoglobin (*54*). This equation is easily adapted to fit experimental data from numerous reactions (*55*). One adaptation is the Michaelis-Menton equation (Equation 1-3), which is essentially a modified example of the Hill equation.

Hemoglobin is an important protein, especially in the realm of allostery, since it is the quintessential allosteric protein in the literature. Hemoglobin has been studied for nearly two centuries because of the high availability of the protein (the concentration of hemoglobin in blood is about 25 mM) and hemoglobin's binding to oxygen is easily detected with spectrophotometric techniques. In 1747, Vinvenzo Menghini was the first to show that blood contained significant amounts of iron by burning the blood and showing that the ashes were magnetic (*56*). Berzelius separated the erythrocyte into two components: a protein component which he named "globin" and a colored "haem" component which contained the iron oxide (*57*). In 1862, Felix Hoppe-Seyler named the red pigment of blood "hemoglobin" and was able to crystallize and describe the spectrum of the protein (*58*). Hoppe-Seyler also showed that oxygen formed a bond with hemoglobin, which he named oxyhemoglobin (*58*). Paul Bert, in 1878, was the first to discover the relationship between pressure and the amount of oxygen when he exposed animals to different barometric pressures and measured the amount of oxygen

in the animal's blood (*59*). In 1903, Christian Bohr described the sigmoidal response of hemoglobin to oxygen and reported the first occurrence of homotropic cooperativity in the literature (*60*). Homotropic cooperativity described the binding of hemoglobin to oxygen such that hemoglobin's affinity for oxygen increased as more oxygen was added. One year later, Bohr, along with Karl Hasselbalch and August Krogh, showed that at higher carbon dioxide levels the affinity of the hemoglobin for oxygen decreased, which later became known as the "Bohr effect" (*61*). This paper was the first to describe heterotropic cooperativity, which is the effect carbon dioxide had on hemoglobin's affinity for oxygen. In more generic terms, homotropic cooperativity is defined as interactions that take place between like ligands and heterotropic cooperativity are interactions that take place between different ligands.

**Classification of Enzymes as Protein**

The relationship between proteins and enzymes was not known during the first couple of decades of the 20$^{th}$ century. In fact, the nature of the composition of enzymes was the subject of another heated debate. Many scientists hypothesized that enzymes were proteins; however, the dominant opinion belonged to Richard Willstätter, a trusted and well respected German scientist who did not believe enzymes were proteins. Instead, Willstätter developed the "carrier theory" for enzymes where a carrier was defined as any colloid, such as a protein or a carbohydrate, which could carry an enzyme. The carrier was able to exchange with other carriers and the composition of the enzyme was an unknown chemical compound (*62*). In 1926, after nine years of trial

and error, James Sumner demonstrated that he could purify and crystallize urease and that these crystals were "purely protein in so far as can be determined by chemical tests" (*63*). Sumner's results were immediately dismissed by Willstätter and his followers. However, four years later John H. Northrop published a paper in which he described the crystallization of pepsin, a well characterized enzyme (*64*). Northrop ran numerous assays on the crystallized pepsin, including solubility, temperature, and rate of diffusion assays. He concluded that pepsin was indeed a protein, supporting Sumner's work. After numerous other reports of enzymes being proteins (a review of these papers in (*62*)), it was finally excepted that enzymes were indeed composed of proteins.

In 1958 there was an explosion of discoveries in the area of proteins and enzymes. Francis Crick gave a speech in 1958 at the Symposium of the Society for Experimental Biology titled "On Protein Synthesis" where he introduced the central dogma of molecular biology, which explained how proteins are synthesized in cells (*65*). During the same year, Daniel E. Koshland introduced the induced fit model for enzyme catalysis which updated Emil Fischer's lock and key model (*66*). The lock and key model assumed a rigid enzyme whereas Koshland's induced fit model assumed a flexible enzyme which allowed the substrate to determine the enzyme's final shape. Max Perutz introduced a novel technique in 1953 which solved a long standing problem in protein crystallography in which he demonstrated that isomorphous replacement of heavy atoms in a protein allowed for the protein's structure to be solved (*67*). This method came to fruition in 1958 when John C. Kendrew and associates published the first ever crystal structure of a macromolecule, which was myoglobin (*68*). Just one year

later, in 1959, Perutz solved the crystal structure for hemoglobin bound to oxygen (*69*)(for an in depth review of Perutz's discoveries see (*70*)), which is the first crystal structure of an allosteric protein.

**Enzyme Regulation**

The 1950's also saw the recognition of three forms of enzyme regulation. One form of enzyme regulation considers the amount of enzyme present inside the cell that is control of gene expression. This form of enzyme regulation was first discovered by Jacques Monod, Germaine Cohen-Bazire, and Melvin Cohn in 1951 (*71*, *72*). Monod and his associates measured the amount of β-galactosidase produced by *Escherichia coli* (*E. coli*) in response to several different β-galactosides. They found that the β-galactosides that acted as inducers of the enzyme did not resemble the substrate, lactose. They discovered the inducers of β-galactosidase were activating gene expression for the enzyme and not directly binding to the enzyme. In 1957, two independent groups of investigators found that genetic control of the production of enzymes can be controlled through gene repression by end-product metabolites. Luigi Gorini and Werner Mass showed that the cellular concentration of arginine or derivatives of arginine in *E. coli* controlled the rate of formation of ornithine transcarbamylase (*73*). Richard A. Yates and Arthur B. Pardee used inhibition studies and radioactive metabolite assays to determine that three enzymes involved in the making of orotic acid in *E. coli* are controlled by a mechanism of enzyme repression at the genetic level (*74*).

The second type of enzyme regulation elucidated in the 1950's is covalent modification of the enzyme itself by a small molecule, such as a phosphate group. George Burnett and Eugene P. Kennedy described in their 1954 paper an enzyme in rat mitochondria that is capable of catalyzing the phosphorylation of a protein substrate by MgATP (*75*). This first description of a protein kinase was soon followed by the discovery of regulation of glycogen phosphorylase via phosphorylation in 1955 (*76-78*). In a series of papers, Edwin G. Krebs and Edmond H. Fischer described how the inactive form of the enzyme, glycogen phosphorylase b, in resting muscle is converted to the active form of the enzyme, phosporylase a, by phosphorylase kinase.

A method was developed in 1950 by Bernard D. Davis that made the isolation of mutant strains of *E. coli* practical and easy (*79*). Thanks to this method another form of enzyme regulation called feedback inhibition was discovered. Aaron Novick and Leo Szilard, using a new instrument they called a chemostat, conducted experiments in which they isolated *E. coli* strains that were deficient in tryptophan synthesis (*80*). They conducted *in-vivo E. coli* experiments which showed that the synthesis of indole-3-glycerol phosphate, a precursor of tryptophan, was rapidly inhibited by the addition of typtophan to the media. Novick and Szilard hypothesized that an enzyme which catalyzes a reaction early on in a metabolic pathway can be inhibited by an end product of the same pathway. H. Edwin Umbarger published a very short, but important, paper in 1956 in which he went one step further than Novick and Szilard by preparing cell-free extracts of *E. coli*, and showed that the addition of isoleucine inhibited the first committed step of the isoleucine metabolic pathway (*81*). Later, in a talk given at the

26th annual Cold Spring Harbor Symposium on Quantitative Biology in 1961, Jacques Monod defined a new name for feedback inhibition when he stated, "From the point of view of mechanisms, the most remarkable feature of the Novick-Szilard-Umbarger effect is that the inhibitor is not a steric analogue of the substrate. We propose therefore to designate this mechanism as 'allosteric inhibition'." (*82*).

**Allostery Theory**

After the discovery of feedback inhibition, two groups of researchers have been credited with developing the "two-site theory" for allosteric enzymes. John C. Gerhart, a graduate student of Arthur B. Pardee, worked with aspartate transcarbamylase and Jean P. Changeux, a graduate student of Monod, worked with threonine deaminase. Gerhart and Pardee knew that aspartate transcarbamylase was inhibited by cytidine triphosphate (CTP), an end product of the pathway. They showed that the inhibition by CTP was reversed by addition of high concentrations of one of the enzyme substrates and that the $V_{max}$ of the enzyme remained the same even in the presence of CTP. Gerhart and Pardee altered aspartate transcarbamylase from *E. coli* by applying heat, urea, and heavy metal ion additions so that the enzyme was no longer sensitive to CTP inhibition; however, the enzyme still catalyzed its substrates. The authors of this paper state:

> It is concluded that the surface of aspartate transcarbamylase contains an exclusive site for binding CTP, the feedback inhibitor. This feedback site is distinct from the active site but appears to influence the function of the latter (*83*).

Changeux and Monod altered threonine deaminase from *E. coli* using methods such as mutagenesis and chemical treatments to create mutants which were not sensitive to inhibition but still active (*84*). The discoveries of Gerhart and Changeux were reported in 1961; therefore, both of these groups are credited with being the first to define allosteric enzymes as enzymes that bind regulating metabolites, also called effectors, at distinct binding sites separate from the substrate binding site or active site. The effector then regulates the activity of the enzyme by altering either the enzyme's affinity for the substrate (K-type) or its catalytic activity (V-type). Furthermore, the effector is an inhibitor if it decreases the protein's affinity for its substrate, and it is an activator if it increases the protein's affinity for its substrate.

Four years after Gerhart and Changeux's publications reporting the allosteric phenomenon, Jacque Monod, Jeffries Wyman, and Jean P. Changeux published their model explaining the behavior of allosteric proteins. They were looking for a simple physical interpretation of the allosteric phenomena in terms of structure (*85*). Their model, also called the concerted model or the MWC model, was based on properties of all known allosteric proteins and enzymes available in 1965. Monod, Wyman, and Changeux compared the 24 allosteric proteins and enzymes and noticed that most of their saturation functions were not linear, like that of a non-allosteric enzyme would be, but were instead sigmoidal. Years before, in 1950, Wyman predicted that hemoglobin was structurally symmetrical based on its symmetrical oxygen saturation (*86*). Wyman's expectation proved to be correct once Perutz came out with his structure of hemoglobin (*69*). Following this observation, Monod, Wyman, and Changeux proposed their model

which basically states that there is a preexisting equilibrium between two possible forms of the enzyme, the T or tense form has a low affinity for the substrate and the R or relaxed form has a high affinity for the substrate (*87*). According to this model, all subunits in the enzyme exist wholly in either the R or T form, so that when the enzyme changes from one form to the other, all subunits do so in a concerted or cooperative manner. The MWC model also states that the substrate and the allosteric activator stabilize the R form of the enzyme just as the allosteric inhibitor stabilizes the T form of the enzyme.

Soon after the release of the MWC model, Koshland, Némethy, and Filmer proposed the KNF or sequential model (*88*). The KNF model uses the same notations as the MWC model, such as R and T; however, there are a few differences. The KNF model predicts that only the subunit that binds the ligand (either substrate or effector) undergoes a conformational change, while the subunits that do not bind the ligand remain unchanged. This allows for negative cooperativity, a condition not allowed for in the MWC model. In other words, the subunit that is bound by the ligand can influence the neighboring subunits. If the bound subunit's influence is favorable, then the cooperativity that ensues is positive. If the bound subunit's influence is unfavorable, then the cooperativity that ensues is negative. Also, the KNF model does not assume a preexisting equilibrium between R and T forms; instead, it predicts that the ligand (either substrate or effector) will influence the conformation the enzyme adopts.

**Allostery and Kinetics**

The discovery of allosteric enzymes initiated research into the kinetics of these unique enzymes. Carl Frieden wrote a paper in 1964 that addressed "the question of how to treat the data for enzymes which are influenced by substances binding specifically to sites other than the enzymatically active site" (*89*). In this paper Frieden introduced the single substrate-single modifier case, shown in Figure 1-1. The single substrate-single modifier case represents a simplified scenario in which there is one substrate and one product bound by the enzyme, and the enzyme possesses one effector site and one substrate site. There may be more than one effector or substrate site per enzyme; however, all similar sites are considered to be independent and identical. Frieden derived equations using both the rapid equilibrium and the steady state assumptions for enzyme mechanisms in which there is a single substrate site and a single effector site (*89*).

J. Wyman, in addition to collaborating with Monod and Changeux on the MWC model, wrote several papers elucidating the general concept of linkage (*90-92*). Wyman explained linkage in his 1948 paper with, "Whenever a molecule possesses two or more different functions there is the likelihood of an interdependence of these functions due to interaction between the groups." (*92*). Wyman believed that through studying the linkage between several reactions within a complex molecule one could describe the structure and function of the molecule. Soon after the publication of the MWC model was released; Wyman published a paper describing allosteric linkage in which he was the first to relate the allosteric nature of a macromolecule to thermodynamics by

introducing the allosteric binding potential (*93*). This binding potential quantified the allosteric response of a macromolecule. Wyman used chemical potentials to imply reciprocity, which means that the binding of the effector has the same influence on the binding of the substrate as the binding of the substrate has on the binding of the effector.

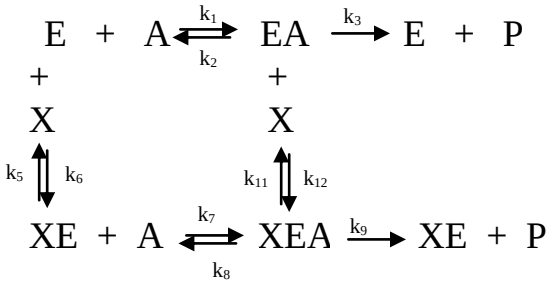


Figure 1-1 Single substrate-single modifier scheme. Where E, A, X, and P represent enzyme, substrate, effector, and product, respectively, and the various k's represent the rate constant of the corresponding reaction.

Gregorio Weber described a new approach to Wyman's linkage theory in papers written between 1968 and 1975. Weber defined allosteric linkage as interactions that occur within a macromolecule between two ligands which bind at distinct sites. Weber demonstrated that allosteric linkage can be written in thermodynamic terms of free energy, in which he introduced the concept of coupling free energy (*94, 95*). Gregory D. Reinhart simplified Wyman's and Weber's ideas into more intuitive relationships. Reinhart applied the kinetic notations first used by W. Wallace Cleland and the single substrate-single modifier scheme created by Frieden (see Figure 1-1) to describe the thermodynamic relationships previously defined by Weber (*89, 94-98*). The relationship between the binding of effector (X) and the binding of substrate (A) was defined as the

coupling free energy which quantifies both the nature and the magnitude of an allosteric effect. The coupling free energy, or $\Delta G_{ax}$, is expressed in terms of standard free energy by using the following equation (*94*, *95*):

$$\Delta G_{ax} = -RT\ln Q_{ax} \tag{1-5}$$

where $Q_{ax}$ is the coupling constant that is equal to the ratio of the following values:

$$Q_{ax} = \frac{K_{ia}^{\circ}}{K_{ia}^{\infty}} = \frac{K_{ix}^{\circ}}{K_{ix}^{\infty}}. \tag{1-6}$$

$K_{ia}^{\circ}$ and $K_{ia}^{\infty\circ}$ are the dissociation constants for A in the absence and saturating presence of X, respectively, and $K_{ix}^{\circ}$ and $K_{ix}^{\infty}$ are the dissociation constants for X in the absence and saturating presence of A. The relationship defined in Equation 1-6 describes the notion of reciprocity, first introduced by Wyman in terms of chemical potential. The dissociation constants can also be defined, with reference to Figure 1-1, as:

$$K_{ia}^{\circ} = \frac{[E][A]}{[EA]} = \frac{k_2}{k_1} \tag{1-7}$$

$$K_{ix}^{\circ} = \frac{[E][X]}{[XE]} = \frac{k_6}{k_5} \tag{1-8}$$

$$K_{ia}^{\infty} = \frac{[XE][A]}{[XEA]} = \frac{k_8}{k_7} \tag{1-9}$$

$$K_{ix}^{\infty} = \frac{[EA][X]}{[XEA]} = \frac{k_{12}}{k_{11}}. \tag{1-10}$$

Therefore, if $\Delta G_{ax}$ is negative (or $Q_{ax} > 1$), then the allosteric effector is an activator and if $\Delta G_{ax}$ is positive (or $Q_{ax} < 1$), the allosteric effector is an inhibitor. When $\Delta G_{ax}$ is equal to zero (or $Q_{ax} = 1$) there is no allosteric effect. The above definitions reveal that $Q_{ax}$ is the equilibrium constant for the following disproportionation equilibrium:

$$XE + EA \overset{Q_{ax}}{\Leftrightarrow} XEA + E. \tag{1-11}$$

In 1987, Reinhart applied Weber's thermodynamic approach to derive relationships between the Hill number, the concentration of the effector, the coupling free energy, and the dissociation constants for a theoretical allosteric homodimer (*99*). Through the mathematical advancements of Frieden, Wyman, Weber, and Reinhart; we now have an effective and descriptive way of describing the allosteric reaction for any enzyme.

One of the first enzymes described using the MWC model was phosphofructokinase (PFK) from *E. coli* (*100*). Daniel Blangy, H. Buc, and Monod published a paper in 1968 detailing the kinetics of the allosteric homotetramer PFK. PFK catalyzes the first committed step of glycolysis, transferring a phosphate group from MgATP to fructose-6-phosphate (F6P) making MgADP and fructose-1-6-bisphosphate (F16BP). Prokaryotic PFK is a highly regulated enzyme that is allosterically inhibited by phosphoenolpyruvate (PEP) and allosterically activated by MgADP. Both PEP and MgADP bind to the same effector binding site. Blangy, Buc, and Monod reported data detailing the kinetics, activation, and inhibition of *E. coli* PFK and concluded that the enzyme was "a perfect K system, i.e. one where the kinetic parameter $V_{max}$ is invariant" (*100*). They also wrote in their conclusions that "The results reported in the present paper and their analysis may be summarized by saying that the kinetic behavior of PFK with respect to its substrate, activators, and inhibitors, is quantitatively accounted for by a model based on the concerted transition theory" (*100*). About twenty years later, Tilman Schirmer and Philip R. Evans had crystallized the substrate bound form and the phosphoglycolate (PGA), a PEP analog, bound form of *Bacillus stearothermophilus* PFK (BsPFK) (*101*). EcPFK and BsPFK share 55% amino

acid identity and both are inhibited by PEP and activated by MgADP. When the crystal structures of the substrate-bound and the PGA-bound enzymes are compared there is a conformational change that occurs in the PGA-bound BsPFK structure relative to the substrate-bound structure. The conformational change includes a difference in the quaternary structures of the two enzyme forms. The quaternary structure of the inhibitor-bound BsPFK has undergone a 7° rotation about the substrate-binding interface, termed the quaternary shift, when compared to the substrate-bound BsPFK. The conformational change also includes the movement of residues E161 and R162 in the active site. When F6P is bound to the enzyme, the positively charged R group of R162 interacts with the negatively charged phosphate group of F6P. In the PGA bound structure, R162 is replaced by the negatively charged R group of E161. Given the structural differences seen between the substrate bound and inhibitor bound structures of BsPFK, Schirmer and Evans were confident that they had all the evidence needed to prove that the MWC model was accurate in describing the allosteric behavior for prokaryotic PFK. In fact, the structural basis for the allosteric nature of BsPFK has been used as an example of allosteric regulation in textbooks (*102, 103*).

Reinhart has provided a great deal of evidence that contradicts many previous predictions concerning prokaryotic PFK. For example, Jennifer Kimmel and Reinhart measured the thermodynamic parameters of active site mutants of BsPFK. They showed that the switching of E161 and R162 in the active sites of the substrate bound and PGA bound structures of BsPFK did not adequately explain the allosteric inhibition of the enzyme by PEP (*104*). The study by Kimmel and Reinhart is supported by the

findings of Braxton, et. al. in which MgADP, a weak activator of BsPFK at moderate temperatures, becomes an allosteric inhibitor at temperatures below 16°C (*105*). A key component of the MWC model is that allosteric activators and inhibitors bind to distinct forms of the enzyme. Accordingly, MgADP would stabilize the active site of BsPFK so that F6P can more readily bind to the enzyme. However, Braxton, et. al. showed that the structure alone could not explain how MgADP becomes an inhibitor at lower temperatures (*105*). Braxton et. al. also pointed out that attributing the allosteric nature of BsPFK to structural perturbations alone addressed the enthalpic component of the coupling free energy, but ignored the entropic component completely [4]. Tlapak-Simmons and Reinhart addressed the differences in the kinetics and allosteric properties of BsPFK with PEP, the native allosteric inhibitor of BsPFK, and PGA, the PEP analog that is present in the inhibited form of BsPFK (*106*). Schirmer and Evans reasoned that the PGA structure would exhibit the same structural characteristics as the PEP structure since the two components are structurally similar (*101*). Tlapak-Simmons and Reinhart showed that while PEP and PGA are both K-type inhibitors of BsPFK, they differ significantly in both their binding affinity and coupling. (*106*). The aforementioned studies provide evidence that does not support the model asserted by Schirmer and Evans.

Other groups have also found contradictions to the MWC and KNF models. In 1984, A. Cooper and D.T.F. Dryden proposed a model for dynamic allostery, in which allosteric regulation occurs without the advent of a conformational change (*107*). R. Ranganathan and S.W. Lockless proposed a new approach in which one could identify

allosteric networks within a protein (*108*). Monomeric and single domain proteins have been shown to be allosteric (*109, 110*). Also, in 2006, Popovych, et. al. reported negative allostery in an enzyme that did not undergo a conformational change (*111*). The view of allostery has been expanded far beyond the restricted confines of the concerted and sequential models. In a recent review, Ruth Nussinov summed up the new view of allostery with (*112*):

1) Allosteric proteins exist in numerous conformations
2) Allostery is thermodynamic phenomenon which can exist as being enthalpically, enthalpically and entropically, or just entropically dominated.
3) Allosteric proteins have multiple conformational and dynamic states meaning that there will be multiple pathways for which the allosteric communication will be relayed.

All in all, it appears that the field of allosteric proteins is still expanding, with new discoveries and ideas being added to the annals of history every day. Maybe Monod had it right almost 50 years ago when he said "In any case, one may predict that "allosteric enzymes" will become a favorite object of research, in the hands of students of the mechanisms of enzyme action" (*82*).

**The Present Study**

The allosteric regulation of BsPFK has been extensively studied throughout the years and been the topic of many interesting journal articles. Many facets of the enzyme's characteristics have been elucidated; however, as demonstrated throughout

chapter I, with every question answered, there follows countless more questions. Such is the case for BsPFK. The current investigation attempts to address a few queries concerning the structure and function relationship of BsPFK.

Chapter II deals with the apo BsPFK crystal structure and its importance to the understanding of the allosteric nature of the enzyme. Chapter III concentrates on the function of the quaternary shift in BsPFK. The variants D12A BsPFK and T156A BsPFK were crystallized and illustrate the enzyme to be in the quaternary shifted position similar to the PGA-bound structure of wild-type BsPFK. Kinetic characterization of both variants demonstrates that the single mutations significantly alter the enzyme's ligand affinities without significantly changing their coupling values. Chapter III also focuses on the roles of D12 and T156 in ligand binding and coupling for BsPFK. The use of methyl TROSY NMR spectroscopy is introduced in Chapter IV as a tool to delve into the structure of BsPFK bound to both inhibitor and substrate simultaneously. In addition, methyl TROSY NMR spectroscopy is attempted with the variant D12A BsPFK in order to obtain additional structural information. Finally, Chapter V summarizes the results discussed throughout the dissertation and alludes to possible future work.

The following dissertation is a humble contribution to the annals of history concerning the regulation of allosteric enzymes. Hopefully, it will provide some clarity for future generations interested in asking questions about BsPFK.

# CHAPTER II

# STRUCTURE OF THE APO FORM OF *BACILLUS STEAROTHERMOPHILUS* PHOSPHOFRUCTOKINASE

Phosphofructokinase (PFK) is under strong metabolic regulation because it catalyzes the first committed step of glycolysis in which it transfers the γ-phosphate from MgATP to fructose-6-phosphate (F6P) making MgADP and fructose-1, 6-bisphosphate (F1,6BP). Not surprisingly, PFK is the subject of intense study and often serves as a key example of an allosteric enzyme (*102*, *103*). Eukaryotic PFKs have very complex regulation involving many effectors (*113*) and, to date, none of those structures have been solved. Insight into the allosteric regulation of eukaryotic PFKs can be gleaned through the study of the much simpler regulation exhibited by prokaryotic PFKs. The two most thoroughly characterized prokaryotic PFKs are from *Escherichia coli* (Ec) and *Bacillus stearothermophilus* (Bs) (*100*, *114*). EcPFK and BsPFK share 55% amino acid identity and both are homotetramers with a molecular weight of 34 KDa per monomer (*115*). Both enzymes are regulated by the K-type effectors phospho(*enol*)pyruvate (PEP), an allosteric inhibitor, and MgADP, an allosteric activator. Furthermore, PEP and MgADP bind to the same allosteric site. EcPFK and BsPFK have two unique dimer-dimer interfaces, the substrate-binding interface and the effector-binding interface. The substrate-binding interface contains the F6P binding site, which is comprised of amino-acids from two adjacent monomers. Likewise, the effector-binding interface possesses the allosteric ligand binding site which is made up

of amino acids from two adjacent monomers. Each homotetramer possesses four identical F6P binding sites and four identical effector binding sites.

Currently, there are seven crystal structures of bacterial ATP-dependent PFKs in the Protein Data Bank (PDB). Of the seven structures, only one does not originate from EcPFK or BsPFK. *Lactobacillus delbrueckii* PFK (LbPFK) contains 56% and 47% amino acid sequence identity to BsPFK and EcPFK, respectively (*116*). Despite the high sequence identity LbPFK shares with EcPFK and BsPFK, LbPFK exhibits a severely diminished capacity to bind both PEP and MgADP (*117*). The structure of LbPFK with $SO_4$ bound to all four active sites and all four effector sites (accession code 1ZXX) was solved by Parichartanakul, et. al. (*117*). The crystal structures of EcPFK include the apo enzyme, which was grown in the absence of ligands (accession code 2PFK) (*118*), and the enzyme bound to its reaction products (accession code 1PFK) (*119*). The latter structure contains the bound reaction products F1,6BP and MgADP in all four active sites, and MgADP is bound to all four effector binding sites. Comparison of the two EcPFK crystal structures to each other reveals that their secondary, tertiary, and quaternary structures are nearly identical.

Each of the three crystal structures of BsPFK contains different combinations of bound ligands. Evans, et. al. crystallized BsPFK in a solution containing F6P and then proceeded to wash the crystal with a phosphate solution. The phosphate solution reportedly displaced any F6P bound, and allowed for the structure of the phosphate bound BsPFK (accession code 3PFK) (*120*) to be determined. The phosphate bound form of BsPFK contains a phosphate molecule at each of the F6P and effector binding

sites for a total of eight bound phosphates. The crystal structure of BsPFK bound to F6P and MgADP in all substrate binding sites and MgADP in all of the effector binding sites (accession code 4PFK)(*121*) was determined by Evans et. al. and will be referred to as the "substrate-bound" BsPFK in the following discussion. BsPFK was also crystallized in the presence of phosphoglycolate (PGA), an analog of the inhibitor PEP, and the structure reveals that PGA is bound to all four effector binding sites (accession code 6PFK)(*101*). In a study comparing the binding affinities and allosteric properties of BsPFK with PGA and PEP, it was found that PGA inhibits BsPFK in a manner similar, though not identical, to PEP (*106*). The structures of the phosphate bound and the substrate-bound enzymes are very similar to each other; however, the PGA-bound BsPFK displays a different conformation. The crystal structure of BsPFK containing the modifications W179F, Y164W revealed that F6P and MgADP were bound in all substrate binding sites and MgADP occupied all four effector binding sites (accession code 1MTO)(*122*). This structure was also found to resemble the substrate-bound form of BsPFK. This variant of BsPFK apparently dissociates in the presence of PEP (*122*).

Before any crystal structures of PFK were solved, the allosteric behavior of EcPFK was described using the concerted transition model proposed by Monod, Wyman, and Changeux (MWC) (*87, 100*). Upon solving the structures of the substrate-bound and the PGA-bound forms of BsPFK, Schirmer and Evans also interpreted the differences in these structures in terms of the MWC model (*101*). The enzyme was described as existing in two states, the substrate-bound form or, R-state, and the PGA-bound form or, T-state. Comparison of the substrate-bound and PGA-bound structures

of BsPFK reveals that the PGA-bound form has undergone a 7° rotation about the substrate binding interface, termed the quaternary shift. The quaternary shift is accompanied by secondary and tertiary changes that include the unwinding of the end of helix 6 and the switching of Arg 162 for Glu 161 in the F6P binding site. Evans, et. al. did not obtain an apo BsPFK structure, but concluded that the structure must assume the T-state conformation because crystals cracked when substrate was removed (*120, 121*). This prediction was a direct result of assuming the enzyme exists in only two-states.

In this paper we present the crystal structure of the apo form of wild-type BsPFK, determined to 2.8 Å resolution. This crystal structure serves as a basis for comparison for any structural changes seen in the binary or ternary complexes. In addition, the tertiary and quaternary structures of apo BsPFK are different from those originally predicted by Evans, et. al. (*120, 121*). Contrary to prior expectations, the apo form of BsPFK resembles the substrate-bound form of the enzyme, and not the PGA-bound form. The structure of the apo form of BsPFK is therefore an important addition to the structural library of allosterically relevant enzyme forms that will help us better understand the structural basis of the allosteric mechanism.

## Materials and Methods

### *Materials*

All chemical reagents used in buffers, protein purifications, and enzymatic assays were of analytical grade, purchased from Sigma-Aldrich (St. Louis, MO) or Fisher Scientific (Fair Lawn, NJ). Creatine kinase and the ammonium sulfate suspension of glycerol-3-phosphate dehydrogenase were purchased from Roche (Indianapolis, IN). The ammonium sulfate suspensions of aldolase and triosephosphate isomerase, and the sodium salts of phosphocreatine, ATP, and phospho(*enol*)pyruvate were purchased from Sigma-Aldrich. The coupling enzymes, obtained as ammonium sulfate suspensions, were extensively dialyzed against 50 mM MOPS-KOH, pH 7.0, 100 mM KCl, 5 mM $MgCl_2$, and 0.1 mM EDTA before use. The sodium salt of F6P was purchased from Sigma-Aldrich or USB Corporation (Cleveland, OH). NADH and DTT were purchased from Research Products International (Mt. Prospect, IL) and the crystallization reagents were purchased from Hampton Research (Aliso Viejo, CA). Mimetic Blue 1 resin used for protein purification was purchased from Prometic Biosciences (Rockville, MD). Deionized distilled water was used throughout.

### *Protein Purification*

The plasmid pBR322/BsPFK (*123*) contains the gene for BsPFK behind the native *Bacillus stearothermophilus* promoter and was received as a generous gift from Simon H. Chang (Louisiana State University). Wild-type BsPFK was expressed in *E.coli* RL257 cells (*124*), which is a strain of *E.coli* lacking both the pfkA and pfkB

genes. The purification of BsPFK was performed as described previously, with a few modifications (*125*). RL257 cells containing the plasmid pBR322/BsPFK were grown at 37°C for 16-18 hours in LB (Lysogeny Broth) ampicillin (Tryptone 10 g/L, yeast extract 5 g/L, and Sodium Chloride 10 g/L, ampicillin 100 ug/ml). Cells were centrifuged and frozen at -20°C for at least 12 hours. The cells were resuspended in purification buffer (10 mM Tris-HCl, 1 mM EDTA pH 8.0) and sonicated in a Fisher 550 Sonic Dismembrator at 0°C in 15 second pulses at setting 6 for 8 minutes. The crude lysate was centrifuged using a Beckman model J2-21 centrifuge at 22,500 x g for an hour at 4°C. The clear supernatant was heated at 70°C for 15 minutes, cooled on ice for 15 minutes, and centrifuged for one hour at 4°C. The supernatant was diluted 4-fold and then loaded onto a Mimetic Blue 1 column that was equilibrated with purification buffer. The column was washed with at least 5 bed volumes of purification buffer, and the enzyme was eluted with a 0 – 1 M NaCl gradient. Fractions containing enzyme were pooled and dialyzed into 20 mM Tris-HCl pH 8.5 and loaded onto a Pharmacia Mono-Q anion exchange column. The enzyme was eluted with a 0 to 1 M NaCl gradient, and fractions containing PFK were combined, concentrated, then dialyzed into EPPS Buffer (50 mM EPPS, 10 mM $MgCl_2$, 100 mM KCl, 0.1 mM EDTA pH 8.0). Concentrated enzyme was stored in EPPS buffer at 4°C. The final enzyme was determined to be pure by SDS-PAGE, and the concentration was ascertained using the absorbance at 280 nm ($\varepsilon$ = 18910 $M^{-1}cm^{-1}$(*126*)).

*Crystallization and Data Collection*

BsPFK was crystallized using the hanging drop vapor diffusion method (*127*) at 16°C. Crystallization was achieved in a 4 µl drop consisting of 1 µl of solvent (0.2 M calcium acetate hydrate, 0.1 M sodium cacodylate trihydrate pH 6.5, and 18% w/v polyethylene glycol 8,000) and 3 µl of protein (stock concentration of BsPFK was 28 mg/mL). Within 24 hours, plate BsPFK crystals were formed. The crystals were briefly soaked in 30% ethylene glycol and then flash-frozen in a liquid $N_2$ stream at 100 K. Diffraction data were collected on the APS beam line 23-ID (insertion device) using a MAR 300 CCD detector (MarMosaic from Marresearch- Charged Coupled Device) (Rayonix LLC, Evanston, IL). The HKL2000 program package (HKL Research, Inc., Charlottesville, VA) (*128*) was used for integration and scaling.

*Structure Determination and Refinement*

The molecular replacement program PHASER (University of Cambridge, UK) (*129*) was used to solve the structure of apo BsPFK using the phosphate-bound crystal structure of BsPFK (3PFK) (*121*) with waters and ions removed as a model. Rigid body refinement followed by simulated annealing refinement at 5000 K was carried out using Phenix (Python-based Hierarchical Environment for Integrated Xtallography, Berkeley, CA) (*130*). Subsequently, refinement was carried out in alternating cycles of manual model building in COOT (Crystallographic Object-Orientated Toolkit, Oxford, UK) (*131*) followed by refinement in Phenix until the R-factors converged. The

steareochemical quality of the final model of the apo BsPFK enzyme was verified by MolProbity (Duke University, Durham, NC) (*132*).

**Results**

Apo BsPFK crystals belong to the space group C2 with unit cell parameters of *a* =201.909 Å, *b* =113.383 Å, *c* =76.627 Å and α=90.00°, β=104.030°, γ=90.00°. Figure 2-1 shows the asymmetric unit that consists of four monomers or a single tetramer with an estimated solvent content of 58.5%. The final structure was refined to R-factor/R-free values of 19.9%/26.01% and has a 2.8 Å resolution. The entire structure consists of 1,276 residues (319 residues per monomer), 326 water molecules, and five calcium ions. The details of the final refinement parameter are shown in Table 2-1.

The five calcium ions are most likely a crystallization artifact since calcium is a main component of the crystallization solution. Figure 2-1 shows the calcium ions and how they appear to bind to the enzyme randomly. Four of the ions associate with aspartate residues and the fifth ion associates with two water molecules and possibly a backbone carbonyl group. Asp 155 from subunits A, B, and C are associated with three of the calcium ions and Asp 307 from subunit D is associated with the fourth ion. Neither Asp 155 nor Asp 307 is involved in the direct binding of any ligand, and the ions are asymmetrically located in the structure. Apart from the non-specifically bound calcium ions, there are no other ligands bound to the enzyme.

Table 2-1 Data collection and refinement statistics[a]

| Data set | Apo-BsPFK |
|---|---|
| Unit cell (Å) | $a$ = 201.909 |
| | $b$ = 113.383 |
| | $c$ = 76.627 |
| | β= 104.030 |
| Space group | C2 |
| Number of molecules per asymmetric unit (Z) | 4 monomers |
| Resolution (Å) | 50-2.8 |
| Completeness (%) | 98.8(99.2) |
| $I/ I$ | 14.61(2.80) |
| $R_{sym}$ | 11.5 (46.0) |
| **Refinement** | |
| Resolution (Å) | 50-2.8 |
| Reflections (working/free) | 38382 (1933) |
| $R_{cryst}$ (%) | 19.90 |
| $R_{free}$ (%) | 26.01 |
| Number of protein atoms/number of waters | 9384/326 |
| Average $B$ factor (Å$^2$) | 42.91 |
| Average $B$ factor for water molecules (Å$^2$) | 44.83 |
| rmsd bond length (Å) | 0.004 |
| rmsd bond angles (deg) | 0.620 |
| **Ramachandran statistics** | |
| most favored | 95.82% |
| allowed | 3.63% |

[a] For details of the crystallization and structure determination, see text. Values in parentheses are for high resolution shells. $R_{sym} = \sum_h \sum_i |I_{hi} - \langle I_h \rangle| / \sum_h \sum_i I_{hi}$, where $I_{hi}$ is the $i$th observation of the reflection $h$, whereas $<I_h>$ is the means intensity of reflection $h$. $R_{cryst} = \sum |F_o| - |F_c| / |F_o|$. $R_{free}$ was calculated with a fraction (5%) of randomly selected reflections excluded from refinement. rmsd, root-mean-square deviations from ideal geometry.

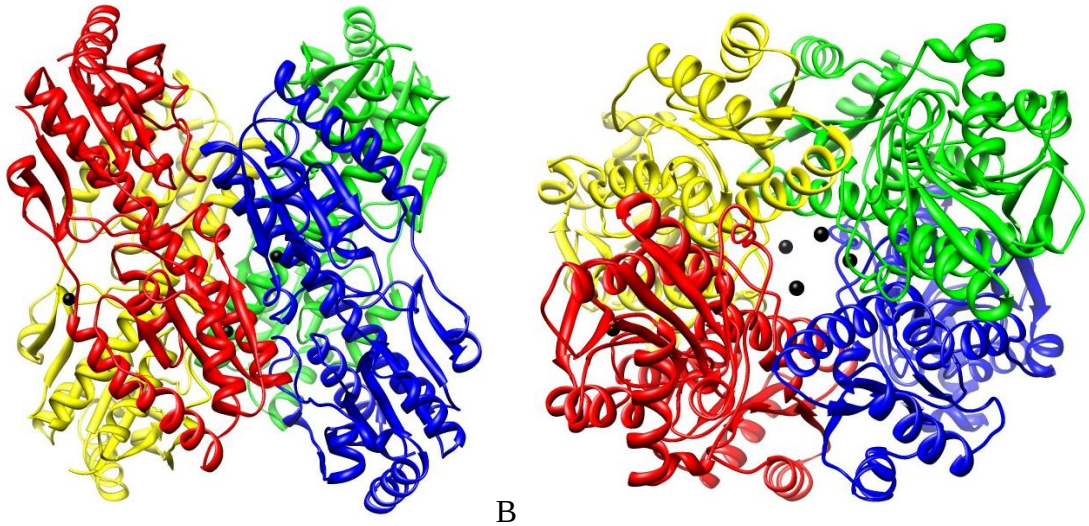

A. B

Figure 2-1 Apo BsPFK tetramer. Subunit A colored blue, subunit B colored green, subunit C colored yellow, subunit D colored red, and calcium ions colored black. (A) View of apo BsPFK showing the substrate binding interface between red and blue monomers and green and yellow monomers, allosteric interface between red and yellow monomers and blue and green monomers. (B) Alternate view, rotated 90° along the horizontal axis.

The root-mean-square deviation (RMSD) between apo BsPFK and the substrate-bound BsPFK is 0.53±0.05 Å for 319 Cα atoms. The RMSD between apo BsPFK and the PGA-bound BsPFK is 0.94±0.05 Å for 319 Cα atoms. Furthermore, comparison of the quaternary structures of the apo, substrate-bound, and PGA-bound forms of the enzyme reveals that the apo BsPFK structure has not undergone the quaternary shift seen in the PGA-bound structure (Figure 2-2). Given the values for the RMSDs and the state of the quaternary structures, it appears that the apo enzyme is more like the substrate-bound form than the PGA-bound form. By contrast, Evans, et. al. (*120, 121*) observed that when crystals formed in the presence of F6P were transferred to a solution lacking any activating ligands, the crystals cracked. Also, crystals grown in the presence of inhibitor cracked when exposed to F6P. The cracking of the crystals was interpreted as being an indicator of the enzyme undergoing a large conformational shift, presumable the quaternary shift. However, it is clear that the enzyme has not undergone the quaternary shift when crystallized only in the presence of the crystallization solvent. One should note, however, that there are also many local differences observed between the apo, substrate-bound, and PGA-bound structures.

The B-factor, or temperature factor, in protein crystal structures is an indicator of the fluctuation of an atom about its mean position. By looking at the distribution of the B-factors for an entire protein sequence, information can be derived about the protein's flexibility and mobility. Large B-factors reflect areas of higher mobility within the crystal structure. Figure 2-3 is a backbone ribbon structural comparison of the crystallographic B-factors for the different wild-type BsPFK crystal structures. The

allosteric interface is seen in Figure 2-3 along the back side of all 3 of the monomers as depicted. The allosteric interface is less flexible than the rest of the monomer for all three wild-type crystal structures. The PGA-bound structure shows more rigidity along the allosteric interface than the other two wild-type crystal structures, which is indicated by the color blue for the lower B-factors (Figure 2-3C). Clearly the substrate-bound

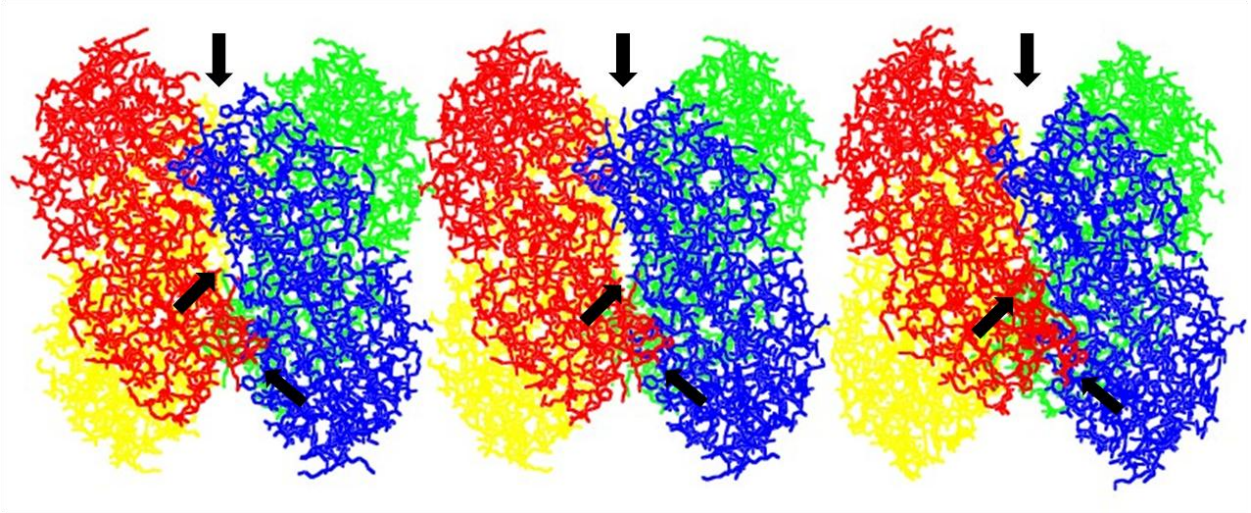

A. B. C.

Figure 2-2 Comparison of wild-type BsPFK crystal structures. (A) Apo BsPFK (B) Substrate-bound BsPFK (accession code 4PFK) (C) PGA-bound BsPFK (accession code 6PFK). The blue monomer was aligned to the blue monomer of the apo structure for each ligand bound structure. Ligands and heteroatoms have been removed for clarity. Each monomer is colored blue, green, yellow, and red. The substrate binding interfaces are between the red and blue monomers and the green and yellow monomers. The effector binding interfaces are between the green and blue monomers and the red and yellow monomers. Areas where there are differences in the tertiary and quaternary structures are pointed out with black arrows.

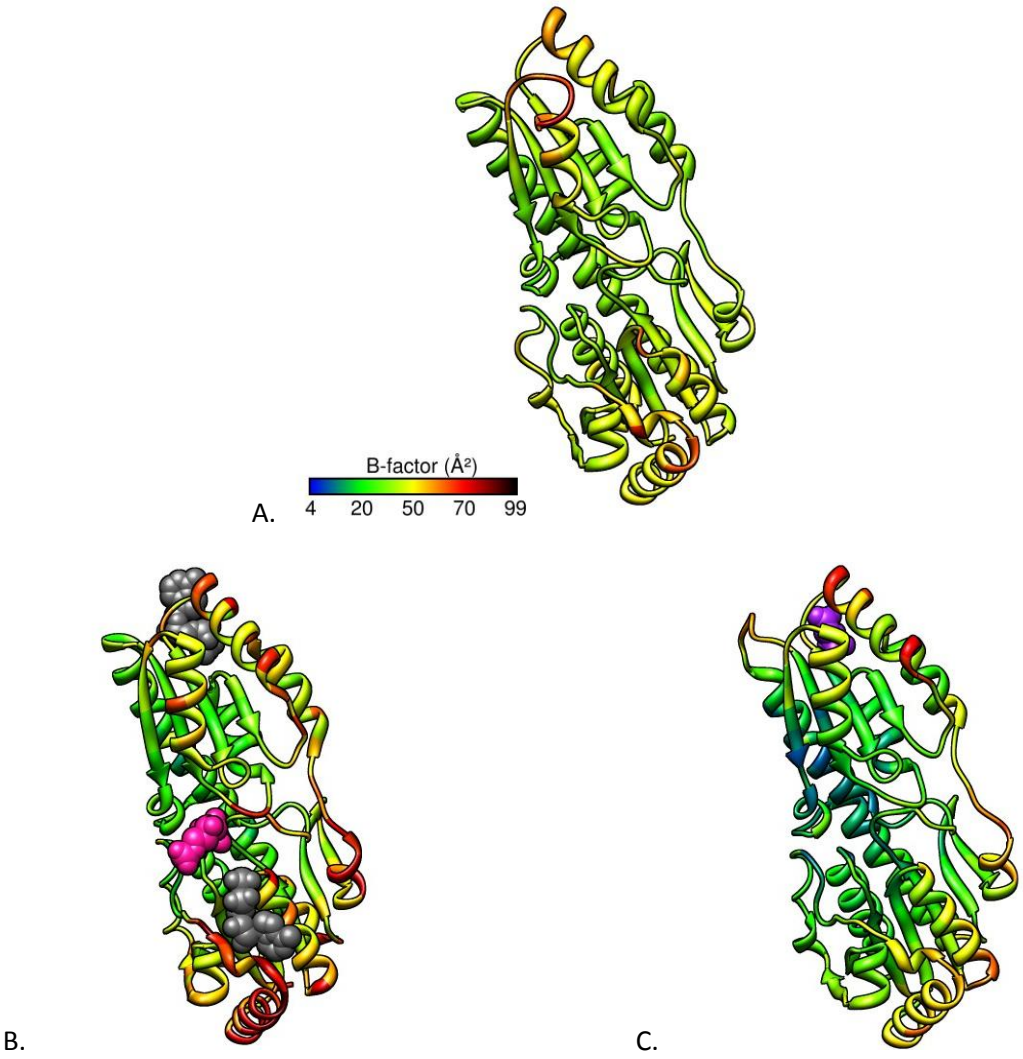


Figure 2-3 Comparison of wild-type BsPFK B-factors. (A) Apo BsPFK (B) Substrate-bound BsPFK (accession code 4PFK) (C) PGA-bound BsPFK (accession code 6PFK). Only monomer A is shown for each structure. Bound ligands are depicted as space filled molecules, with ATP colored gray, F6P colored pink, and PGA colored purple

structure shown in Figure 2-3B is more flexible overall when compared to the apo and PGA-bound structures, with one exception being residues 156-162, which are across the allosteric interface from residue D12. In the PGA-bound structure, residues 156-162 are in a loop conformation and in the substrate-bound and apo structures this region is in a helix conformation. Residues 156-162 have higher B-factor values for the PGA-bound structure than the apo and substrate-bound structures. The B-factors for the apo structure are not identical to either ligand bound structure, but the apo structure does appear to be more flexible than the PGA-bound structure and slightly less flexible than the substrate-bound structure.

Figure 2-4 compares the F6P binding site of the apo BsPFK to the substrate-bound and the PGA-bound forms of BsPFK. Overall, the orientations of the residues in the active site for the apo structure appear to correspond better with the active site residues of the substrate-bound BsPFK than the PGA-bound BsPFK. However, there are a few key residues with significant changes in orientation that have altered interactions that could not have been predicted without the apo BsPFK crystal structure. For instance, Arg 72 interacts with the phosphate groups of ATP in the substrate-bound enzyme. In the PGA-bound BsPFK where ATP is no longer bound, Arg 72 forms a salt-bridge with Glu241 across the substrate-binding interface. The orientation of Arg 72 in apo BsPFK is dramatically different from both liganded forms of BsPFK. In apo BsPFK, Arg72 does not form a salt-bridge with Glu241.

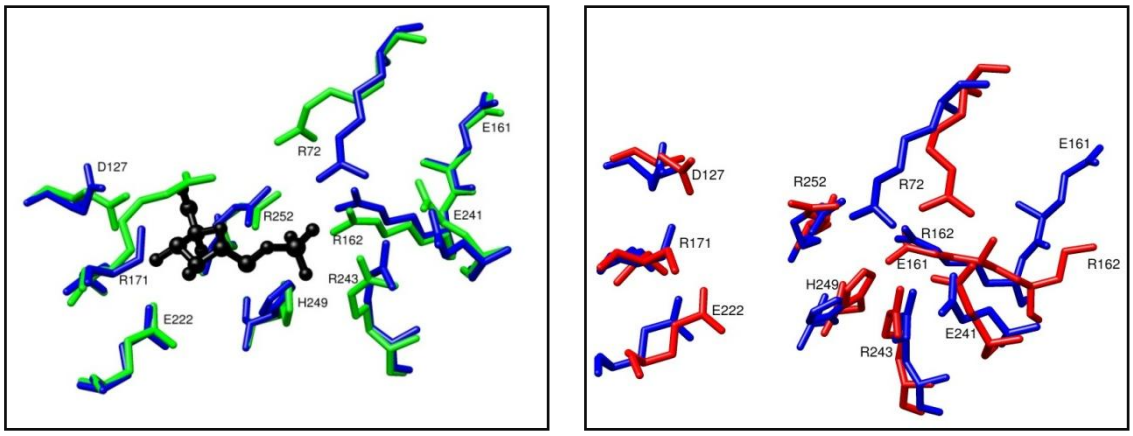


A. B.

Figure 2-4 Overlay of residues in the Fru-6-P binding site of BsPFK. (A) Apo residues in blue, substrate-bound BsPFK residues in green, and Fru-6-P in black ball and stick. (B) Apo residues in blue and PGA-bound BsPFK residues in red. All residues are labeled.

His 249 is another residue that exhibits a difference in its orientation in the apo structure as compared to either liganded structure. In the substrate-bound enzyme, His 249 interacts with the phosphate group of F6P. His 249 forms a hydrogen bond across the substrate binding interface with Glu 161 in the PGA-bound structure. In the apo structure, His 249 forms a hydrogen bond with Tyr 164 across the binding interface. The breaking of the hydrogen bond between His 249 and Tyr 164 when PEP binds to the enzyme may be the basis for the substrate-binding interface being the weaker of the two interfaces. Both wild-type and a tryptophan-shift mutant of BsPFK exhibit reversible dissociation of the tetramer along the active site interface in the presence of PEP. Perhaps the formation of a hydrogen bond across the substrate-binding interface between His 249 and either Tyr 164 or Glu 161 is important for tetramer stability. Therefore, the

addition of PEP may cause a perturbation between these residues and in the quaternary structure of the enzyme to weaken the substrate binding interface. Such weakening has been observed with BsPFK where it was demonstrated that the addition of PEP to the enzyme induced the dimers of BsPFK to exchange along the substrate-binding interface (*133*).

Figure 2-4 shows the relative positions of Glu 161 and Arg 162 in the active sites of the substrate-bound, PGA-bound, and apo crystal structures. In the substrate-bound BsPFK structure, the positively charged Arg 162 interacts with the negatively charged phosphate group of F6P, and in the PGA-bound structure, the negatively charged Glu 161 replaces Arg 162, thereby repelling F6P from the active site. These structural features were used to rationalize the MWC model for BsPFK (*101*). Prior to this, the apo BsPFK structure was presumed to be in the T-state; therefore, according to assumptions made based on the MWC model, Glu 161 should be poised in the active site of the apo crystal structure ready to repel F6P (*120, 121*). However, Arg 162 is in the active site of the apo BsPFK crystal structure, with the apo positions of both Arg 162 and Glu 161 matching quite well with the substrate-bound positions (Figure 2-4).

Figure 2-5 compares the effector binding site of apo BsPFK to the substrate-bound form and the PGA-bound form, respectively. The orientation of the 8-H loop (residues 213-215) in the apo structure resembles that of the substrate-bound enzyme, except the loop is slightly more open in the apo structure. Arg 211 is not well ordered in the apo structure and can only be visualized in subunit D, where the orientation of Arg 211 is significantly different from both of the liganded structures. Arg 211 interacts with

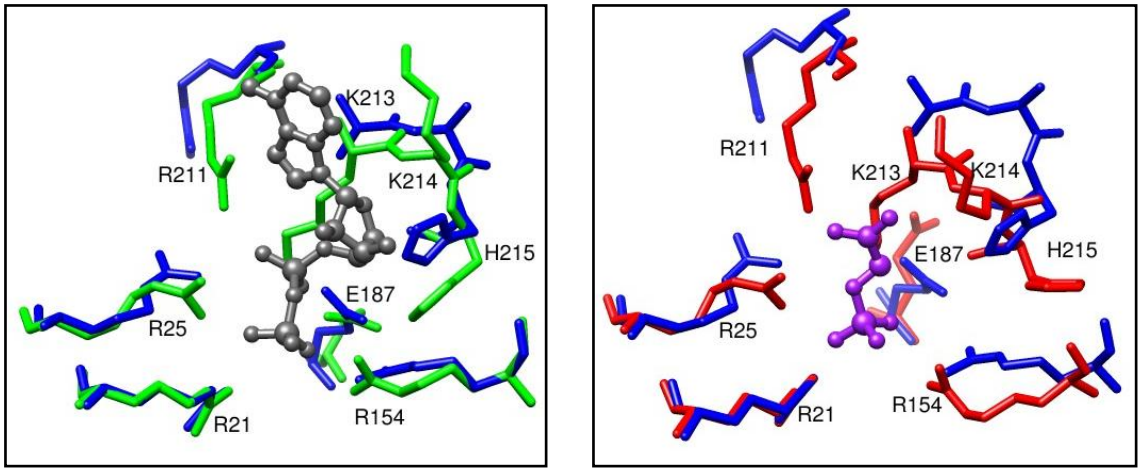


A. B.

Figure 2-5 Overlay of residues in the effector binding site of BsPFK. (A) Apo residues in blue, substrate-bound BsPFK residues in green, and ADP in gray ball and stick. (B) Apo residues in blue, PGA-bound BsPFK residues in red, and PGA in purple ball and stick.

the α-phosphate of ADP in the substrate-bound BsPFK. In the PGA-bound BsPFK, Arg 211 interacts with the carboxylate group of PGA. Arg 211 also interacts with the backbone carbonyl oxygen of Ile 320 in both of the liganded structures. However, in the apo BsPFK structure, Arg 211 is positioned so that it interacts only with a water molecule. Therefore, Arg 211 no longer binds with the backbone oxygen of Ile 320. The position of Glu 187 also shows significant deviation relative to both substrate-bound and PGA-bound enzymes. In the substrate-bound structure, the R group of Glu 187 is coordinated to the magnesium ion of ADP and interacts with Lys 213. In the PGA-bound structure, the R group rotates away from the ligand and interacts with Lys 213 and Ser 216. However, in the apo structure, Glu 187 forms a hydrogen bond with a water molecule and no other residue.

**Discussion**

When considering the mechanistic basis of allosteric behavior in enzymes, it is important to interpret both the structural and the thermodynamic characteristics of the enzyme simultaneously. The two-state model that has been proposed to explain the allosteric mechanism for BsPFK is based on the differences between the crystal structures of the substrate-bound and the PGA-bound enzymes (*101*) and structure alone does not address the issue of reciprocity. Reciprocity acknowledges that whatever affects an allosteric ligand has on the binding of the substrate; the same effect is felt by the allosteric ligand when the substrate binds. There is no apparent structural reciprocity seen in the active and effector binding sites of BsPFK. In addition, it is not apparent

whether the structural differences seen between the two liganded species are a consequence of ligand binding the enzyme or are attributable to the inherent nature of the enzyme. An apo BsPFK structure allows for the assessment of actual ligand-induced effects on the structure of the enzyme and thereby serves as an important reference structure.

The importance of the apo structure of BsPFK is further underscored when considering the origin of the coupling free energy between an effector (X) and a substrate (A) that quantifies both the nature and the magnitude of a K-type allosteric effect. The coupling free energy, or $\Delta G_{ax}$, is determined using the following equation (*94, 95*):

$$\Delta G_{ax} = -RT\ln Q_{ax} \tag{2-1}$$

where $Q_{ax}$ is the coupling constant that is given by:

$$Q_{ax} = \frac{K_{ia}^{\circ}}{K_{ia}^{\infty}} = \frac{K_{ix}^{\circ}}{K_{ix}^{\infty}}. \tag{2-2}$$

$K_{ia}^{\circ}$ and $K_{ia}^{\infty}$ are the dissociation constants for A in the absence and saturating presence of X, respectively, and$K_{ix}^{\circ}$ and $K_{ix}^{\infty}$ are the dissociation constants for X in the absence and saturating presence of A, respectively. Therefore, if $\Delta G_{ax}$ is negative (or $Q_{ax} > 1$), then the allosteric effector is an activator and if $\Delta G_{ax}$ is positive (or $Q_{ax} < 1$), the allosteric effector is an inhibitor. When $\Delta G_{ax}$ is equal to zero (or $Q_{ax} = 1$) there is no allosteric effect. The above definitions reveal that $Q_{ax}$ is the equilibrium constant for the following disproportionation equilibrium:

$$XE + EA \overset{Q_{ax}}{\Longleftrightarrow} XEA + E \tag{2-3}$$

where E is the apo enzyme, EA is the enzyme bound to the substrate, XE is the enzyme bound to the effector, and XEA is the ternary complex formed when both substrate and effector are bound. This equilibrium depicts the different forms that BsPFK can assume in the presence of substrate and allosteric effector. All four enzyme species are involved in determining the value of $Q_{ax}$. The two-state model is based exclusively on a consideration of the XE and the EA forms that describes only the left side of the disporportionation equilibrium and ignores the entire right side; and therefore does not adequately describe the coupling free energy of the reaction.

The four species of enzyme that contribute to the allosteric mechanism have free energies of formation of their own. In other words, the coupling free energy can be defined by subtracting the free energy of formations of the EA and XE from that of XEA and E (*98*):

$$\Delta G_{ax}=(G_{XEA}+G_E)-(G_{EA}+G_{XE}). \quad (2\text{-}4)$$

This equation can be converted to the following equivalent expression:

$$\Delta G_{ax}=\left(G_{XEA}-G_E\right)-\left[\left(G_{EA}-G_E\right)+\left(G_{XE}-G_E\right)\right]. \quad (2\text{-}5)$$

Further simplification of the above equation can be done by denoting the differences in the parenthesis with a $\delta$ such that:

$$\Delta G_{ax}=\delta G_{XEA}-(\delta G_{EA}+\delta G_{XE}). \quad (2\text{-}6)$$

With the above expression it is clear that the free energy of the apo form of the enzyme is crucial to the overall coupling free energy of the allosteric reaction. Note that $\Delta G$ and $\delta G$ are two different expressions, where $\Delta G$ considers the free energy implications of the free ligand and $\delta G$ does not, hence the reason for the different symbols. Given the

fact that the free energy of the apo enzyme must be subtracted from each enzyme form addresses the importance of the apo structure. The structure of the apo BsPFK allows for the structural perturbations that occur from each ligand binding event to be observed. Therefore, it may be possible to determine some of the structural contributions to the free energy of binding of the liganded forms of the enzyme.

In order to fully describe $\Delta G_{ax}$ in terms of structure, all four structures of the enzyme are needed. The above expression demonstrates the necessity of obtaining as much information as possible about all forms of the enzyme, particularly the form bound to both F6P and PEP simultaneously (XEA). The difference between the free energy of the XEA form and the combined free energies of the binary complexes is what determines the actual coupling free energy. The model adopted by Schirmer and Evans describes the allosteric inhibition of BsPFK by using only two of the four species, and virtually ignores the E and XEA forms (*101*). Although the structure of XEA has not yet been determined, we are now one step closer to understanding the structural implications of the allosteric inhibition of BsPFK with the addition of the apo BsPFK structure.

Strictly using a structurally based model to describe an allosteric mechanism tends to oversimplify the regulation of the enzyme. However, reconciling the structures of BsPFK with the experimentally measured thermodynamic parameters of the enzyme will lead to understanding the structure-function relationship of the allosteric mechanism. With the addition of the apo BsPFK structure, there are now more relevant structures to the allosteric regulation of BsPFK than any other PFK enzyme. More

importantly, the apo BsPFK structure serves as a necessary reference structure for comparison to the liganded structures. The obvious next step would be to obtain the structure of the XEA form of BsPFK. Along with the thermodynamic data already collected on the XEA form of BsPFK, this structure would go a long way in helping us better understand the basis for allosterism in BsPFK.

# CHAPTER III

# REDEFINING THE ROLE OF THE QUATERNARY SHIFT IN *BACILLUS STEAROTHERMOPHILUS* PHOSPHOFRUCTOKINASE

Phosphofructokinase (PFK) is a highly regulated enzyme that catalyzes the first committed step of glycolysis. PFK transfers the γ-phosphate of Mg-ATP to fructose-6-phosphate (F6P) producing fructose-1, 6-bisphosphate and Mg-ADP. The PFK from the moderate thermophile, *Bacillus stearothermophilus* (Bs), is a homotetramer of 34 KDa per monomer that forms a rigid dimer of dimers which consists of two unique dimer-dimer interfaces. The substrate interfaces comprise the binding sites for F6P, for which there are four identical binding sites per homotetramer. The effector interfaces contain the binding sites for the allosteric ligands, for which there are four identical effector binding sites per homotetramer. The allosteric binding sites are capable of binding either MgADP or phosphoenolpyruvate (PEP). For BsPFK, MgADP serves as a very weak activator and PEP is a very strong inhibitor. Both PEP and MgADP alter the affinity BsPFK has for F6P without changing the enzyme's maximal activity; therefore, both allosteric ligands are considered to be K-type effectors.

The regulation and structure of BsPFK has been the subject of study for over three decades (*120*). Ever since 1990, with the publication of Schirmer and Evan's paper titled "Structural basis for the allosteric behavior of phosphofructokinase" (*101*), the structural basis for the allosteric nature of BsPFK has been used as an example of allosteric regulation (*102, 103*). Schirmer and Evans compared the crystal structures of

the substrate bound BsPFK and the inhibitor bound BsPFK. The substrate bound BsPFK consists of the enzyme bound to F6P and MgADP in all four substrate binding pockets and MgADP bound in all four effector binging sites (accession code 4PFK) (*121*). The inhibitor bound BsPFK consists of the enzyme bound to the PEP analog, phosphoglycolate (PGA), in all four effector binding sites (accession code 6PFK) (*101*). When the crystal structures of the substrate bound and the PGA bound enzymes are compared there is a conformational change that occurs in the PGA bound BsPFK. The conformational change includes a difference in the quaternary structures of the two enzyme forms. The quaternary structure of the inhibitor bound BsPFK has undergone a 7° rotation about the substrate binding interface, termed the quaternary shift, when compared to the substrate bound BsPFK. The conformational change also includes the movement of residues E161 and R162 in the active site. When F6P is bound to the enzyme, the positively charged R group of R162 interacts with the negatively charged phosphate group of F6P. In the PGA bound structure, R162 is replaced by the negatively charged R group of E161. Given the structural differences seen between the substrate bound and inhibitor bound structures of BsPFK, Schirmer and Evans proposed the concerted transition or Monod, Wyman, Changeux (MWC) model (*87, 101*) to describe the allosteric behavior of BsPFK (*101*). More specifically, they proposed that the allosteric inhibition of BsPFK was due to the quaternary shift and the switching of E161 and R162 in the active site (*101*).

In the years since Schirmer and Evans introduced their model, several studies have suggested that the MWC model is insufficient in describing the mechanism of

inhibition for BsPFK (*104-106*). Kimmel and Reinhart measured the thermodynamic parameters of active site mutants of BsPFK. They showed that the switching of E161 and R162 in the active sites of the substrate bound and PGA bound structures of BsPFK did not adequately explain the allosteric inhibition of the enzyme by PEP (*104*). The study by Kimmel and Reinhart is supported by the findings of Braxton, et. al. in which MgADP, a weak activator of BsPFK at moderate temperatures, becomes an allosteric inhibitor at temperatures below 16°C (*105*). A key component of the MWC model is that allosteric activators and inhibitors bind to distinct forms of the enzyme. Accordingly, MgADP would stabilize the active site of BsPFK so that F6P can more readily bind to the enzyme. However, Braxton, et. al. showed that the structure alone could not explain how MgADP becomes an inhibitor at lower temperatures (*105*). Braxton et. al. also pointed out that attributing the allosteric nature of BsPFK to structural perturbations alone addressed the enthalpic component of the coupling free energy, but ignored the entropic component completely [4]. Tlapak-Simmons and Reinhart addressed the differences in the kinetics and allosteric properties of BsPFK with PEP, the native allosteric inhibitor of BsPFK, and PGA, the PEP analog that is present in the inhibited form of BsPFK (*106*). Schirmer and Evans reasoned that the PGA structure would exhibit the same structural characteristics as the PEP structure since the two components are structurally similar (*101*). Tlapak-Simmons and Reinhart showed that while PEP and PGA are qualitatively the same, they are quantitatively different (*106*). The aforementioned studies provide evidence that does not support the model asserted by Schirmer and Evans. However, the role of the quaternary shift in

BsPFK is still questionable. Schirmer and Evans delegate the allosteric inhibition of BsPFK to the switching of E161 and R162 in the active site and the quaternary shift. The former has already been addressed by Kimmel and Reinhart (*104*), the latter is addressed in the following study.

A sequence comparison of all available bacterial ATP-dependent PFKs (approximately 150 amino acid sequences) reveals that only 14 residues are completely conserved. Of the 14 residues, seven are glycines, two are involved in substrate binding or catalysis, and five do not directly bind to any ligand. Of the two residues that are necessary in binding a ligand, R252 binds directly to the 6-phosphate group of F6P and D127 acts as a catalytic base. The five 100% conserved residues that do not directly bind to any ligand are D12, N17, P123, D129, and T156. According to the F6P bound BsPFK crystal structure, D12 interacts with R252 within its own monomer and with T156, S159, and H160 in the adjacent monomer across the substrate-binding interface (Figure 3-1A). In the PGA bound BsPFK structure, residues 156-160 (last turn of helix 6) adopt a loop conformation that results in D12 potentially interacting with only T158 across the substrate-binding interface. Therefore, in the inhibitor bound structure, the hydrogen bond between D12 and R252 no longer exists as it did in the substrate bound structure (Figure 3-1B). N17 forms hydrogen bonds with backbone atoms of residues within its own monomer, bonds that remain unchanged in the substrate bound and inhibitor bound forms. P123 and D129 form no apparent hydrogen bonds with any residues. As indicated before, T156 forms a hydrogen bond with D12 in the adjacent monomer in the substrate bound enzyme. When PGA is bound to BsPFK, T156 no

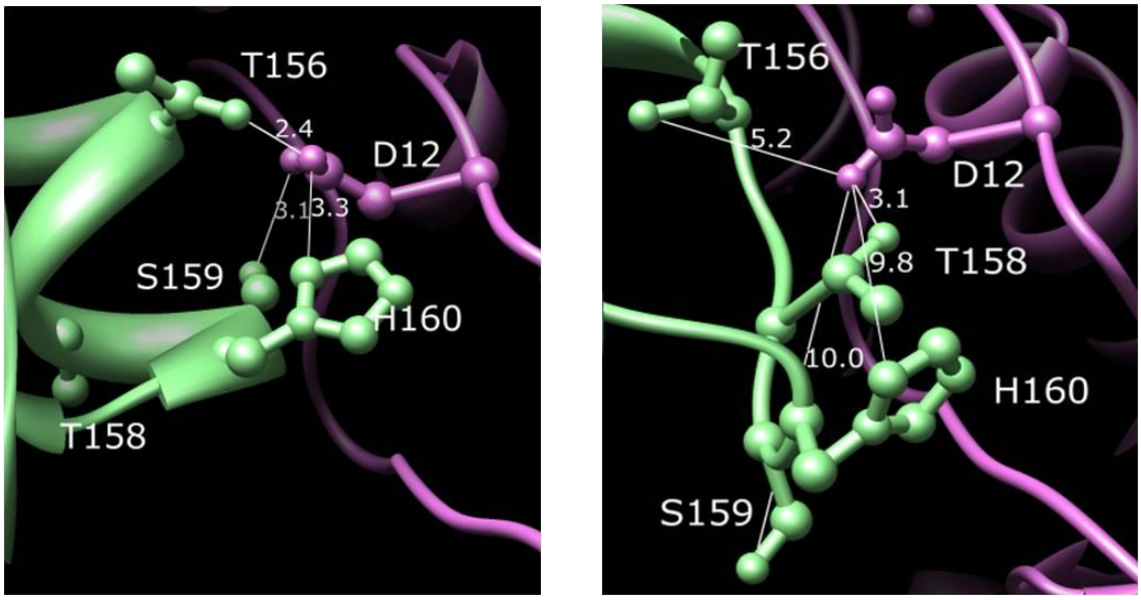


A. B.

Figure 3-1 Crystal structure of D12 region in wild-type BsPFK. (1A) Crystal structure of wild-type BsPFK bound to F6P and MgADP(*121*). (1B) Crystal structure of wild-type BsPFK bound to PGA (*101*). Distances are indicated and are in Å.

longer interacts with D12; instead T156 forms a hydrogen bond with the OH group of Y164 within its own monomer. Therefore, out of all of the completely conserved residues, D12 and T156 are the only two residues that do not directly bind to any ligand, are located along a dimer-dimer interface, and form hydrogen bonds that dramatically change depending on whether substrate or inhibitor is bound. D12 is the only residue of the group that can interact with up to four residues (T156, S159, H160, and R252) when the substrate is bound to the enzyme, three of these residues belonging to helix 6 in the adjacent monomer. In addition, D12 continues to interact with loop 6F across the substrate-binding interface when PGA is bound.

The highly conserved nature and lack of direct ligand interactions of D12 and T156 is an intriguing facet of the amino acid sequence of bacterial PFKs. Furthermore, the residues D12 potentially interacts with when the enzyme is in the substrate bound form, S159 and H160, are both 96% conserved among the ATP-dependent PFKs compared. These four residues are located along the substrate binding interface. This dimer-dimer interface is the same interface that undergoes the quaternary shift in the PGA bound structure of BsPFK. In an attempt to understand the role of these highly conserved residues, alanine scanning mutagenesis was performed on D12 and the residues D12 potentially interacts with across the interface (T156, T158, S159, and H160). Previous work performed by Ortigosa, et. al. noted the importance of D12A in experiments designed to isolate each of the four unique heterotropic interactions found in BsPFK (*134*). The D12A mutation was made in concert with other mutations; therefore, the characteristics of the single mutant were never fully investigated. The

following data describes the kinetic and structural characteristics of the variants D12A BsPFK and T156A BsPFK. In addition, the kinetic and coupling parameters of T158A, S159A, and H160A are described. The mutations, D12A and T156A, both significantly alter the binding of PEP and F6P without appreciably changing the coupling constant when compared to wild-type BsPFK. In addition, two crystal structures of D12A BsPFK and one crystal structure of T156A BsPFK are introduced. Figure 3-2 compares the D12 region of apo BsPFK (Figure 3-2A), substrate bound BsPFK (Figure 3-2B), PGA bound BsPFK (Figure 3-2C), apo D12A BsPFK (Figure 3-2D), PEP bound D12A BsPFK (figure 3-2E), and PEP bound T156A BsPFK (Figure 3-2F). Both the apo and PEP bound structures of D12A BsPFK and the PEP bound structure of T156A BsPFK are in the quaternary shifted position characteristic of the PGA bound wild-type BsPFK structure. The fact that D12A BsPFK and T156A BsPFK crystal structures are in the quaternary shifted position and still experience allosteric inhibition by PEP brings to question the traditional role of the quaternary shift proposed by Schirmer and Evans.

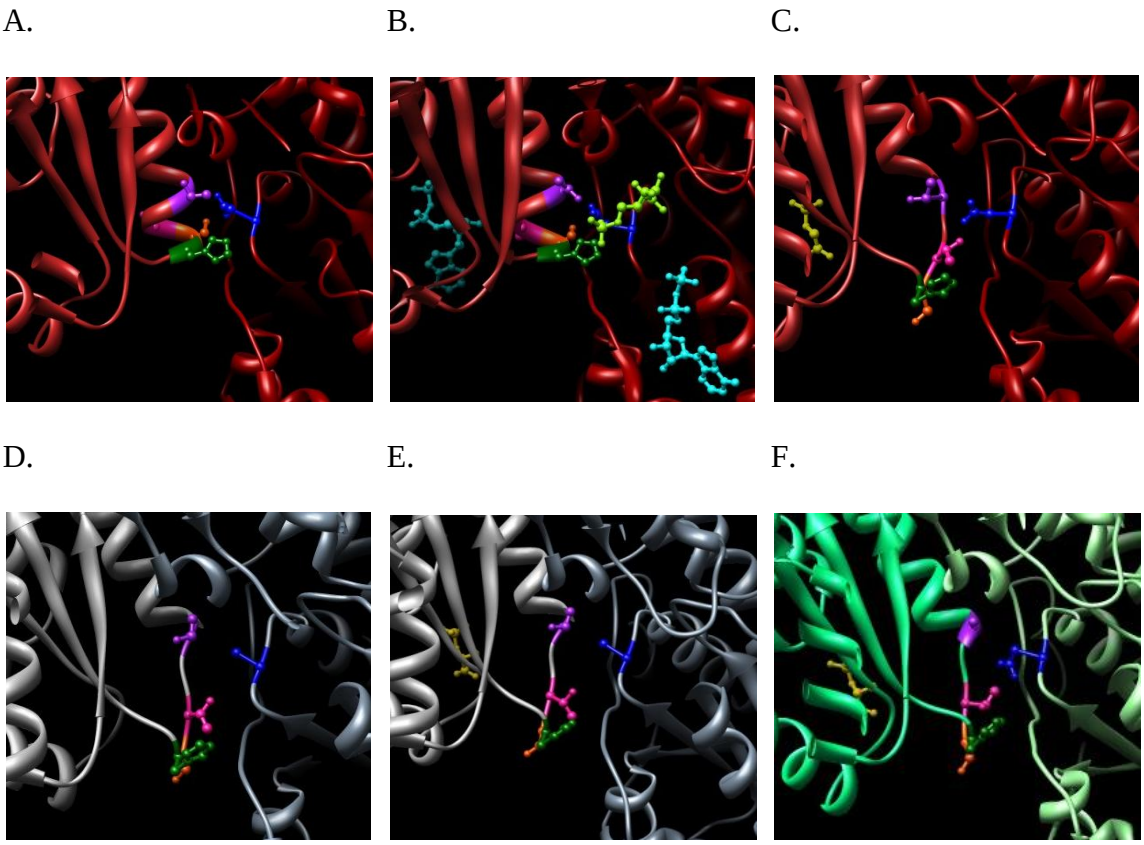


Figure 3-2 Comparison of the D12 region between wild-type and variants of BsPFK crystal structures. (A) Wild-type apo. (B) Wild-type substrate bound. (C) Wild-type PGA bound. (D) D12A apo. (E) D12A PEP bound. (F) T156A PEP bound. Wild-type BsPFK is red ribbon, D12A BsPFK is grey ribbon, and T156A is green ribbon. Residue D12 (or D12A) is blue, T156 (or T156A) is purple, T158 is pink, S159 is orange, and H160 is green. ADP is light blue, Fru-6-P is light green, PGA is yellow, and PEP is gold.

## Materials and Methods

### *Materials*

All chemical reagents used in buffers, protein purifications, and enzymatic assays were of analytical grade, purchased from Sigma-Aldrich (St. Louis, MO) or Fisher Scientific (Fair Lawn, NJ). Creatine kinase and the ammonium sulfate suspension of glycerol-3-phosphate dehydrogenase were purchased from Roche (Indianapolis, IN). The ammonium sulfate suspensions of aldolase and triosephosphate isomerase, and the sodium salts of phosphocreatine, ATP, and PEP were purchased from Sigma-Aldrich. The coupling enzymes were extensively dialyzed against 50 mM MOPS-KOH, pH 7.0, 100 mM KCl, 5 mM $MgCl_2$, and 0.1 mM EDTA before use. The sodium salt of F6P was purchased from Sigma-Aldrich or USB Corporation (Cleveland, OH). NADH and DTT were purchased from Research Products International (Mt. Prospect, IL) and the crystallization materials were purchased from Hampton Research (Aliso Viejo, CA). DE52 and Memetic Blue 1 resin used in protein purifications were purchased from Whatman (Maidstone, England) and Promatic BioSciences (Rockville, Maryland), respectively. Site-directed mutagenesis was performed using the QuikChange Site-Directed Mutagenesis System from Stratagene (La Jolla, CA). Oligonucleotides were synthesized and purchased from Integrated DNA Technologies, Inc (Coralville, IA). DNA modifying enzymes and dNTP's were purchased from Stratagene (Cedar Creek, TX), New England Biolabs (Ipswich, MA), or Promega (Madison, WI). Deionized distilled water was used throughout.

*Site-directed Mutagenesis*

The plasmid pBR322/BsPFK (*123*) contains the gene for BsPFK behind the native *Bacillus stearothermophilus* promoter and was received as a generous gift from Simon H. Chang (Louisiana State University). Mutagenesis was performed following the QuikChange Site-Directed Mutagenesis protocol. Two complementary oligonucleotides were used to make the mutant genes and only the template oligo is shown below. The underlined bases designate the codon for the alanine that replaced the specific residue indicated.

D12A: G TTG ACA AGC GGC GGC <u>GCC</u> TCG CCG GGA ATG

T156A: C GAC AAA ATC CGC GAC <u>GCC</u> GCG ACG TCG

T158A: CGC GAC ACG GCG <u>GCC</u> TCG CAC GAG

S159A: GAC ACG GCG ACG <u>GCC</u> CAC GAG CGG AC

H160A: CG GCG ACG TCG <u>GCC</u> GAC CGG ACG TAC G

Wild-type and all mutant BsPFKs were expressed in *E.coli* RL257 cells (*124*), which is a strain of *E.coli* lacking both the PFK-1 and PFK-2 genes.

*Protein Purification for Wild-type, T158A, S159A, and H160A BsPFK*

The purification of both wild-type and variant BsPFKs was performed as described previously, with a few modifications (*125*). RL257 cells containing the appropriate plasmid were grown at 37°C for 16-18 hours in LB (Lysogeny Broth) ampicillin (Tryptone 10 g/L, yeast extract 5 g/L, and Sodium Chloride 10 g/L, ampicillin 100 ug/ml). Cells were pelleted and frozen for at least 12 hours. The cells were

resuspended in purification buffer (10 mM Tris-HCl, 1 mM EDTA pH 8.0) and sonicated at 0°C in 15 second pulses for 8 minutes with a Fisher 550 Sonic Dismembrator. The crude lysate was centrifuged using a Beckman model J2-21 centrifuge equipped with a JA20 rotor at 22,500 x g for one hour at 4°C. The clear supernatant was heated at 70°C for 15 minutes, cooled on ice for 15 minutes, and centrifuged as before. The diluted supernatant for the wild-type protein was loaded onto a Mimetic Blue 1 column. The column was equilibrated with purification buffer before loading the supernatant containing the protein of interest. The column was washed with at least 5 bed volumes of purification buffer and the enzyme was eluted with a 0 – 1 M NaCl gradient. Enzyme containing fractions were pooled and dialyzed into 20 mM tris-HCl pH 8.5 and loaded onto a Pharmacia Mono-Q anion exchange column. The enzyme was eluted with a 0 – 1 M NaCl gradient and PFK containing fractions were combined, concentrated, then dialyzed into EPPS Buffer ( 50 mM EPPS, 10 mM $MgCl_2$, 100 mM KCl, 0.1 mM EDTA pH 8.0). Concentrated enzyme was stored in EPPS buffer at 4°C. The final enzyme was determined to be pure by SDS-PAGE and the concentration was ascertained using the absorbance at 280 nm ($\varepsilon = 18910\ M^{-1}cm^{-1}$(*126*)).

*Protein Purification for D12A and T156A BsPFK*

Protein purification for D12A BsPFK and T156A BsPFK were carried out as described above, with the following exceptions. T156A BsPFK lost a significant amount of activity during the heating step unless 1 mM F6P was added to the supernatant before heating. F6P was not added to any other buffer for the duration of the

purification for T156A BsPFK. D12A BsPFK and T156A BsPFK did not respond to the Mimetic Blue 1 resin the same as wild-type so that the supernatant was loaded onto a DE52 column. The DE52 column was prepared and treated the same as the Mimetic Blue 1 column.

*Crystallization and Data Collection*

The apo and the PEP bound D12A BsPFKs and the T156A BsPFK were crystallized using the hanging drop vapor diffusion method at 16°C. Apo D12A BsPFK was obtained through extensive dialysis of the mutant enzyme in EPPS buffer containing 50 mM EPPS, 10 mM $MgCl_2$, 100 mM KCl, 0.1 mM EDTA, 10 mM F6P pH 8.0 followed by extensive dialysis in F6P free EPPS buffer. The crystallization condition for the Apo D12A BsPFK structure was a 4 µl drop consisting of 2 µl of solvent (0.2 M magnesium chloride hexahydrate, 0.1 M tris hydrochloride pH8.5, and 30% w/v polyethylene glycol 4,000) and 2 µl of protein (stock concentration of apo D12A BsPFK was 35 mg/mL stored in EPPS buffer). PEP bound D12A BsPFK was obtained through purification of the enzyme as directed above. The PEP bound to the enzyme is indigenous *Escherichia coli* PEP. The crystallization condition for the PEP bound D12A structure was a 6 µl drop consisting of 2 µl of solvent (0.1 M sodium citrate tribasic dehydrate pH 5.6, 20% v/v 2-propanol, 20% w/v polyethylene glycol 4,000) and 4 µl of protein (stock concentration of D12A BsPFK was 34 mg/mL stored in EPPS buffer). The crystallization condition for the T156A BsPFK structure was either 2 µl of solvent (0.1M HEPES sodium pH 7.5 and 1.4 M Sodium citrate tribasic dehydrate) and either 3

or 4 µl protein (stock concentration of T156A BsPFK was 13 mg/ml). The T156A BsPFK crystal structure is bound to four PEP molecules, just as the PEP bound D12A BsPFK. And just as the D12A BsPFK is bound to the indigenous *Escherichia coli* PEP, so is the T156A BsPFK. Numerous attempts were made to crystallize T156A BsPFK without the inhibitor bound; however, none were successful. In addition, attempts were made to crystallize the variants T158A, S159A, and H160A BsPFKs. All proteins yielded crystals, but the quality of the crystals were insufficient and did not produce quality data.

Within 2-3 days crystals formed for both species (D12A and T156A BsPFK) of enzyme. Variant BsPFK crystals were briefly soaked in cryogenic mother liquor containing 30% ethylene glycol and then flash-frozen in a liquid $N_2$ stream at 100 K. Diffraction data for the apo and PEP bound D12A BsPFK crystals were collected on an Advanced Photon Source (APS) beam line 23-ID (insertion device) using a MAR 300 CCD detector (MarMosaic from Marresearch- Charged Coupled Device) (Rayonix LLC, Evanston, IL). The high resolution data of T156A BsPFK was collected at beamline 19-ID on an Area Detector Systems Corporation Q315 area detector at the Advanced Photon Source, Argonne National Laboratory. The HKL2000 program package (HKL Research, Inc., Charlottesville, VA) (*128*) was used for integration and scaling of the PEP bound D12A crystals, while d*TREK (Rigaku Americas, Woodlands, TX) was used for integration and scaling of the apo D12A and T156A crystals (*128, 135*). Data collection details are summarized in Table 3-1.

Table 3-1 Data collection and refinement statistics for apo and PEP bound D12A BsPFK structures[b]

| Data set | D12A apo | D12A-PEP | T156A-PEP |
|---|---|---|---|
| Unit cell (Å) | $a$ = 96.05 | $a$=96.65 | a=96.405 |
| | $b$ = 112.66 | $b$=112.97 | b=111.575 |
| | $c$ = 129.73 | $c$=131.04 | c=129.448 |
| Space group | $P2_12_12_1$ | $P2_12_12_1$ | $P2_12_12_1$ |
| Number of molecules per asymmetric unit (Z) | 4 monomers | 4 monomers | 4 monomers |
| Resolution (Å) | 40-2.3 | 65-2.0 | 45-2.5 |
| Completeness (%) | 100.0(100.0) | 97.0(78.2) | 100.0(100.0) |
| $I/\sigma I$ | 12.2(3.1) | 13.3(2.7) | 36.49 (5.68) |
| $R_{merge}$ | 11.5 (46.0) | 5.3(38.9) | 10.6 (46) |
| **Refinement** | | | |
| Resolution (Å) | 40-2.3 | 50-2.00 | 45-2.5 |
| Reflections (working/free) | 63108 (3204) | 89745(4715) | |
| $R$ (%) | 20.07 | 18.86 | 16.6 |
| $R_{free}$(%) | 25.39 | 23.48 | 23.78 |
| Number of protein atoms/number of waters | 9517/329 | 9574/626 | 9429/312 |
| Average $B$ factor (Å$^2$) | 48.41 | 28.96 | 50.5 |
| Average $B$ factor for water molecules (Å$^2$) | 44.21 | 43.53 | 53.1 |
| Rmsd Bond length (Å) | 0.004 | 0.012 | 0.005 |
| Rmsd Bond angles (degrees) | 0.517 | 1.355 | 0.637 |
| **Ramachandran statistics** | | | |
| Most favored | 97.3% | 97.2% | 97.79% |
| Allowed | 2.5% | 2.8% | 0.08% |

[a] Values in parentheses are for high resolution shells. $R_{sym} = \sum_h\sum_i|I_{hi} - \langle I_h\rangle|/\sum_h\sum_i I_{hi}$, where $I_{hi}$ is the $i$th observation of the reflection $h$, whereas $\langle I_h\rangle$ is the means intensity of reflection $h$. [b] $R_{cryst} = \sum||F_o| - |F_c||/|F_o|$. $R_{free}$ was calculated with a fraction (5%) of randomly selected reflections excluded from refinement.

*Structure Determination and Refinement*

Molecular replacement program PHASER (University of Cambridge, UK) (*129*) was used to solve the structure of the apo and PEP bound BsPFKs using the phosphate bound crystal structure of BsPFK (PDB accession code 3PFK) (*121*) with waters and ions removed as the search model. Rigid body refinement followed by simulated annealing refinement at 5000K was carried out using Phenix (Python-based Hierarchical Environment for Integrated Xtallography, Berkely, CA) (*130*) for the apo structure while CCP4 Refmac (York Structural Biology Laboratory, University of York, Heslington, UK) with TLS refinement (translation, libration and screw-rotation) (Science and Technology Facilities Council, Daresbury, UK) were used for the refinement of the PEP bound protein(*136, 137*). Subsequently, refinement was carried out in alternating cycles of manual model building in COOT (Crystallographic Object-Orientated Toolkit, Oxford, UK) (*131*) followed by refinement until the R-factors converged. The stereochemistry of the final models of the BsPFK enzymes were verified by MolProbity (Duke University, Durham, NC) (*132*).

*Kinetic Assays*

Activity measurements for PFK were carried out in a 0.6 mL reaction volume of EPPS buffer containing 50 mM EPPS, 10 mM $MgCl_2$, 100 mM KCl, 0.1 mM EDTA, 2 mM DTT, 0.2 mM NADH, 3 mM ATP, 250 μg aldolase, 50 μg of glycerol-3-phosphate dehydrogenase, 5 μg of triosephosphate isomerase, 40 μg/mL of creatine kinase and 4 mM phosphocreatine at pH 8.0 and 25 °C. F6P and PEP were added at varied

concentrations as indicated. Assays were started by the addition of 6 μL of appropriately diluted PFK and the reaction was monitored as the absorbance at 340 nm decreased over time. Dilution of T156A BsPFK in EPPS buffer resulted in significant loss of activity; therefore, all dilutions of T156A BsPFK were done in EPPS buffer containing 1 mM F6P. The addition of F6P resulted in T156A BsPFK remaining stable throughout the duration of the assays. The rate of the reaction was measured on Beckman Series 600 spectrophotometers. One unit of PFK activity is described as the amount of enzyme needed to produce 1 μmol of F16BP per minute.

*Data Analysis*

Data were fit to the following equations using the least-squares fitting analysis of Kaleidagraph software (Synergy). Initial velocity activities, that were measured in the kinetic assays where the F6P concentration was saturable, were fit to the Hill equation (*138*):

$$\frac{v}{E_T} = \frac{V_{max}[A]^{n_H}}{K_{1/2}^{n_H} + [A]^{n_H}} \qquad (3\text{-}1)$$

where v is the initial rate, $E_T$ is the total enzyme active site concentration, [A] is the concentration of the substrate F6P, $V_{max}$ is the maximal velocity, $K_{1/2}$ is the concentration of F6P that gives one-half the maximal specific activity, and $n_H$ is the Hill coefficient. In the D12A BsPFK kinetic assays, the $K_{1/2}$ is unattainable at higher concentrations of inhibitor because the F6P titration does not reach saturation; therefore, the data were fit to the following equation:

$$\frac{v}{E_T} = \frac{k_{cat}}{K_{1/2}}[A]. \quad (3\text{-}2)$$

The allosteric responses of BsPFK to PEP were quantified by plotting either the $K_{1/2}$ from Equation 3-1 or the reciprocal of $V_{max}/K_{1/2}$ from equation 3-2 versus the PEP concentration and fitting these data to the following equation (*96*):

$$K_a = K_{ia}^{\circ} \frac{K_{iy}^{\circ} + [Y]}{K_{iy}^{\circ} + Q_{ay}[Y]} \quad (3\text{-}3)$$

where $K_a$ is equal to $K_{1/2}$ when data were fit to Equation 3-1 or $K_{1/2}/V_{max}$ when data were fit to Equation 3-2, [Y] is the concentration of the inhibitor PEP, $K_{ia}^{\circ}$ is the dissociation constant for F6P in the absence of PEP, $K_{iy}^{\circ}$ is the dissociation constant for PEP in the absence of F6P, and $Q_{ay}$ is the coupling coefficient which describes both the nature and the magnitude of the allosteric response (*96, 99*). $Q_{ay}$ describes an inhibitor when it is less than one and an activator when it is greater than one. There is no allosteric response when $Q_{ay}$ equals to one.

**Results**

BsPFK, like many oligomeric enzymes, contains ligand binding sites that lie along the interface of two subunits, such that every active site and effector site is comprised of residues from adjacent monomers. BsPFK contains four substrate binding sites that are formed along one dimer-dimer interface (substrate interface) and four effector binding sites formed along the other dimer-dimer interface (allosteric interface). Located in the C-4a loop, along the active site interface, is the completely conserved amino acid D12, which does not directly interact with any ligand. Comparison of the

substrate bound and apo wild-type BsPFK crystal structures reveals that an intra-subunit hydrogen bond exists between R252 (R252 directly binds to the 6-phosphate of F6P(*101*)) and D12 regardless of whether or not F6P is bound (Figure 3-2A and 3-2B). According to the PGA bound structure, the R252-D12 interaction is lost when the inhibitor analog is bound to the enzyme (Figure 3-2C). The relationship between these two residues was first manipulated by making the double mutant R252A/D12A in order to create specific hybrids in BsPFK (*134*). Interestingly, the specific activity of the double mutant and the single mutant, R252A, are comparable to the wild-type enzyme (*125, 134*). However, the specific activity of D12A BsPFK, as shown in Figure 3-3, is almost 7 fold lower than wild-type BsPFK. Equation 3-1 was used to fit both the wild-type and the variants data. The apparent dissociation of F6P ($K_{1/2}$) for D12A BsPFK is augmented by 50-fold compared to that of wild-type, which makes performing complete F6P titrations at high concentrations of inhibitor impossible due to the inability of the enzyme to be fully saturated by substrate. The F6P binding of H160A BsPFK is only diminished 2-fold when compared to wild-type; however, this small augmentation in substrate binding was significant enough to necessitate a different approach to obtaining kinetic data. Therefore, in an attempt to measure the nature and magnitude of the allosteric effect between F6P and PEP for D12A BsPFK and H160A BsPFK, only data in the linear region of the F6P titration curves were fit to Equation 3-2. This linear

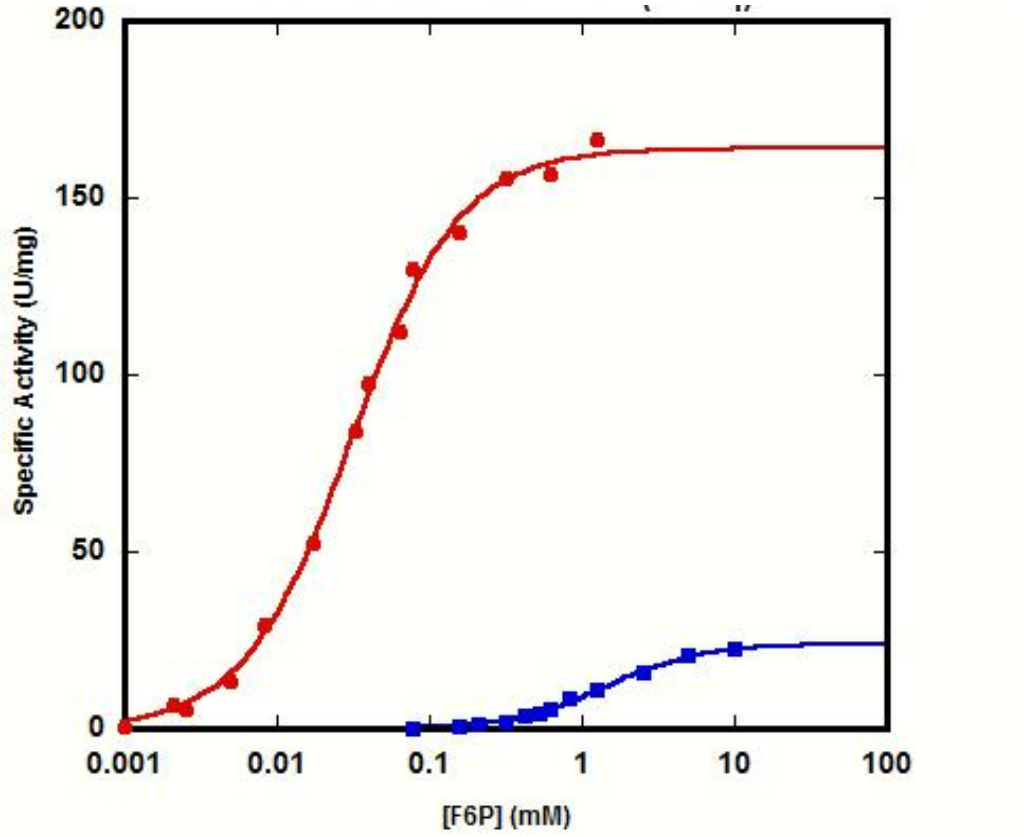


Figure 3-3 Specific activity versus F6P concentration for wild-type and D12A BsPFK. Wild-type BsPFK is represented by red circles and D12A BsPFK is represented by blue squares. Solid lines represent the best fit of the data to Equation 3-1.

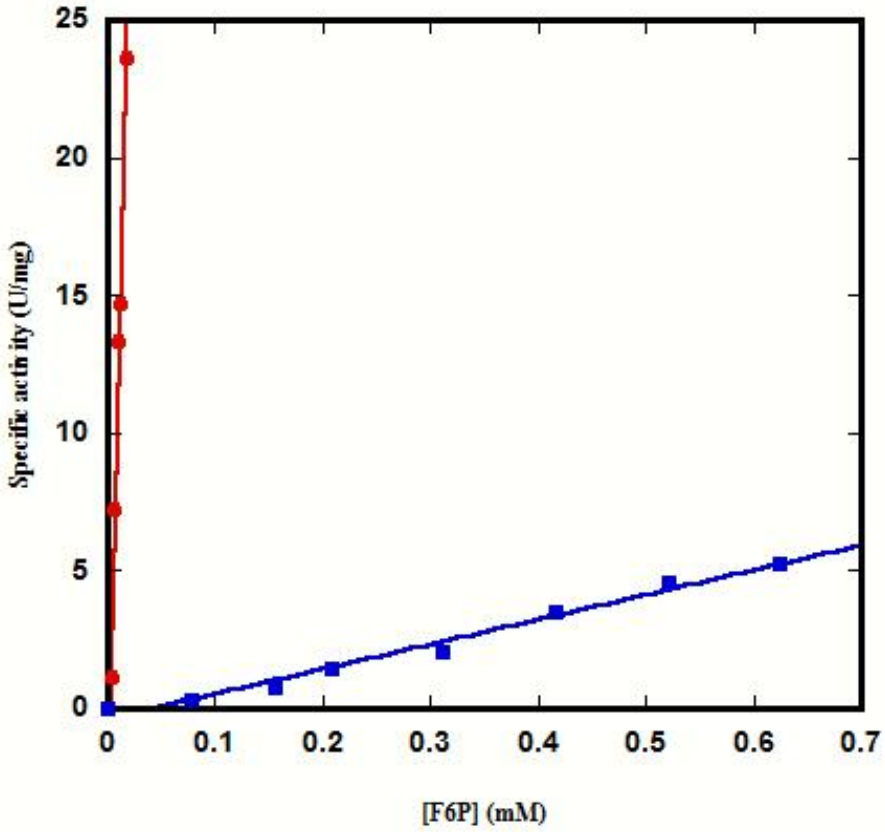


Figure 3-4 Specific activity versus F6P concentration under first-order conditions for wild-type and D12A BsPFK. Wild-type BsPFK is in circles and red. D12A BsPFK is in squares and blue. Solid lines represent the best fit of the data to Equation 3-2.

region, shown for both wild-type and D12A in Figure 3-4, is indicative of the first binding event of F6P to the enzyme, assuming that the hill number remains relatively constant.

Figure 3-5 compares plotting $K_{1/2}$ or $K_m/V_{max}$ versus the PEP concentration for wild-type BsPFK in order to demonstrate the efficacy of using $K_m/V_{max}$ in Equation 3-3. The apparent dissociation constant for PEP in the absence of F6P and the coupling parameter, $Q_{ay}$, for both methods are within error of each other. The apparent dissociation constant for F6P is the only parameter of Equation 3-3 that is not comparable between the two techniques; however, by simply fitting Equation 3-1 to a F6P titration curve in the absence of PEP and taking the $K_{1/2}$ from this fit can the $K_{ia}^{\circ}$ be approximated. Figure 3-6 illustrates the $K_m/V_{max}$ versus the PEP concentration for wild-type, D12A, and H160A BsPFKs. Table 3-2 compares the kinetic and coupling parameters of wild-type, D12A, and H160A BsPFKs. D12A BsPFK has a dissociation constant for F6P, $K_{ia}^{\circ}$, of 1.4±0.1 mM, which is almost a 50-fold increase in substrate binding affinity compared to wild-type BsPFK. In addition, D12A BsPFK has a dissociation constant for PEP, $K_{iy}^{\circ}$, of 0.45 ± 0.01 uM, which is a 100-fold increase in binding affinity compared to wild-type BsPFK. Most striking, however, is that the coupling parameter for D12A is remarkably similar to that of wild-type.

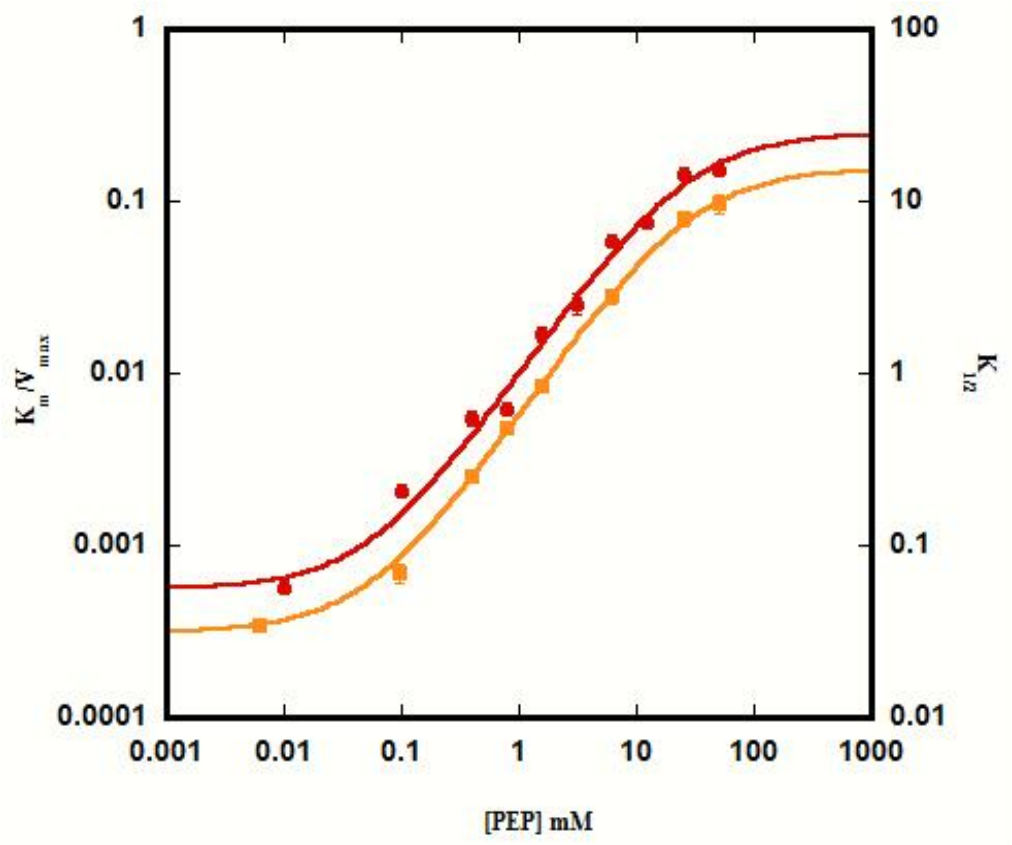


Figure 3-5 K vs. PEP concentration plot comparing $K_m/V_{max}$ and $K_{1/2}$ methods for wild-type BsPFK. Data points from $K_m/V_{max}$ method in red circles. Data points from $K_{1/2}$ method in orange squares. Solid lines represent the best fit to Equation 3-3.

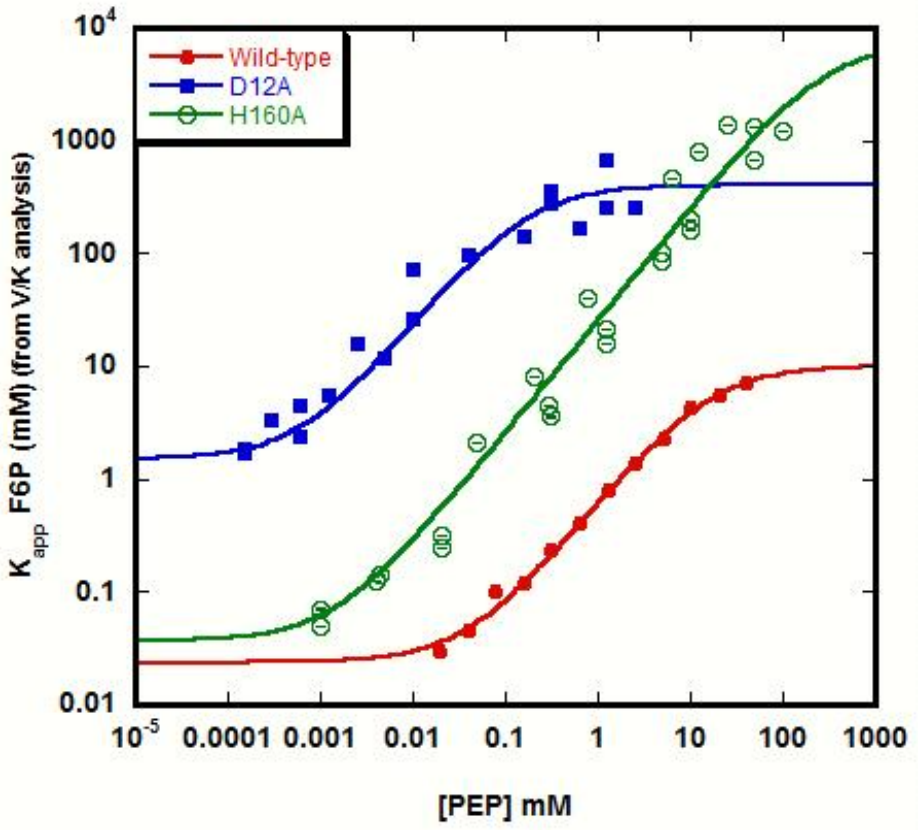


Figure 3-6 Influence of PEP on the $Km/V_{max}$ of wild-type, D12A, and H160A BsPFKs. Wild-type is represented by red circles, D12A is represented by blue squares, and H160A is represented by open green circles. Solid lines represent the best fit to Equation 3-3.

Table 3-2 Steady-state kinetic and coupling parameters for wild-type, D12A, and H160A BsPFKs

| | Wild-type | D12A | H160A |
|---|---|---|---|
| Specific Activity (U/mg) | 163 ± 3 | 24 ± 1 | 70 ± 2 |
| $K_{ia}^{\circ}$ (mM) | 0.030 ± 0.002 | 1.4 ± 0.1 | 0.056 ± 0.002 |
| $K_{iy}^{\circ}$ (mM) | 0.060 ± 0.004 | 0.00045 ± 0.00001 | 0.001 ± 0.00005 |
| $Q_{ay}$ | 0.002 ± 0.0003 | 0.003 ± 0.0001 | 0.000005± 0.0000004 |

Table 3-3 Steady-state kinetic and coupling parameters for variant BsPFKs

| | T156A | T158A | S159A |
|---|---|---|---|
| Specific Activity (U/mg) | 50 ± 3 | 70 ± 3 | 140 ± 4 |
| $K_{ia}^{\circ}$ (mM) | 0.52 ± 0.005 | 0.017 ± 0.0005 | 0.025 ± 0.003 |
| $K_{iy}^{\circ}$ (mM) | 0.0021 ± 0.00004 | 0.098 ± 0.004 | 0.012 ± 0.001 |
| $Q_{ay}$ | 0.002 ± 0.0007 | 0.009 ± 0.0003 | 0.0005 ± 0.00006 |

Given the remarkable binding and coupling characteristics of D12A BsPFK, the same kinetic and coupling parameters for T156A, T158A, S159A, and H160A were measured. Figure 3-6 and Figure 3-7 compare the $K_m/V_{max}$ or the $K_{1/2}$, respectively, versus the PEP concentration for wild-type and all of the variants of BsPFK. In addition, Tables 3-2 and 3-3 display the kinetic and coupling parameters for the mutant forms of BsPFK. The dissociation constants for F6P for T158A, S159A, and H160A are comparable to that of wild-type BsPFK. While the $K_{ia}^{\circ}$ for S159A is almost identical to wild-type, T158A shows an almost 2-fold enhanced binding for F6P and H160A shows an almost 2-fold diminished binding for F6P. However, the $K_{ia}^{\circ}$ for T156A is 0.52 ± 0.005 mM, which is a 17-fold decrease in the substrate binding when compared to wild-type. The PEP binding of the mutant BsPFKs is a bit more varied than the F6P binding. T156A, S159A, and H160A all exhibit enhanced PEP binding, though to different

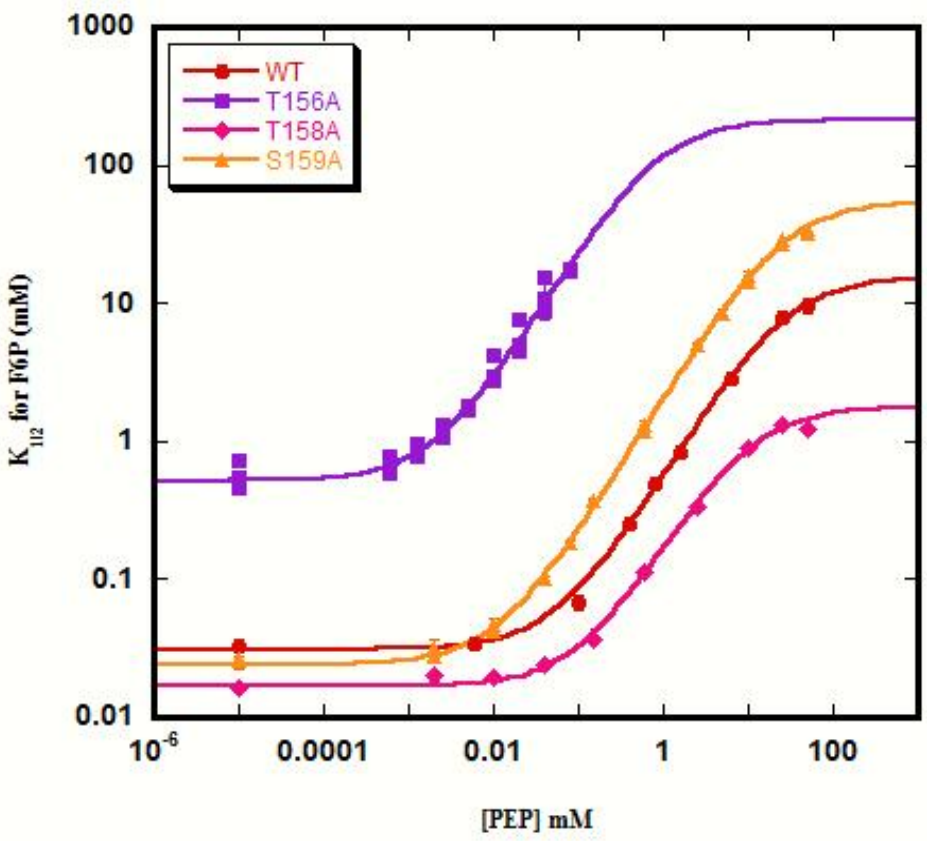


Figure 3-7 Influence of PEP on $K_{1/2}$ for F6P of wild-type, T156A, T158A, and S159A BsPFKs. Wild-type is represented by red circles, T156A is represented by purple squares, T158A is represented by pink diamonds, and S159A is represented by orange triangles. Solid lines represent the best fit to Equation 3-3.

degrees. Compared to wild-type, S159A and H160A enhance PEP binding by 5- and 15-fold, respectively, and T156A enhances the inhibitor binding by 28-fold. T158A, unlike the other variants, exhibits a diminished PEP binding of 0.098 ± 0.004, which is almost a 2-fold increase compared to that of wild-type. Considering only the binding characteristics of the variant BsPFKs, D12A and T156A BsPFKs are the only two mutants that show a significant enhancement in PEP binding while also exhibiting a diminished F6P binding.

The coupling constants of the variants of BsPFK range dramatically depending on the mutation. T158A is the only mutant BsPFK that shows a significant decrease in coupling, with a $Q_{ax}$ of 0.009 ± 0.0003. Both S159A and H160A BsPFKs exhibit enhanced coupling, when compared to wild-type. However, the coupling parameter for T156A BsPFK is remarkably similar to that of wild-type and D12A BsPFKs. Therefore, it appears that the kinetic and coupling parameters of T156A BsPFK compare with those of D12A BsPFK, while the parameters for T158A, S159A, and H160A do not.

D12A exhibits a significant decrease in specific activity and shows a dramatic effect on the binding of both F6P and PEP without being directly bound to either ligand. The unique response of D12A raises some question with regard to the structural integrity of the enzyme. Specifically, has some structural perturbation occurred that could explain not only the low activity and poor F6P binding, but also the magnitude of the enhanced PEP binding? Diffraction quality crystals of D12A bound to PEP were obtained. The PEP binding of this mutant is enhanced to such a degree that the

indigenous PEP during cell growth (i.e. protein production) stayed bound to the enzyme throughout the extensive purification and dialysis processes. Figure 3-8 shows the electron density of PEP in the effector binding pocket of D12A BsPFK. The crystals belong to the space group $P2_12_12_1$ with unit cell dimensions of a=96.65, b=112.97, and c=131.04. The asymmetric unit consists of 4 subunits, or one tetramer. The final structure was refined to R-factor/R-free values of 18.86%/23.48% and has a 2.0 Å resolution. Given the kinetic and coupling similarities between D12A BsPFK and T156A BsPFK, diffraction quality crystals of T156A BsPFK were obtained. The crystal structure of T156A BsPFK has four PEP molecules bound to the effector binding sites. The crystals belong the same space group as PEP bound D12A BsPFK crystals, and the unit cell dimensions of T156A BsPFK are a=96.405, b=111.575, and c=129.448. The final structure was refined to R-factor/R-free values of 16.6%/23.78% and has a 2.5 Å resolution. The details describing the diffraction data and refinement statistics are displayed in Table 3-1.

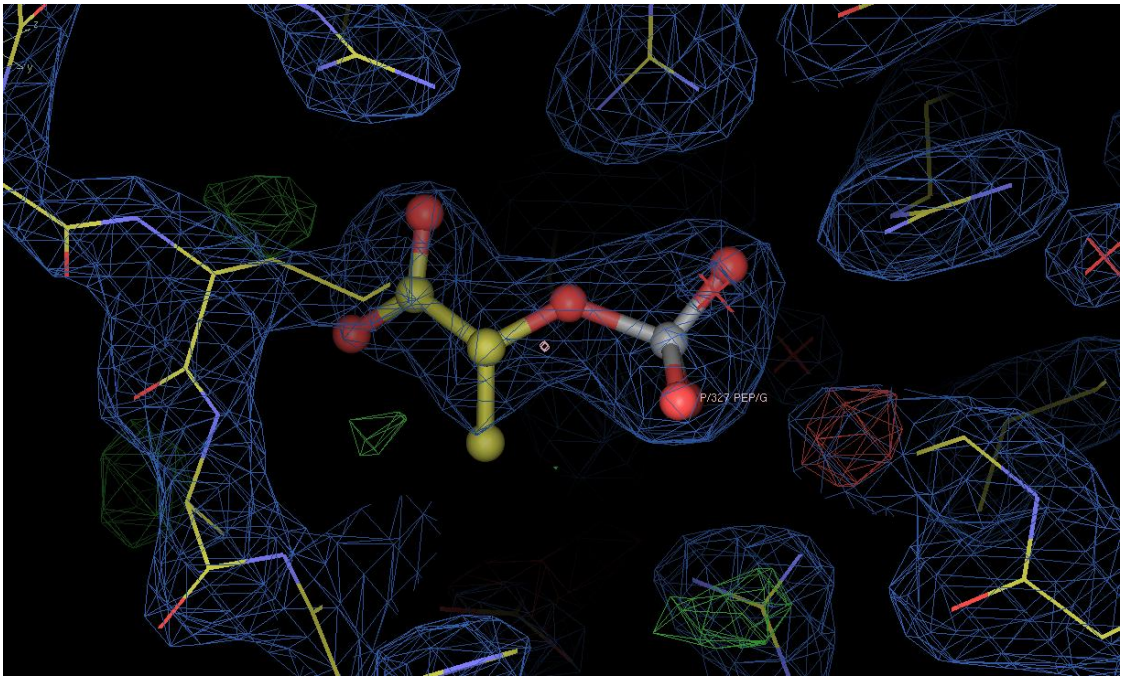


Figure 3-8 Electron density map showing the electron cloud fitting PEP that is bound in the effector binding site in D12A BsPFK.

The fact that PEP is bound to the mutant enzymes demonstrates not only the extremely tight PEP binding of D12A and T156A BsPFKs, but also that PEP has a small dissociation constant. The purification process included two columns, one of which is a strong anion exchange column, as well as numerous dialysis steps. In order to remove the PEP from the D12A BsPFK, the reciprocal binding nature of BsPFK was exploited. Specifically, PEP inhibits the binding of F6P; therefore, the binding of F6P must also inhibit the binding of PEP to the same degree. Ligand reciprocity was utilized by dialyzing the PEP bound D12A BsPFK in a solution containing F6P for over 48 hours, then subsequently removing any substrate from the enzyme by dialyzing for at least 24 hours in buffer containing no ligand. Both the PEP bound and the apo D12A BsPFKs form stable tetramers, as concluded through comparison to wild-type BsPFK on a native gel (data not shown). Diffraction quality crystals of Apo D12A BsPFK were obtained by using the aforementioned dialysis method. The apo crystals belong to the space group $P2_12_12_1$ with unit cell dimensions of a=96.05, b=112.66, and c=129.73. The asymmetric unit consists of 4 subunits, or a single tetramer. The final structure was refined to R-factor/R-free values of 20.07%/25.39% and has a 2.3 Å resolution. The details describing the diffraction data and refinement statistics are displayed in Table 3-1. Several attempts were made to crystallize an apo form of T156A BsPFK. However, every crystal form contained PEP. This may be attributed to the possibility that PEP stabilized the crystal; and if the inhibitor was removed, the enzyme was unstable enough not to be able to form a crystal lattice.

There are no significant structural differences between the apo and PEP forms of D12A BsPFK, except for a slight deviation in residues K214, H215, and D59. When the available wild-type BsPFK structures (substrate bound, PGA bound, and apo) are compared, loop 8-H (residues 213-215) undergoes a hinge motion in response to effector binding. Loop 8-H is open in the apo structure, but closes when ADP is bound and closes to a larger extent when PGA is bound. Figure 3-9 is an overlay of the residues in the effector binding site for the apo and PEP structures of D12A BsPFK. In the PEP bound structure of D12A, K214 forms a hydrogen bond with Y69, a hydrogen bond that does not exist in the apo version of D12A. The hydrogen bond formed between K214 and Y69 pulls K214 out of the binding pocket and causes H215 to tilt towards the $CH_2$ group of PEP. The change in the orientation of D59 observed between the apo and bound D12A structures is a result of the ligand binding since the same residue overlays perfectly with the PGA bound structure of wild-type. Figure 3-10 is an overlay of the effector site residues in the PEP bound D12A structure and in the PGA bound wild-type structure. The positions of the residues are very similar between the inhibitor bound proteins except for K214 and H215. The imidazole ring of H215 is closer to the $CH_2$ group of PEP in the D12A structure, and in the PGA structure the ring is orientated away from the ligand. The region around the mutation is unaffected by the amino acid substitution. Residues 156-162 (6-F loop) are in the same orientation for apo D12A, PEP bound D12A, and PGA bound wild-type. In addition, the active sites are comparable between the three inhibited forms of BsPFK. Both of the D12A structures have undergone the quaternary shift that is characteristic of the inhibited form of BsPFK.

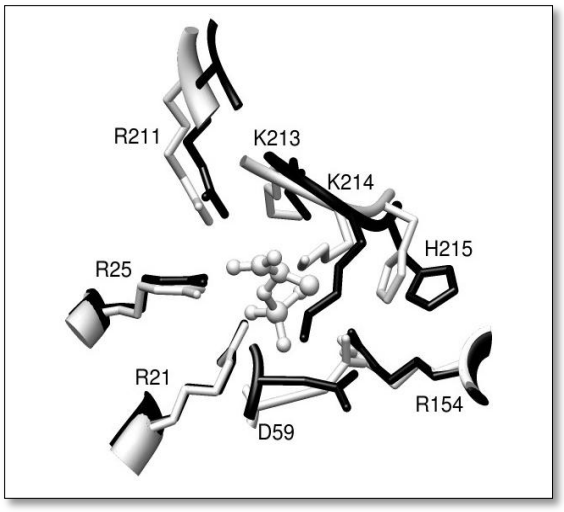


Figure 3-9 Overlay of residues in the effector binding site of D12A BsPFK. Apo D12A BsPFK is in black and PEP bound D12A BsPFK is in gray. PEP is shown in ball and stick mode.

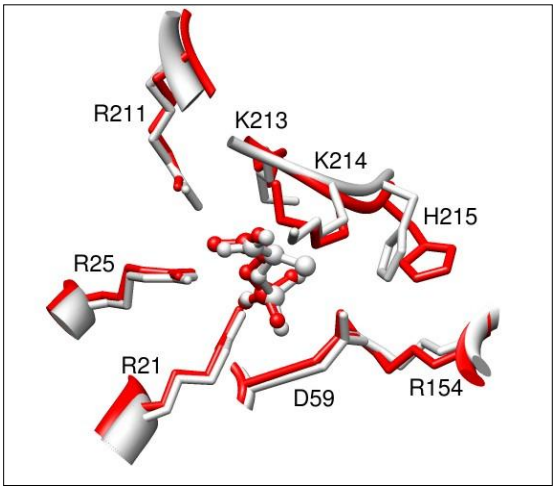


Figure 3-10 Overlay of residues in the effector binding site for inhibitor bound BsPFK. Wild-type PGA bound BsPFK in red, with PGA in red and ball and stick mode, and PEP bound D12A is in gray with PEP in gray and ball and stick mode.

The PEP bound T156A BsPFK crystal structure is similar to the structures of the D12A BsPFK enzymes and the PGA bound wild-type enzyme. Figure 3-2F shows the D12 region for the T156A BsPFK crystal structure, which displays the 6-F loop in a similar orientation to that of the other inhibitor bound BsPFK crystal structures. In addition, the quaternary structure of T156A BsPFK is similar to that of both D12A and PGA bound wild-type BsPFK crystal structures. Figure 3-11 compares the B-factors for the apo D12A (Figure 3-11A), PEP bound D12A (Figure 3-11B), and PEP bound T156A (Figure 3-11C) BsPFK crystal structures. The B-factor, or temperature factor, in protein crystal structures is a refinement parameter that describes the fluctuation of an atom about its mean position. B-factors give an estimate of the flexibility of an atom in a protein crystal structure; therefore, a large B-factor indicates higher mobility. Comparisons of the B-factors for the variant BsPFK crystal structures (Figure 3-11) reveal that the structures are remarkably similar to each other, which is not surprising given the overall similarity in the structures. All of the variant enzymes structures shown here share similar quaternary structures which resemble that of the PGA-bound structure, and they are not as flexible as the substrate-bound form of the enzyme shown in Figure 2-3B. However, none of the variant BsPFK crystal structures are as rigid as the PGA-bound enzyme, which is shown in Figure 2-3C. Overall, when comparing all of the BsPFK B-factors, the variant structures resemble the apo BsPFK enzyme the most, though they are not exact matches to apo BsPFK.

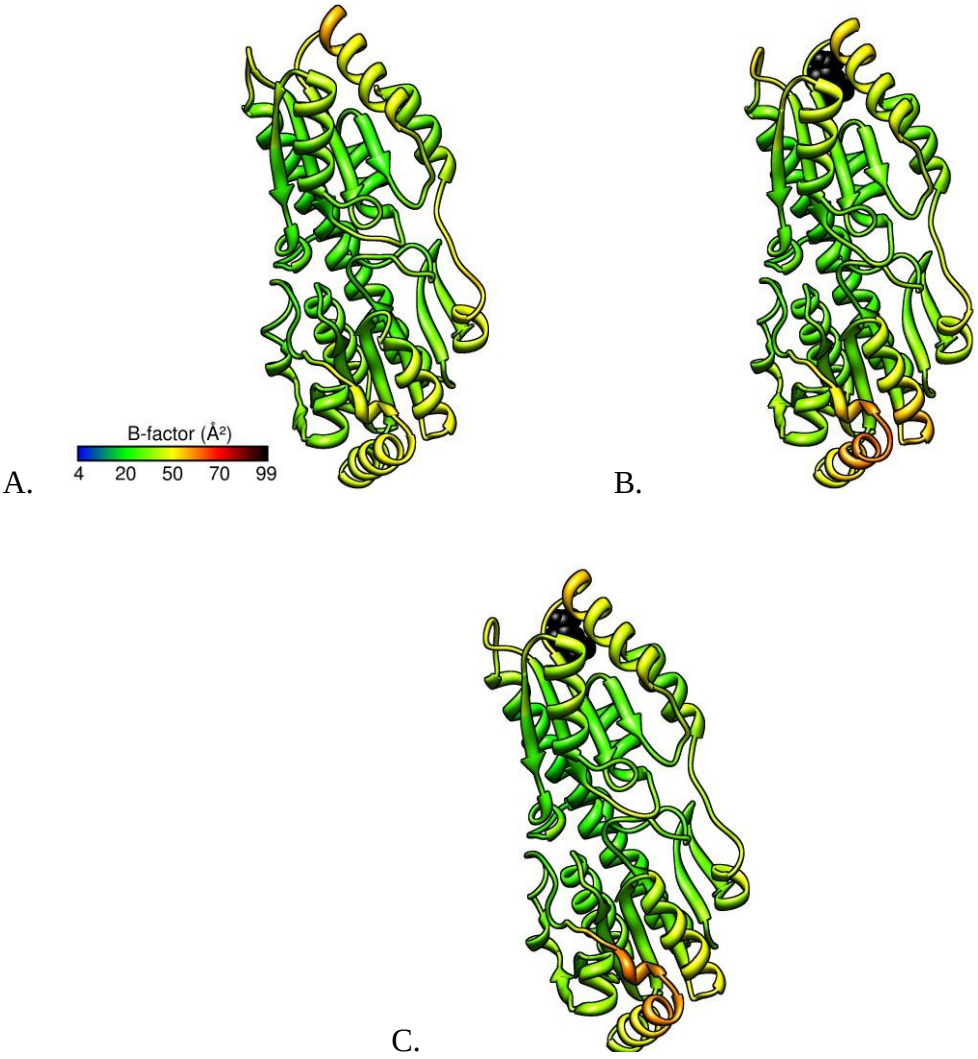


Figure 3-11 Comparison of the variant BsPFK B-factors. (A) Apo D12A BsPFK (B) PEP-bound D12A BsPFK (C) PEP-bound T156A BsPFK . Only monomer A is shown for each structure. PEP is shown as a black space filled molecule.

The unavailability of an apo form of T156A BsPFK is unfortunate, but not detrimental to the overall conclusions that can be drawn from the PEP bound T156A BsPFK crystal structure. When one considers that the quaternary shift causes the enzyme to be more favorable for PEP binding, then the fact that T156A BsPFK is bound to PEP could imply that the apo form of T156A BsPFK may be in the quaternary shifted position as well.

**Discussion**

The model introduced by Schirmer and Evans describing the allosteric nature of BsPFK attributes the mechanism of PEP inhibition to the conformational changes observed in the enzyme (*101*). This proposal is based solely on the structural differences observed between two crystal structures of BsPFK, the F6P bound structure and the PGA bound structure. In contrast, the current study, as well as previous studies conducted with BsPFK, provides evidence that does not support the proposal made by Schirmer and Evans (*104-106*, *134*). The crystal structure of the apo D12A BsPFK shows the enzyme has undergone the quaternary shift; however, analysis of its coupling parameters shows that the mutant enzyme exhibits inhibition that is equivalent to that of wild-type. If the quaternary shift was the action for PEP inhibition, then D12A BsPFK would not exhibit coupling since the enzyme has adopted the quaternary shift before any ligand was added. In essence, the mutant enzyme would exhibit characteristics similar to the wild-type enzyme that had already been saturated by inhibitor. The $K_{ia}^{\infty}$ (dissociation constant for F6P in the saturating presence of PEP) for wild-type BsPFK is

15 mM. The $K_{ia}^{\circ}$ (dissociation constant for F6P in the absence of PEP) for D12A BsPFK is 1.2 mM, which is about 10-fold lower that the $K_{ia}^{\infty}$ of wild-type. D12A BsPFK exhibits a binding for F6P in the absence of PEP that is comparable to the F6P binding of wild-type when in the saturating presence of PEP. However, even with the poor F6P binding D12A BsPFK exhibits, the mutant enzyme still shows heterotropic inhibition on par with that of wild-type.

Given that D12 potentially interacts with multiple residues across the substrate interface, each potential interaction was dissected through mutagenesis, kinetic, and coupling analysis. T158 is the only residue across the substrate interface that could potentially interact with D12 when the inhibitor is bound to the enzyme and it the only potential D12 interaction that is not highly conserved. T158A is the only mutant enzyme tested that showed a significant enhancement in F6P binding and a diminished PEP binding. In addition, T158A is the only mutation that showed a diminished coupling parameter. It is obvious from the kinetic and coupling data discussed here that the potential hydrogen bond formed between D12 and T158 when PEP is bound to the enzyme is not the interaction that is responsible for the D12A BsPFK binding and coupling characteristics.

Likewise, the binding characteristics of S159A BsPFK and H160A BsPFK do not follow the trends seen with D12A BsPFK. Whereas, S159A does cause a slight enhancement in PEP binding, the F6P binding remains comparable to that of wild-type. Also, H160A does enhance PEP binding and diminish F6P binding; however, not nearly to the extent that D12A does. Interestingly, the coupling coefficients for S159A BsPFK

and H160A BsPFK show greater inhibition than wild-type. In fact, the coupling of H160A BsPFK is significantly enhanced when compared to wild-type. Fully saturating amounts of F6P and PEP were not achieved, as is evidenced by the lack of points in the upper plateau of the K vs. X plot in Figure 3-6 and the high error value for the coupling coefficient (Table 3-2). It may be that H160A BsPFK resembles the apo wild-type BsPFK structure since its F6P binding is similar to that of wild-types (Figure 3-6). All crystals grown for H160A BsPFK so far have exhibited low resolution.

T156 has many similarities with D12. Both residues are located along the substrate binding interface, directly across from each other. Both residues are 100% conserved among all available bacterial ATP-dependent PFK sequences. Neither residue directly binds to a ligand. In addition, when each residue is replaced by an alanine, the coupling and kinetic characteristics are also similar to each other. D12A and T156A enhance PEP binding 100- and 28-fold, respectively and diminish F6P binding 50- and 17-fold, respectively. However, the coupling parameters for D12A and T156A are remarkably similar to that of wild-type.

Caution must be exercised when considering structures alone to describe an allosteric mechanism. Allostery, by its very nature, is a thermodynamic phenomenon that is composed of both enthalpic and entropic components. Structures, though insightful, do not address entropic events (dynamics) and should be used as a tool, not the basis, for an allosteric mechanism. In fact, there is growing evidence that proteins are dynamic ensembles of conformational states, leading to the idea that all proteins have the potential to be allosteric (*109*). Accordingly, monomeric and single domain

proteins have been shown to be allosteric (*109, 110*). Quaternary structure was once thought to be a requirement for allostery; however, it may be just a coincidence that many allosteric enzymes are oligomeric.

The diminished specific activity of D12A BsPFK when compared to wild-type BsPFK is a potential complication. Comparison of the mutant enzymes R252A and R252A/D12A to each other reveals that the addition of the D12A mutation did not significantly alter the specific activity of the enzyme (*125, 134*). The question arises whether or not the D12A enzyme intrinsically has a lower specific activity or is a small percentage of the total enzyme active? We are reasonably sure that the D12A enzyme forms stable homotetramers, both in the presence and absence of PEP. Comparison of the active sites of the apo D12A and the apo wild-type BsPFKs shows a very small perturbation in the orientation of R252. The D12-R252 interaction, when completely removed in the double mutant, may allow for the proper orientation of the substrate in the binding pocket. However, if the negative charge of D12 is removed and the positive charge of R252 is unaffected, then the orientation of R252 may hinder the binding of F6P. In order to address this problem, many attempts to produce crystals of D12A BsPFK bound to F6P were tried; however, none of them were successful.

Schirmer and Evans assumed that the PGA BsPFK structure is equivalent to the PEP structure, an assumption that can't be proven without an actual wild-type PEP structure. However, the PEP bound variants of BsPFK and PGA bound wild-type BsPFK structures are very similar. The structure of the effector binding pockets of the PGA bound wild-type BsPFK, apo D12A BsPFK, and the PEP bound variants of BsPFK

are analogous. Therefore, there are no obvious structural explanations to define why PEP binds to D12A BsPFK 100-fold tighter and T156A BsPFK 28-fold tighter than wild-type. Structure alone does not consider that the dissociation and coupling constants for PGA are not the same as that for PEP in wild-type BsPFK (*106*). The differences observed in the structures of the substrate bound and the PGA bound wild-type enzymes are not sufficient in explaining the mechanism of inhibition in BsPFK. If structure alone did constitute the mechanism for inhibition, then one might predict from the kinetic and coupling characteristics of D12A BsPFK that there would be some structural differences seen between PEP bound D12A BsPFK, PEP bound T156A BsPFK, and PGA bound wild-type BsPFK. However, there are not any significant differences between the three inhibitor bound enzymes. In other words, there are no obvious differences in the effector binding pockets of D12A BsPFK and PGA bound wild-type that would explain the large augmentation in PEP binding for the mutant enzyme.

We have not uncovered the mechanism for PEP inhibition of BsPFK, but we have shown a new possible role for the quaternary shift. The quaternary shift, envisioned at one time as the mechanism for allosteric inhibition of BsPFK, may have a significant role in ligand binding. D12A BsPFK and T156A BsPFK have undergone the quaternary shift, exhibit significant changes in ligand binding when compared to wild-type, and possess coupling constants that are comparable to that of wild-type. These data lead to the idea that the quaternary shift is necessary for ligand binding and not heterotropic inhibition. Further research into the actual dynamics of inhibition of BsPFK

must be conducted before a plausible mechanism for allosteric inhibition can be proposed.

## Conclusion

Presented in this paper are the first ever reported PFK crystal structures bound to their native inhibitor, PEP. Whereas, crystal structures of wild-type BsPFK bound to PEP have been elusive; D12A BsPFK and T156A BsPFK both exhibit crystal structures with PEP bound. This strong PEP binding is most likely due to the variant enzymes possessing the quaternary shifted structure resembling the PGA-bound structure of wild-type BsPFK. In addition, D12 and T156 form a strong hydrogen bond across the substrate-binding interface that when broken allows the enzyme to undergo the quaternary shift. This quaternary shift most likely enhances the binding of PEP and diminishes binding of F6P. In addition, the quaternary shift appears to have little impact on the coupling of BsPFK.

# CHAPTER IV

# A SOLUTION NMR STUDY OF *BACILLUS STEAROTHERMOPHILUS* PHOSPHOFRUCTOKINASE

The phosphofructokinase (PFK) from the moderate thermophilic prokaryote *Bacillus stearothermophilus* (Bs) is a 136 kDa enzyme that catalyzes the first committed step of glycolysis in which the substrates fructose-6-phosphate (F6P) and MgATP are converted to fructose-1,6-bisphosphate (F1,6BP) and MgADP. Researchers have known for nearly thirty years that BsPFK is a homotetramer that is allosterically regulated by the K-type inhibitor phosphoenolpyruvate (PEP) and the K-type activator MgADP (*1, 2*). Also, both effectors bind to identical binding sites located along one dimer-dimer interface, termed the allosteric-binding interface, and the substrate, F6P, binds along the other dime-dimer interface, termed the substrate-binding interface. In 1990, the crystal structure of BsPFK bound to phosphoglycolate (PGA), a PEP analog, in all four effector sites was compared to the crystal structure of BsPFK bound to F6P and MgADP in all four active sites and MgADP in all four effector sites, which will be referred to as the "substrate-bound" BsPFK (*101*). This comparison revealed that the substrate-bound enzyme has undergone a 7° rotation about its substrate-binding interface, termed the quaternary shift. The quaternary shift is accompanied by secondary and tertiary changes that include the unwinding of the end of helix 6 and the switching of Arg 162 for Glu 161 in the F6P binding site.

Due to the apparent differences seen between the substrate-bound and the PGA-bound structures, the allosteric behavior of BsPFK was described using the concerted transition model proposed by Monod, Wyman, and Changeux (MWC) (*87, 101*). The MWC model predicts that allosteric enzymes such as BsPFK exist in equilibrium between two states, the tense or, T state, and the relaxed or, R state. The T state represents the inhibitor bound enzyme and the R state represents the substrate bound enzyme. There has been growing kinetic evidence that the MWC model does not adequately describe the allosteric behavior of prokaryotic PFK (*104, 134, 139*). For example, the role of the switching of E161 and R162 in the F6P binding site was addressed by Kimmel and Reinhart where they showed, contrary to what was previously predicted, that the switching of E161 and R162 in the active sites of the substrate bound and PGA bound structures of BsPFK did not adequately explain the allosteric inhibition of the enzyme by PEP (*104*). In addition, as discussed in Chapter III and contrary to what was predicted by the MWC model, the quaternary shift of BsPFK is thought to have a substantial role in ligand binding and a lesser role in the allosteric inhibition by PEP. These conclusions were drawn from experiments performed with the variant D12A BsPFK. This single mutation when compared to wild-type BsFPK caused a 100-fold decrease in the binding affinity for PEP, a 50-fold increase in the binding affinity for F6P, but did not alter the coupling constant. Also, the crystal structure of D12A BsPFK indicated that the enzyme had undergone the quaternary shift.

The actions of a K-type inhibitor such as PEP can be quantitatively described by a coupling free energy, $\Delta G_{ax}$ (*94, 95*). The $\Delta G_{ax}$ is expressed in terms of standard free energy by the following equation:

$$\Delta G_{ax} = -RT\ln Q_{ax} \quad (4\text{-}1)$$

where $Q_{ax}$ is the coupling constant for the following dissociation constant:

$$Q_{ax} = \frac{K_{ia}^{\circ}}{K_{ia}^{\infty}} = \frac{K_{ix}^{\circ}}{K_{ix}^{\infty}}. \quad (4\text{-}2)$$

$K_{ia}^{\circ}$ and $K_{ia}^{\infty}$ are the substrate dissociation constants in the absence and saturating presence of the effector, respectively, and $K_{ix}^{\circ}$ and $K_{ix}^{\infty}$ are the effector dissociation constants in the absence and saturating presence of the substrate, respectively. Therefore, $Q_{ax}$ describes the following disproportionation equilibrium:

$$XE + EA \overset{Q_{ax}}{\Longleftrightarrow} XEA + E \quad (4\text{-}3)$$

where E is the apo enzyme, XE is the effector bound enzyme, EA is the substrate bound enzyme, and XEA is the enzyme bound to both the effector and the substrate simultaneously, also called the tertiary complex.

The MWC model limits its interpretation of the allosteric behavior of the enzyme to the binary complexes on the left side of the disproportionation equilibrium shown above, and it doesn't acknowledge the tertiary complex or the apo enzyme. By contrast, when kinetic studies are analyzed as described above, all four enzyme forms contribute to the value of the coupling constant. Crystal structures of BsPFK representing the two binary complexes were solved in 1981 and 1990 prematurely leading to the proposal of the concerted model (*101, 121*). As discussed in Chapter III, the apo BsPFK crystal

structure was solved, providing a much needed basis for comparison of the changes introduced in the formation of each binary complex of BsPFK as well as the first structural information pertaining to the right side of the disproportionation equilibrium. Also, the apo crystal structure revealed that the unliganded enzyme resembles the substrate bound form of BsPFK in many respects. This result directly disagreed with the prediction made earlier by the MWC model (*120*, *121*). Obtaining structural information of the XEA form in which the enzyme is bound to both the inhibitor and the substrate simultaneously is the obvious next step in understanding the allosteric mechanism for BsPFK. However, crystallization of XEA have proven to be elusive. In addition, structural data derived from crystal structures offer a static snapshot of the enzyme that may be influenced by crystal contacts and the crystallization conditions. With this in mind, methyl TROSY NMR was employed in order to gain more structural information about BsPFK in all four states of ligation relevant to the allosteric coupling.

Development of novel labeling techniques has opened up the use of NMR to study high molecular weight proteins such as aspartate transcarbamoylase (*140*), protease ClpP (*141*), 20S proteosome (*142*), and malate synthase G (*143*). In the following chapter, hetero-nuclear single-quantum coherence (HMQC) experiments were conducted with deuterated wild-type and D12A BsPFKs which were specifically labeled with δ-$^{13}C^{1}H_3$-isoleucine. By doing this, only the isoleucines present in the enzymes were visualized in chemical shift correlation maps of $^{13}C$ and $^{1}H$. Interestingly, there are 30 isoleucines in one monomer of BsPFK, most of which are well resolved in the NMR spectra. The deuterated and [Ileδ1-$^{13}CH_3$] wild-type BsPFK was exposed to saturating

amounts of F6P and PEP, and for the first time solution NMR data are presented that depict all four enzyme forms of the disproportionation equilibrium including the elusive ternary complex. NMR spectra show several cross peaks with chemical shifts unique to each enzyme form; indicating that each enzyme form takes a different structure. The ternary complex quite interestingly does not resemble either binary complex, but has cross peaks with chemical shifts unique to the ternary complex. D12A BsPFK was labeled for NMR experiments because it is known from the crystal structures that the variant is in the quaternary shifted position and still undergoes substantial inhibition by PEP. Therefore, we were interested in identifying the peaks that might change when PEP and F6P are added, thus causing shifts in cross peaks. The chemical shift spectra for the labeled D12A BsPFK were not as well resolved as the wild-type spectra; however, the variant spectra do show promising results.

## Materials and Methods

### *Materials*

All chemical reagents used in buffers, protein purifications, and enzymatic assays were of analytical grade, purchased from Sigma-Aldrich (St. Louis, MO) or Fisher Scientific (Fair Lawn, NJ). Creatine kinase and the ammonium sulfate suspension of glycerol-3-phosphate dehydrogenase were purchased from Roche (Indianapolis, IN). The ammonium sulfate suspensions of aldolase and triosephosphate isomerase, and the sodium salts of phosphocreatine, ATP, and phosphoenolpyruvate were purchased from Sigma-Aldrich. The coupling enzymes in ammonium sulfate suspensions were

extensively dialyzed against 50 mM MOPS-KOH, pH 7.0, 100 mM KCl, 5 mM $MgCl_2$, and 0.1 mM EDTA before use. The sodium salt of F6P was purchased from Sigma-Aldrich or USB Corporation (Cleveland, OH). NADH and DTT were purchased from Research Products International (Mt. Prospect, IL) and the isotopically labeled materials were purchased from Cambridge Isotope laboratories, Inc (Andover, MA). Mimetic Blue 1 resin used for protein purification was purchased from Prometic Biosciences (Rockville, MD). Deionized distilled water was used throughout. Shigemi NMR tubes purchased from Shigemi, Inc. (Allison Park, PA) were used for all NMR experiments. Shigemi tubes are specialized NMR tubes that allow for the use of small protein volumes around ~300 µl.

*Protein Purification of [Ileδ1-$^{13}CH_3$] BsPFK*

The plasmid pBR322/BsPFK (*123*) contains the gene for BsPFK behind the native *Bacillus stearothermophilus* promoter and was received as a generous gift from Simon H. Chang (Louisiana State University). This plasmid was modified to place the BsPFK gene behind an inducible lac promoter in pALTER as described previously (*126*). Wild-type BsPFK was expressed in *E.coli* RL257 cells (*124*), which is a strain of *E.coli* lacking both the pfkA and pfkB genes. Protein expression of the deuterated and $^{13}C^{1}H_3$-isoleucine labeled BsPFK was performed as described previously by Tugarinov, V. et. al., with a few modification (*143*). Following transformation, cells were picked from a single bacterial colony that was grown on solid Lysogeny Broth (LB)/tet/$H_2O$ media (Tryptone 10 g/L, yeast extract 5 g/L, and Sodium Chloride 10 g/L, tetracycline

12.5 μg/ml). These cells were transferred to a 5-ml culture of LB/tet/$H_2O$ media and allowed to grow in a shaking incubator at 37°C until the cell density reaches an $OD_{600}$ of 0.7-0.8 (~ 4 hours). The 5-ml culture was spun down with a speed of 1,200g at room temperature and the pellet was very gently resuspended in 1 ml of M9/$H_2O$ media (0.048 M $Na_2HPO_4$ (dibasic), 0.022 M $KH_2PO_4$ (monobasic), 9 mM NaCl, 19 mM $NH_4Cl$, 0.2 % Glucose, 2 mM $MgSO_4$, 100 uM $CaCl_2$, 10 ug/ml Thiamine, 10 ug/ml $FeSO_4$, 12.5 ug/ml Tetracycline) which contained unlabeled glucose and $NH_4Cl$. Aliquots of the resuspension were added to 20 ml of the unlabeled M9/$H_2O$ media until the starting $OD_{600}$ was 0.1. The culture was grown until the $OD_{600}$ reached 0.6, which took between 8-10 hours. The culture was then centrifuged and resuspended in 100 ml of labeled M9/$D_2O$ media (containing [$^2H$,$^{13}C$] glucose and $^{15}NH_4Cl$) so that the beginning $OD_{600}$ was 0.1. These cells were grown until the $OD_{600}$ was between 0.4-0.5 (4-7 hours), then the cells were diluted to 200 ml by the addition of 100 ml labeled M9/$D_2O$ media and were grown until the $OD_{600}$ reached 0.4-0.5 (2-3 hours). At this time the culture was diluted with labeled M9/$D_2O$ media to a volume that equaled 1 L once the α-ketobutyrate was added and allowed to grow until the $OD_{600}$ was 0.25 (2-3 hours). At this time, 70 mg/L of [3-$^2H_2$] ,$^{13}C$ α-ketobutyrate was added to the culture. Following a previously established protocol, [3-$^1H$],$^{13}C$ α-ketobutyrate was deuterated by incubating the $^{13}C$ α-ketobutyrate at pH 10.5 in $D_2O$ for 12-14 hours prior to its addition (*144*). The pH meter was calibrated with $H_2O$ buffers. The culture was allowed to grow for approximately one hour until the $OD_{600}$ was between 0.3-0.4. Protein expression was induced with the addition of 1 mM IPTG and the cells were allowed to grow for no more

than 8 hours. Wild-type BsPFK and D12A BsPFK were expressed as indicated above, with the following exceptions: [$^2$H] glucose was the sole carbon source for cells expressing wild-type BsPFK and [$^2$H] glucose and [$^2$H] glycerol were the carbon sources for cells expressing D12A BsPFK.

Cells were centrifuged and frozen at -20°C for at least 12 hours and they were resuspended in purification buffer (10 mM Tris-HCl, 1 mM EDTA pH 8.0) and sonicated in a Fisher 550 Sonic Dismembrator at 0°C in 15 second pulses at setting 6 for 8 minutes. The crude lysate was centrifuged using a Beckman model J2-21 centrifuge at 22,500 x g with a JA-20 rotor for an hour at 4°C. The clear supernatant was heated at 70°C for 15 minutes, cooled on ice for 15 minutes, and centrifuged agian for one hour at 4°C. The wild-type BsPFK supernatant was diluted 4-fold and loaded onto a Mimetic Blue 1 column that was equilibrated with purification buffer. The column was washed with at least 5 bed volumes of purification buffer, and the enzyme was eluted with a 0 – 1 M NaCl gradient. The D12A BsPFK supernatant was diluted four-fold and loaded onto a DE52 column that was equilibrated with purification buffer. Enzyme containing fractions were pooled and dialyzed into 20 mM Tris-HCl pH 8.5 for wild-type BsPFK and 20 mM Tris-HCl pH 7.5 for D12A BsPFK and loaded onto a Pharmacia Mono-Q anion exchange column that had been equilibrated with the appropriate buffer. The enzymes were eluted with a 0 – 1 M NaCl gradient and PFK containing fractions were combined, concentrated, then dialyzed into EPPS Buffer (50 mM EPPS, 10 mM $MgCl_2$, 100 mM KCl, 0.1 mM EDTA pH 8.0). Concentrated enzyme was further dialyzed and stored in HEPES/$D_2O$ Buffer (10 mM deuterated HEPES pH 8.0 (uncorrected), 5 mM

$MgCl_2$, 10 mM KCl, and 0.1 mM EDTA) at 4°C. Apo D12A BsPFK was created following the same procedure as described in chapter 2 except HEPES/$D_2O$ buffer was used instead of EPPS buffer. The final enzyme was determined to be pure by SDS-PAGE and the concentration was ascertained using the absorbance at 280 nm ($\varepsilon$ = 18910 $M^{-1}cm^{-1}$(*126*)). Water was used in all buffers unless $D_2O$ is indicated. The final enzyme concentrations achieved for NMR experiments were between 0.4 – 0.5 mM in monomer. About 300 µl of protein was added to a Shigemi NMR tube. F6P and PEP solutions that were added to the NMR protein samples were diluted in $D_2O$ and were made as concentrated as possible in order to add the smallest possible volume.

*NMR Spectroscopy*

NMR experiments were performed on a Varian Inova 600 MHz spectrometer, using a conventional pulsed-field gradient triple resonance probe. Two-dimensional $^{1}H$-$^{13}C$ HMQC methyl correlation experiments were acquired on samples of $^{15}N$, $^{2}H$, [$\delta^{13}C^{1}H$] Ile only wild-type BsPFK (labeled wild-type BsPFK) and $^{15}N$, $^{2}H$, [$\delta^{13}C^{1}H$] Ile only D12A BsPFK (labeled D12A BsPFK) using the pulse schemes described previously (*145*). A relaxation delay of 2 seconds was used and the total evolution times in the $^{1}H$ and $^{13}C$ dimensions were 80 ms and 33 ms, respectively. The net acquisition time was 22 hours and the temperature was set to 25°C for all experiments. NMR data were processed and analyzed with nmrPipe(*146*) and analyzed using Sparky (*147*).

**Results**

Figure 4-1 depicts the apo wild-type BsPFK crystal structure with the thirty NMR labeled isoleucines per monomer highlighted. There is very good coverage of the enzyme with isoleucine. When the apo wild-type BsPFK crystal structure is compared to the wild-type substrate bound and PGA bound crystal structures, the regions of the enzyme that appear to change the most occur around the ligand binding sites and the residues directly around D12, which is discussed in Chapters II and III. Specific activity and ligand binding for the labeled wild-type and D12A enzymes were comparable to their unlabeled counterparts, as shown in Table 4-1. In addition, the activities of the labeled enzymes did not diminish over the course of the NMR experiments. It should be noted that an inducible plasmid was necessary to express the proteins in minimal media.

The spectra for both the wild-type and mutant enzymes indicate that the protein is folded. The wild-type BsPFK spectra have better dispersion than the D12A spectra; however, numerous cross-peaks are very well resolved. Figure 4-2 shows overlays of the chemical shift correlation maps of $^{13}C$ and $^{1}H$ of [Ileδ1-$^{13}CH_3$] wild-type BsPFK. The comparison is between apo BsPFK, F6P-bound BsPFK, and PEP-bound BsPFK. There are several distinct peaks in all three spectra; however, the most significant and dramatic differences are seen between the apo and the PEP-bound forms of the enzyme. This observation is supported by the solved crystal structures for wild-type BsPFK, where the largest structural difference seen is between the apo and PGA bound crystal structures. There are several isoleucines located in and around the regions that undergo change; therefore, sensing ligand binding as well as other structural changes should be

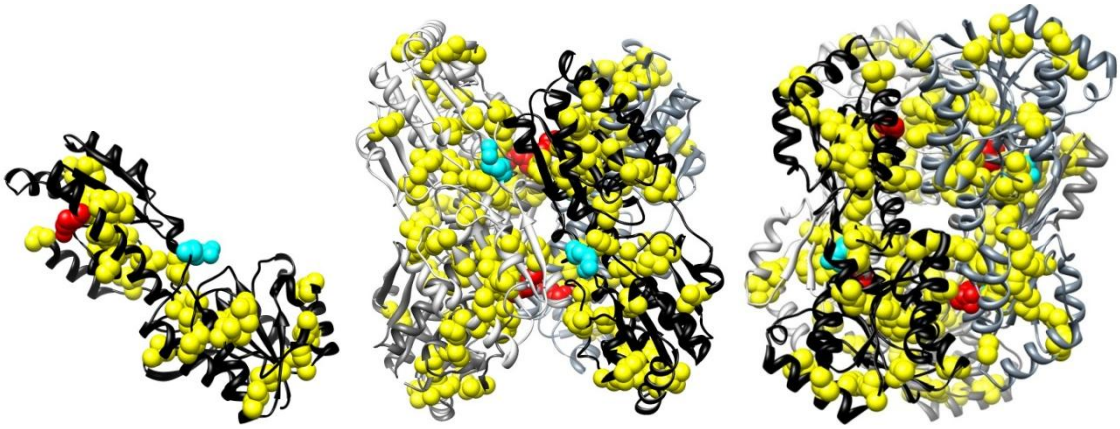

A. B. C.

Figure 4-1 Apo BsPFK with the isoleucines highlighted. There are 30 Ile per monomer, each colored yellow, F6P binding residue colored blue, effector binding residue colored red. A) View of individual monomer. B) View of tetramer along substrate binding interface with the four monomers colored black and gray. C) View of tetramer along effector binding interface with the four monomers colored black and gray.

Table 4-1 Cross-peak coordinates and signal/noise data for unique cross-peaks in NMR spectra.

| Label | Cross-peak $^{13}C$, $^{1}H$ (ppm) | Signal/Noise | | | | | | |
|---|---|---|---|---|---|---|---|---|
| | | Wt-Apo | Wt-F6P | Wt-PEP | Wt-F6P/PEP | D12A-Apo | D12A-F6P | D12A-PEP |
| A | 12.257, 0.666 | | | 63 | | | | 21 |
| B | 13.008, 0.508 | | | 64 | | | | 19 |
| C | 14.216, 1.079 | | | 51 | | | | 15 |
| D | 14.619, 0.987 | | | 57 | | | | 21 |
| E | 11.149, 0.501 | | 40 | | | | | |
| | 11.125, 0.414 | | | | 23 | | | |
| | 11.195, 0.441 | | | | | | 9 | |
| F | 11.149, 0.616 | | 21 | | | | | |
| | 11.132, 0.629 | | | | | | 7 | |
| G | 14.871, 1.007 | | | | | 17 | 11 | |
| | 14.999, 1.015 | 40 | 26 | | | | | |
| H | 14.193, 0.593 | | | | | 26 | 17 | |
| | 14.200, 0.619 | 113 | | | | | | |
| | 14.188, 0.568 | | 54 | | | | | |
| I | 14.300, 0.671 | | 45 | | | | | |
| | 14.500, 0.686 | | | 79 | | | | |
| | 14.400, 0.678 | | | | | | 14 | |
| | 14.449, 0.692 | | | | | | | 28 |
| J | 15.908, 0.702 | 43 | | | | | | |
| | 15.915, 0.732 | | 27 | | | | | |
| | 16.169, 0.721 | | | 33 | | | | |
| | 15.937, 0.696 | | | | 14 | | | |
| K | 10.922, 0.542 | 52 | | | | | | |
| L | 11.392, 0.647 | 31 | | | | | | |
| M | 11.253, 0.587 | | | | 11 | | | |
| N | 14.401, 1.022 | | | | 15 | | | |
| O | 12.678, 0.846 | 20 | 13 | 24 | | 76 | 55 | 140 |
| P | 14.326, 0.839 | | | | | 43 | 32 | |
| | 14.200, 0.835 | | | | | | | 129 |
| | 14.300, 0.862 | 126 | 70 | | | | | |
| | 14.400, 0.881 | | | 16 | | | | |
| Q | 15.000, 0.920 | | | | | 11 | | |
| | 15.100, 0.920 | | | | | | | 11 |
| R | 13.711, 0.932 | | | | | 23 | 36 | 267 |
| S | 10.978, 0.770 | | | | | 13 | 10 | 11 |
| T | 11.325, 0.071 | | | | | 12 | 8 | 13 |
| U | 14.449, 0.747 | | | | | | 33 | 25 |
| V | 11.870, 0.767 | | | | | | 7 | 16 |
| W | 0.844, 1.248 | | | | | | | 13 |

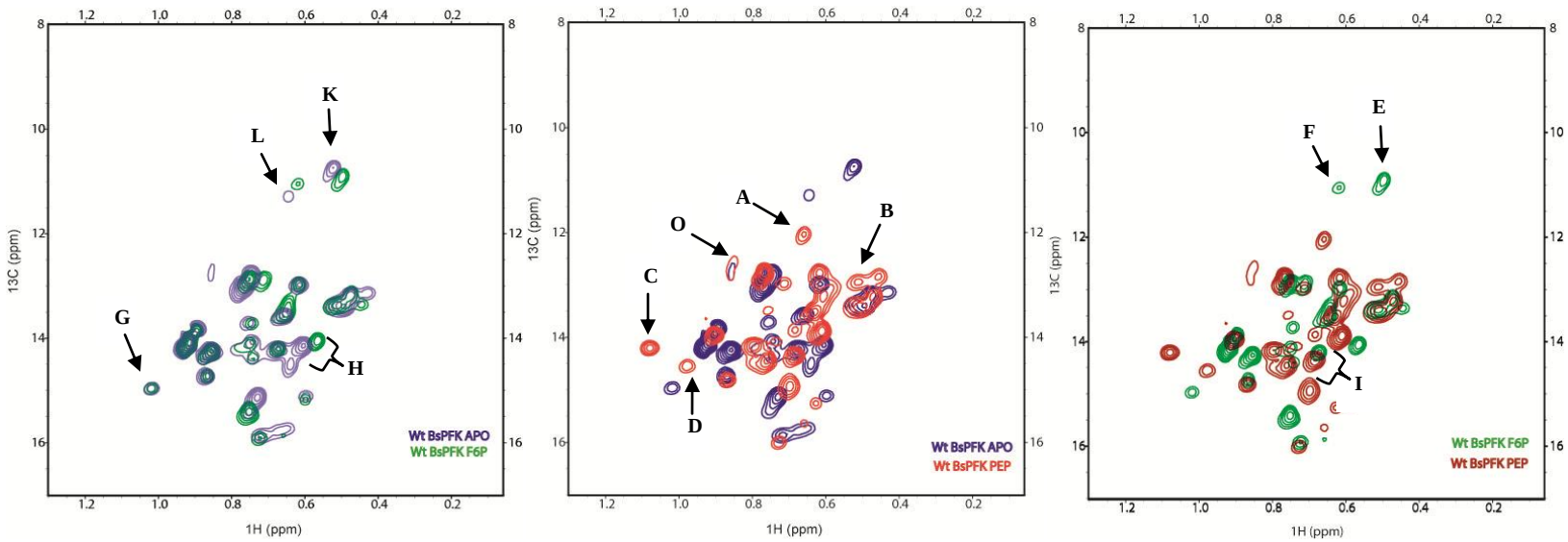


A. B. C.

Figure 4-2 $^{13}C$-$^{1}H$ HMQC spectra of deuterated, Ile-[$\delta^{13}CH_3$]-labeled wild-type BsPFK. A) Overlay of wild-type apo and F6P-bound. B) Overlay of wild-type apo and PEP-bound. C) Overlay of wild-type F6P-bound and PEP-bound. Apo is in blue, F6P-bound is in green, and PEP-bound is in red. Cross-peaks are labeled according to Table 4-1.

detectable. The ternary complex of wild-type BsPFK shown in Figure 4-3 compared to apo, F6P-bound, and PEP-bound BsPFK spectra has several cross-peaks that are different from the other enzymes.

Figure 4-4 shows overlays of the chemical shift correlation maps of the variant $^{13}C$ and $^{1}H$ [Ileδ1-$^{13}CH_3$] D12A BsPFK, where the apo, F6P-bound, and PEP-bound D12A BsPFKs are compared. Only a few peaks in the D12A BsPFK spectra are resolved enough to distinguish any change when ligands bind. Figure 4-5 shows a comparison of the chemical shift correlation maps of the liganded wild-type enzyme with the liganded D12A enzyme. Even with the poor resolution, there are numerous peaks that can be concluded to be a result of a particular ligand binding. There are also some peaks that are entirely characteristic of either D12A or wild-type BsPFK.

In order to determine if particular cross-peaks were noteworthy in each spectrum, all of the spectra were analyzed using Sparky. Sparky gives precise coordinates, signal to noise ratios, and intensity values for each cross-peak. Through comparing each resolvable cross-peak to its counterpart in every NMR sample spectrum, some predictions can be made. Table 4-1 summarizes the coordinates of each interesting cross-peak with its signal to noise ratio and which spectrum it occurs in. In addition, if there is not a signal to noise ratio for a particular spectrum, then there was no apparent signal for the cross peak in that spectrum. For example, cross-peaks labeled a, b, c, and D are found only in the wild-type-PEP and D12A-PEP bound spectra; therefore, these cross-peaks are good indicators for PEP binding.

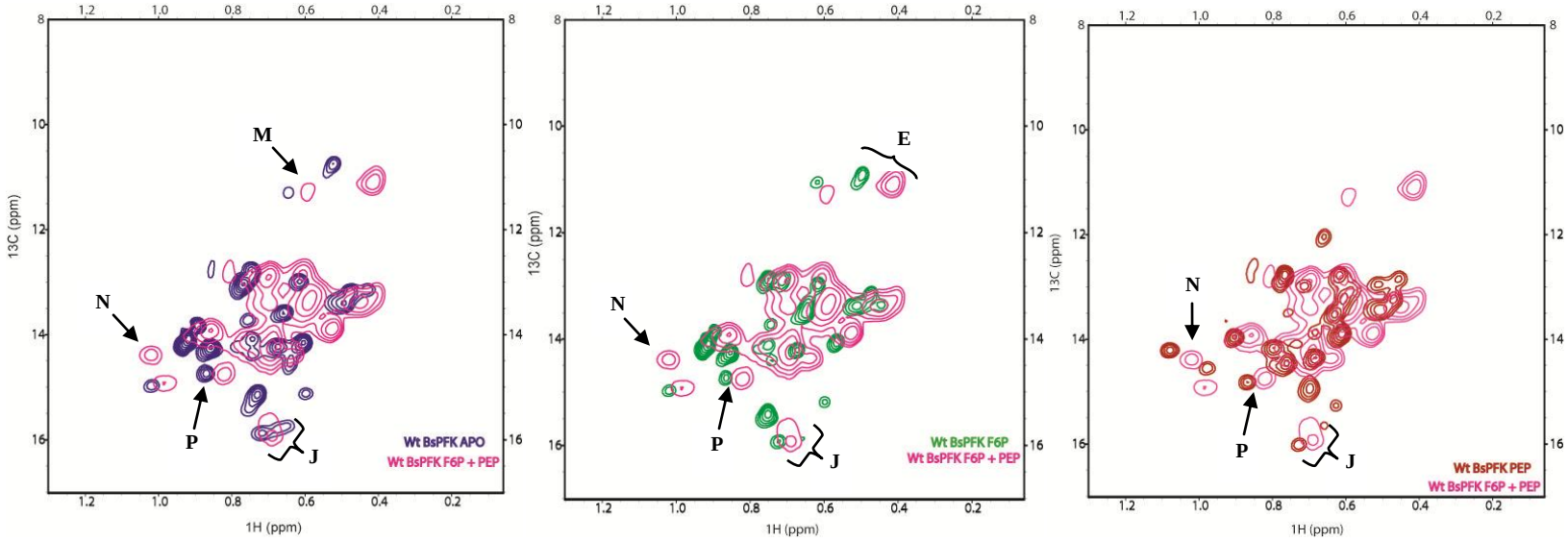


A. B. C.

Figure 4-3 $^{13}C$-$^{1}H$ HMQC spectra of deuterated, Ile-[$\delta^{13}CH_3$]-labeled wild-type BsPFK compared with wild-type BsPFK ternary complex. A) Apo and ternary complex. B) F6P-bound and ternary complex. C) PEP-bound and ternary complex. Ternary complex is pink, apo is blue, F6P-bound is blue, and PEP-bound is red. Cross-peaks are labeled according to Table 4-1.

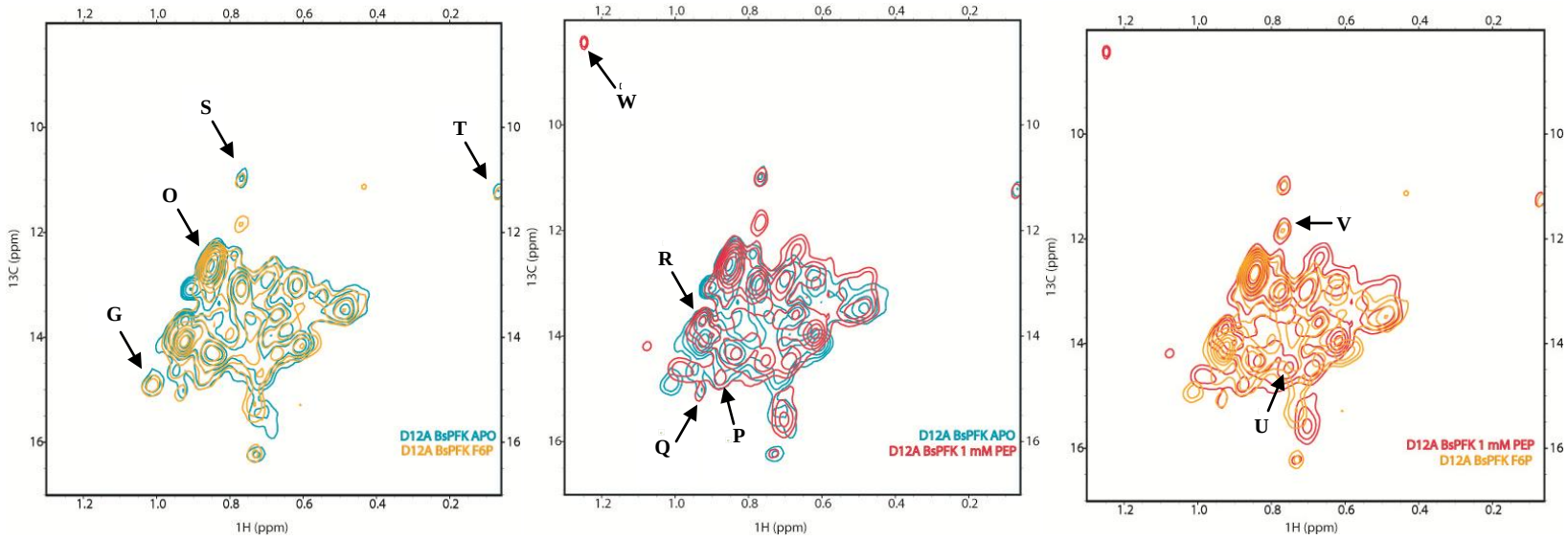


A. B. C.

Figure 4-4 $^{13}C$-$^{1}H$ HMQC spectra of deuterated, Ile-[$\delta^{13}CH_3$]-labeled D12A BsPFK. A) Apo and F6P-bound. B) Apo and PEP-bound. C) F6P-bound and PEP-bound. Apo is in light blue, F6P bound is in gold, and PEP bound is in dark pink. Cross-peaks are labeled according to Table 4-1.

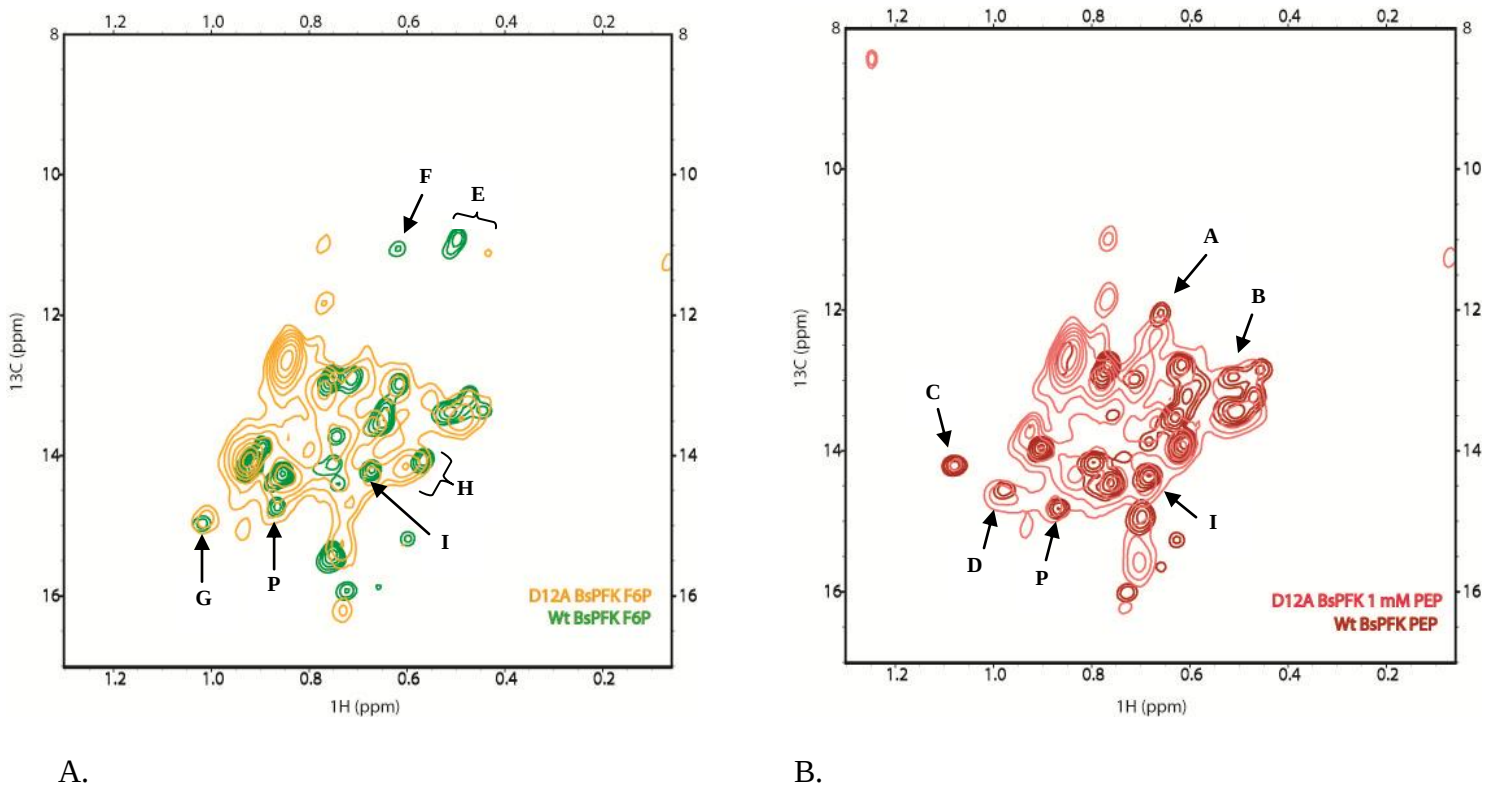


A. B.

Figure 4-5 $^{13}C$-$^{1}H$ HMQC spectra of deuterated, Ile-[$\delta^{13}CH_3$]-labeled wild-type and D12A BsPFK. A) F6P-bound wild-type (green) and F6P-bound D12A (gold). B) PEP bound wild-type (red) and PEP bound D12A (dark pink). Cross-peaks are labeled according to Table 4-1.

Cross-peaks labeled E, F, G, and H may be indicative of F6P binding. Cross-peak E is in wild-type-F6P bound, wild-type-F6P/PEP bound, and D12A-F6P bound spectra at slightly different coordinates; however, there are no definite peaks near these coordinates in the other spectra. This peak appears to be a result of F6P binding; and is the only F6P binding cross-peak that appears in the ternary complex. Cross-peak F does not have a similar peak in the ternary complex spectrum; however, it only occurs in the F6P bound samples. Interestingly, peaks G and H are present in both apo and F6P-bound enzymes and each peak appears to decrease in signal when F6P is added. Also, the cross-peaks for F, G, and H do not exist in the ternary complex. Cross-peak I is also not present in the ternary complex, but it is present in all of the singly liganded spectra for both wild-type and D12A enzymes. In addition, the signal to noise ratio is higher for the PEP bound spectra than the F6P spectra.

Cross-peak J appears only in wild-type spectra while peaks R, S, and T appear only in D12A spectra. The signal to noise ratio for peak R is one of the more prominent peaks in the D12A spectra. Less prominent, but still significant is cross-peak S, which is somewhat near peaks in the wild-type apo and wild-type-F6P-bound spectra; however, peak T is solely indicative of D12A BsPFK since it is not near any other peak in any other spectrum. Also, peak Q is found only in D12A apo and PEP-bound spectra with the same signal to noise ratio in each spectrum. Cross-peak Q has slightly different coordinates in the two spectra, which may be indicative of slight changes that occur within the enzyme as a result of further changes in the structure upon PEP binding. Cross-peaks U and V are present in the ligand bound spectra of D12A BsPFK; therefore,

these peaks may be indicative of ligand binding for D12A BsPFK. Cross-peak W is present only in the PEP bound D12A BsPFK spectra and its chemical shift is far removed from the other peaks. Cross-peak W may be an important indicator of PEP binding in D12A BsPFK. Cross-peaks K and L are found only in the wild-type apo spectrum; so they must represent wild-type apo BsPFK. Cross-peaks M and N are only in the ternary complex spectrum. Interestingly, peak N is located between cross-peaks C and D from the wild-type PEP bound spectrum. Cross-peaks O and P are found in every BsPFK spectra except for the ternary complex; so the absence of these peaks are a good indicator of the ternary complex.

**Discussion**

The development of transverse relaxation-optimized spectroscopy (TROSY) experiments (*148*) coupled with selective isotope labeling of proteins (*149*) has allowed for the study of increasingly larger macromolecules with NMR spectroscopy. Traditionally, using heteronuclear multiple quantum coherence (HMQC) to obtain the chemical shifts of hetero-nuclei that are J-coupled in a large protein would give correlation maps that are indecipherable. TROSY is a method that can be attached to any experiment and selects only the sharpest doublet component of the signal. This causes half of the signal to be lost; however, it also accounts for a large gain in signal to noise ratio which is needed when studying large proteins via NMR. Applying TROSY-HMQC experiments to proteins that have been selectively labeled with isotopes accounts for the growing amount of NMR experimental evidence of large proteins. The labeling

strategy used for BsPFK involved incorporating isoleucines which were selectively protonated at the δ-1 methyl group. This is simply done by adding α-ketobutyrate, a precursor to isoleucine, to the cell culture. Figure 4-6 shows how [3-$^{1}$H],$^{13}$C α-ketobutyrate, [$^{12}$C, $^{2}$H] glucose, and $^{15}NH_4Cl$ are incorporated into isoleucine, and as a result all of the isoleucine residues in the enzyme contain one NMR active methyl group. By labeling only the isoleucine residues, very nice coverage of the enzyme was obtained along with resolved cross-correlation spectra.

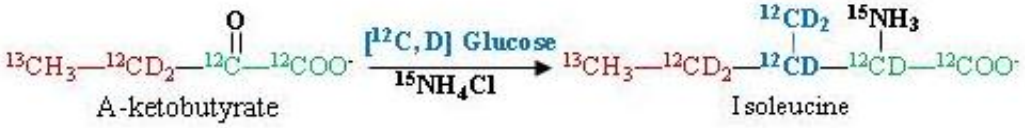


Figure 4-6: Structure of the α-ketobutyrate precursor added to the minimal media, and how each component of the media is incorporated into the end product isoleucine.

One of the hardest obstacles to overcome when performing any kind of protein NMR experiment is to produce large amounts of clean labeled protein. It was found that an inducible promoter for BsPFK is required when growing the cells in M9 minimal media. The *Escherichia coli* (*E. coli*) cells used for the expression of BsPFK did not contain any native PFK; therefore, the only PFK being produced in the cell would be from the plasmid. And since the carbon source given to the cells was glucose, one would expect the use of PFK to be necessary. However, PFK was not obtained in any

noticeable amounts when the non-inducible native *Bacillus stearothermophilus* promoter was used. It could be that a sufficient amount of PFK was produced to allow carbohydrate metabolism to go forward in the cells but not enough to allow for detection. Nevertheless, sufficient quantities of BsPFK were obtained when the inducible promoter was used.

As discussed in Chapter III, D12A BsPFK, when compared to wild-type, has a 50-fold diminished F6P binding in the absence of PEP. However, D12A BsPFK has been shown to bind indigenous PEP from the *E. coli* cell and remain bound to the inhibitor through extensive dialysis and affinity column purifications. When growing the labeled NMR D12A BsPFK sample, it became apparent that there was at least a 30% reduction in cells when compared to the wild-type BsPFK cells. The variants enhanced PEP binding coupled with diminished F6P binding led the possibility that the cells were not able to produce wild-type amounts of PFK due to insufficient quantities of a carbon source. Therefore, in addition to [$^2$H] glucose, [$^2$H] glycerol was added to the media for D12A BsPFK. Once this was accomplished, the production of D12A BsPFK cells matched that of wild-type BsPFK cells.

D12A BsPFK spectra show poorer dispersion than wild-type BsPFK spectra. This may be due to D12A BsPFK having more flexibility or conformational variability in solution than wild-type BsPFK. The substitution of Asp12 in D12A BsPFK removes numerous inter- and intra-subunit interactions; all of which may cause the structure of D12A BsPFK to be more variable. Addition of ligands helped to tighten up some of the peaks for D12A BsPFK; however, a larger field instrument is most likely needed to

better resolve the cross-peaks for D12A BsPFK. The resolved cross-peaks of wild-type and D12A BsPFK in conjunction with their crystal structures can be used as probes to follow the conformation of the enzyme in different liganded states. Once the peaks for D12A BsPFK are better resolved and the peaks are assigned, it may be possible to detect precisely which parts of the protein move when PEP and/or F6P bind the enzyme. Since apo D12A BsPFK is already in the quaternary shifted position, it may be possible to pinpoint which areas of the enzyme are involved in the allosteric communication between PEP and F6P.

Just as the crystal structures predict, apo wild-type BsPFK NMR spectra are similar to that of F6P-bound wild-type BsPFK spectra, whereas PEP-bound BsPFK spectra shows a great number of differences when compared with both apo and F6P-bound BsPFK. There are enough differences seen between all of the spectra to conclude that each enzyme has its own unique structural characteristics. The ternary complex shows several peaks that are distinct and unique to the ternary complex alone, as well as some peaks that are present in every spectrum except the ternary complex spectrum. Even with the assignment of the peaks being unknown at this point, it is still safe to conclude that the ternary complex is indeed unique and different from the other three forms of BsPFK. This is the first structural evidence that supports a F6P-PEP-bound BsPFK species and it shows that the ternary complex is not identical to either the presumed R or T-state structures.

# CHAPTER V

# SUMMARY

The two-state model used to describe the allosteric nature of BsPFK was based on a comparison between the substrate bound and PGA bound crystal structures of the enzyme, which revealed a conformational change in the PGA bound structure (*101*). This conformational change includes a 7° rotation about the substrate-binding interface, termed the quaternary shift. Additionally, in the substrate-bound form of the enzyme, the positively charged R group of R162 interacts with the negatively charged phosphate group of F6P, and in the PGA-bound structure, R162 is replaced by the negatively charged R group of E161. The two-state model proposed that these conformational changes were the structural basis for the allosteric regulation of BsPFK. However, a previous study performed in the Reinhart Lab proved that the switching of E161 and R162 in the active site of the substrate bound and PGA bound structures of BsPFK did not adequately explain the allosteric inhibition of the enzyme by PEP (*104*). With the limited role of E161 and R162 in the allosteric coupling revealed, the role of the quaternary shift was still a question. Therefore, the current study focused on the role of the quaternary shift in the allosteric regulation of BsPFK which was addressed through the use of X-ray crystallography, NMR spectroscopy, and enzyme kinetics.

First, the crystal structure for the apo enzyme was determined to 2.8 Å resolution. Contrary to expectations based on the two-state model, we showed that apo BsPFK had not undergone the quaternary shift characteristic of the PGA bound

structure. In addition, the apo BsPFK structure provided a true blank slate in which to compare all liganded and mutated forms of the enzyme. A few key residues located in the substrate binding and effector binding sites of the apo enzyme were shown to form unique and different orientations when compared to the liganded forms of BsPFK. Now the basis for any structural conclusions concerning BsPFK can be made using a reference state enzyme form. The importance of the apo BsPFK crystal structure was further emphasized through discussing the coupling free energy of the allosteric mechanism. The free energies of formation for the species for the left hand side of the disproportionation equilibrium (Equation 2-3) must equal the free energies of formation for the right hand side of the equilibrium. The two binary forms of BsPFK on the left hand side of the equilibrium are represented by the liganded crystal structures of Evans, et. al. (*101*) And now for the first time the apo BsPFK structure represents a form on the right hand side of the equilibrium. It is very important to note that the crystal structure of the ternary complex is still unknown; however, the apo BsPFK crystal structure fills an important hole in the structural library of allosterically relevant crystal structures.

Next, the role of the quaternary structure was investigated using the variants D12A BsPFK and T156A BsPFK. D12 and T156 are noteworthy residues in BsPFK because they are located along the substrate binding interface, and they are both 100% conserved among 150 prokaryotic ATP-dependent PFKs compared. Furthermore, D12 has the potential of interacting with T156, T158, S159, and H160 across the substrate binding interface. When D12 and T156 are mutated to an alanine, both their kinetics and structure undergo very interesting changes. D12A BsPFK, when compared to wild-type

BsPFK, has a 50-fold diminished F6P binding and a 100-fold enhancement in PEP binding. T156A BsPFK, when compared to wild-type BsPFK, shows a 30-fold increase in PEP binding affinity and a 17-fold decrease in F6P binding affinity. In addition, D12A BsPFK and T156A BsPFK both exhibit a coupling constant that is nearly identical to wild-type. Both the apo and PEP bound crystal structures of D12A BsPFK and the PEP bound crystal structure of T156A BsPFK show that the enzymes have undergone the quaternary shift and the end of helix 6 has become a loop. Therefore, D12A BsPFK is in the "inhibited" form before PEP every binds to the enzyme, which may explain the tighter binding for PEP; however, it does not account for the wild-type coupling constant.

The fact that the quaternary shift has occurred in D12A BsPFK and still exhibits PEP inhibition means that the quaternary shift is not central to the coupling of BsPFK. In addition, T156A BsPFK possesses very similar kinetic and structural characteristics to D12A BsPFK. To determine if the breaking of the interaction between D12 and T156 is causing the unique characteristics of the variants, additional single mutations were made near T156 and D12. Specifically, D12 potentially interacts with T158 across the substrate-binding interface when BsPFK is bound to PGA and D12 may interact with S159 and H160, in addition to T156, when BsPFK is bound to substrate. Therefore, T158, S159, and H160 were each mutated to an alanine, respectively, and characterized. T158A BsPFK was the only variant that showed a slight enhancement in F6P binding, a very small decrease in PEP binding, and a diminished coupling when compared to wild-type. The variant S159A BsPFK, when compared to wild-type, did not substantially

alter the F6P binding, but did enhance both the PEP binding and the coupling. H160A BsPFK diminished the binding for F6P two-fold while enhancing the PEP binding 15-fold, when compared to wild type. However, the coupling constant for H160A BsPFK demonstrated a very large enhancement when compared to wild-type. The variants T158A BsPFK, S159A BsPFK, and H160A BsPFK did not reveal similar kinetic and coupling trends to D12A BsPFK and T156A BsPFK; therefore, these residues must not be a major contributor to the strength of the hydrogen bond between D12 and T156. It is concluded that D12 and T156 must form an important hydrogen bond across the substrate interface that when broken allows the enzyme to undergo the quaternary shift. Thereby, both of the variants that induce the quaternary shift still undergo PEP inhibition and substantially alter the binding affinities for the substrate and inhibitor. In conclusion, the role of the quaternary shift appears to be involved in ligand binding, but not in the coupling.

In order to glean additional structural information about wild-type and D12A BsPFK, methyl TROSY NMR was employed. Deuterated and [Ileδ1-$^{13}CH_3$] labeled wild-type and D12A BsPFK were prepared so that only the delta methyl group on all of the thirty Ile would be detectable by NMR. HSQC experiments of the labeled enzymes were performed with the enzymes exposed to saturating amounts of PEP and F6P. Comparison of the wild-type spectra revealed that there are numerous chemical shifts that are unique to each form of the enzyme. The PEP-bound spectrum, when compared to the apo spectrum, shows a significant change in chemical shifts. The F6P-bound spectrum is not identical to the apo spectrum, but is much more similar to the apo

spectrum than the PEP-bound spectrum. Interestingly, the spectrum showing the enzyme bound to both F6P and PEP simultaneously has several chemical shifts that are different from the other wild-type spectra. These are the first NMR solution structural data of the ternary complex in BsPFK.

The D12A BsPFK methyl TROSY NMR experiments were not as successful as the wild-type experiments. However, even though the chemical shifts were not as well resolved as wild-type, there were numerous chemical shifts in the D12A BsPFK spectra that indicated ligand binding. Additional experiments with a higher field spectrometer will give better resolution hopefully providing structural information about which parts of the enzyme are involved in the PEP inhibition of D12A BsPFK. Also, a higher field instrument will allow for assignment of the Ile residues to be determined. The chemical shift assignments will need to be completed in order to identify which parts of the enzyme are moving and to compare to the existing crystal structure.

In conclusion, the two-state model proposed by Evans, et. al.(*101*) oversimplifies the allosteric mechanism of BsPFK, which is evident from the previous work done by Ortigosa, et. al., Kimmel, et. al., and Tlapak-Simmons, et. al.(*104, 106, 134, 150*) as well as the work discussed in the current dissertation. The structural data presented in Chapters II, III, and IV illustrate the verity that BsPFK is capable of more than just two structures. In fact, Chapter II proved through the description of the apo structure of BsPFK that the enzyme without any ligands bound is different from the two previously solved liganded crystal structures of BsPFK. The apo BsPFK crystal structure may be more like the substrate-bound enzyme, but it must be realized that the structures are not

exactly the same. This is also true for the variant BsPFK crystal structures presented in Chapter III, which are more like the PGA-bound structure of BsPFK, but are not exactly the same. In fact, in comparing the quaternary shift of all of the crystal structures, none of the newly presented crystal structures have identical quaternary structures to the substrate-bound or the PGA-bound enzymes. The wild-type apo and the variant BsPFKs all exhibit quaternary structures that vary by at least one degree from the liganded wild-type BsPFK quaternary structures. The structural data support the kinetic data presented in Chapter III, emphasizing the fact that the mechanism for the allosteric inhibition of BsPFK cannot be easily explained with the crystal structures we currently have determined. The work presented here provides strong evidence that the quaternary structure is not central to the allosteric communication between PEP and F6P in BsPFK. Through introducing four new crystal structures and the first ever solution NMR data of BsPFK we have effectively shown that the structure of BsPFK cannot be delegated to just two simple structures. There are in fact now six unique crystal structures of BsPFK; therefore, the two-state model is extremely oversimplified. The structural, kinetic, and coupling data presented in this dissertation demonstrate that the allosteric inhibition of BsPFK is much more complicated than previously predicted. Furthermore, the mechanism for PEP inhibition will not be fully understood until we understand the energetic and structural characteristics of the ternary complex.

# REFERENCES


1. Descartes, R. (1998) Discourse on the Method for Conducting One's Reason Well and for Seeking Truth in the Sciences (D. A. Cress, Trans.) pp 1-33, Hackett Publishing Company, Indianapolis. (1637)
2. Karssen, Z. (2005) Scientific Publishing: A European Strength, E-Content (Bruck, P. A., Buchhol Z. A., Karssen, Z., Zerfass, A., Eds.) pp 97-108, Springer, Berlin.
3. Beccari, I. B. (1745) De frumento. *De Bononiensi Scientiarium de Artium Instituto alque Academia Commentarii 2*, 122-127.
4. Beach, E. F. (1961) Beccari of Bologna: The discoverer of vegetable protein. *Journal of the History of Medicine and Allied Sciences 16*, 354-373.
5. Rouelle, H. M. (1773) Observations sur les fecules ou parties vertes des plantes et sur la matiere [sic] glutineuse ou vegeto animale. *Journal de Medicine, Chirurgie, Pharmacie 40*, 59-67.
6. Teich, M., and Needham, D. M., Eds. (1992) A Documentary History of Biochemistry 1770-1940, pp 1-80, Associated University Press, Leicester, UK.
7. Fourcroy, A. F. (1799) D'un memoire du cit. Fabroni, sur les fermentations vineuse, putride, aceteuse, et sur l'etherification. *Annales de Chimie [et de Physicque] 31*, 299.
8. Hartley, H. (1950) Origin of the word 'protein'. *Nature 168*, 368-376.

9. Mulder, G. J. (1839) Ueber die zusammensetzung einiger thierischen substanzen. *Journal fur Praktische Chemie 16,* 129-151.

10. Berzelius, J. J. Letters (1916) Correspondence entre Berzelius et G. J. Mulder, Almqvist and Wiksells, Uppsala, Sweden.

11. Mulder, G. J. (1838) Over proteine en hare ver bindingen en ontledingsproducten. *Natuur- en Scheikundig Archief 6,* 87-162.

12. Planche, L. A. (1810) Note sur la sophistication de la resine de jalap et les moyens de la connaitre. *Bulletin de Pharmacie 2,* 578-580.

13. Planche, L. A. (1820) Experiences sur les substances qui developpent la couleur bleue dans la resine de gaiac. *Journal de Pharmacie et des Sciences Accessoires 6,* 16-25.

14. Payen, A. and Persoz, J.F. (1833) Mémoire sur la diastase, les principaux produits de ses réactions, et leurs applications aux arts industriels. *Annales des Chimie et des Physique 53,* 73-92.

15. Schwann, T. (1836) Ueber das wesen des verdauugsprocesses. *Annalen der Pharmazie 20,* 28-33.

16. Berzelius, J. J. (1836) Einige ideen uber eine bei der bildung organischer verbindungen in der lebenden natur wirksame, aber bisher nicht bemarkte kraft. *Jahres-Ber. 15,* 237-245.

17. Thenard, L. J. (1803) Sur la fermentation vinuese. *Annales de Chimie [et de Physicque] 46,* 294-320.

18. Cagniard-Latour, C. (1838) Memoire sur la fermentation vineuse. *Annalen der Pharmazie 68*, 206-222.

19. Schwann, T. (1837) Vorlaufige mittheilung, betreffend versuche uber die weingarung und faulniss. *Poggendorffs Annalen der Physik und Chemie 11*, 184-192.

20. Barnett, J. A. (2003) Beginnings of microbiology and biochemistry: The contribution of yeast research. *Microbiology 149*, 557-567.

21. Kützing, F. T. (1837) Microscopische untersuchungen uber die hefe und essigmutter, nebst mehreren andern dazu gehorigen vegabilischen gebilden. *Journal fur Praktische Chemie 2*, 385-409.

22. Anonymous. (1839) Das entrathselte geheimniss der geistigen gahrung. *Annalen der Pharmazie 29*, 100-104.

23. Liebig, J. V. (1839) Ueber die erscheinungen der gahrung, faulniss und verwesung und ihre ursachen. *Annalen der Pharmazie 30*, 250-286.

24. Berzelius, J. (1836) Considerations respecting a new power which acts in the formation of organic bodies. *Edinburgh New Philosophical Journal 21*, 223-228.

25. Berzelius, J. (1839) Weingahrung. *Jahres-Bericht uber die Fortschritte der Physischen Wissenschaften von Jocabo Berzelius 18*, 400-403.

26. Traube, M. (1858) Zur theorie der gahrungs- und verwesungsercheinungen, wie der fermentwirkungen uberhaupt. *Poggendorffs Annalen der Physik und Chemie 103*, 331-333.

27. Pasteur, L. (1861) Experiences et vues nouvelles sur la nature des fermentations. *Comptes Rendus des Seances de l'Acadamie des Sciences 52*, 1260-1264.

28. Pasteur, L. (1860) Memoire sur la fermentation alcoolique. *Annales de Chimie [et de Physicque] 58*, 323-426.

29. Berthelot, M. P. E. (1860) Sur la fermentation glucosique du sucre de canne. *Comptes Rendus des Seances de l'Acadamie des Sciences 50*, 980-984.

30. Pasteur, L. (1860) Note sur la fermentation alcoolique. *Comptes Rendus des Seances de l'Acadamie des Sciences 50*, 1083-1194.

31. Kuhne, W. (1876) Ueber das verhalten verschiedener organisirter und sog. ungeformter fermente. *Verhandlungen des Heidelberger Naturhistorisches - Medizinischen Vereinigung 1*, 194-199.

32. Friedmann, H. C. (1997) New Beer in an Old Bottle: Eduard Buchner and the Growth of Biochemical Knowledge (Cornish-Bowden, A., Ed.) pp 17-225, Universitat de Valencia, Valencia.

33. Buchner, E. (1897) Alkoholische gahrung ohne hefezellen. Vorlaufige Mittheilung. *Berichte der Deutschen Chemischen Gesellschaft 30*, 117-124.

34. Bertrand, G. (1895) Sur la laccase et sur le pouvoir oxydant de cette diastase. *Comptes Rendus des Seances de l'Acadamie des Sciences 120*, 266-269.

35. Robert, E. and Kohler, J. (1973) The Enzyme Theory and the Origin of Biochemistry. *Isis 64*, 181-196.

36. Bertrand, G. (1897) Sur l'intervention du manganese dans les oxydation provoquees par la laccase. *Comptes Rendus des Seances de l'Acadamie des Sciences 124*, 1032-1035.

37. Young, A. H. and Young, W. J. (1906) The alcoholic ferment of yeast juice. *Proceedings of the Royal Society of London 77*, 405-420.

38. Young, A. H. and. Young, W. J. (1906) The alcoholic ferment of yeast-juice. Part II. The coferment of yeast juice. *Proceedings of the Royal Society of London 78*, 369-375.

39. Ostwald, W. F. (1894) Ueber die katalyse. *Zeitschrift fur Physikalische Chemie 15*, 705-706.

40. Hill, A. C. (1898) Reversible zymohydrolysis. *Journal of the Chemical Society, Transactions 73*, 634-658.

41. O'Sullivan, C. and Tompson, F. W. (1890) Invertase: A contribution to the history of an enzyme or unorganized ferment. *Journal of the Chemical Society, Transactions 57*, 834-931.

42. Thierfelder, H. and Fischer, E. (1894) Verhalten der verschiedenen zucker gegen reine hefen. *Berichte der Deutschen Chemischen Gesellschaft 27*, 2031-2037.

43. Fischer, E. (1894) Einfluss der configuration auf die wirkung der enzyme. *Chemische Berichte 27*, 3479.

44. Armstrong, E. F. (1904) Studies on enzyme action. II.--The rate of the change, conditioned bysucroclastic enzymes, and its bearing on the law of mass action. *Proceedings of the Royal Society of London 73*, 500-516.

45. Armstrong, E. F. (1904) Studies on enzyme action. III.--The influence of the products of change on the rate of change conditioned by sucroclastic enzymes. *Proceedings of the Royal Society of London 73*, 516-526.

46. Brown, A. J. (1902) Enzyme action. *Journal of the Chemical Society, Transactions 81*, 373-388.

47. Henri, V. (1902) Théorie générale de l'action de quelques diastases. *Comptes Rendus des Seances de l'Acadamie des Sciences 135*, 916-919.

48. Duclaux, E. (1898) Lois generales de l'action des diastases. *Annales de l'Institut Pasteur 12*, 96-127.

49. Cornish-Bowden, A. (1999) The origins of enzymology. *The Biochemist 19*, 36-38.

50. Sorensen, S. P. L. (1909) Enzymstudien. II. Uber die messung und die bedeutung der wasserstoffionenkonzentration bei enzymatischen prozessen. *Biochemische Zeitschrift 21*, 131-304.

51. Menten, L. M. a. M. (1913) Die kinetik der invertinwirkung. *Biochemische Zeitschrift 49*, 333-369.

52. Slyke, D. D. V., and Cullen, G. E. (1914) The mode of action of urease and of enzymes in general. *J. Biol. Chem. 19*, 141-180.

53. Briggs, G. E., and Haldane, J. B. (1925) A note on the kinetics of enzyme action. *Biochem. J. 19*, 338-339.

54. Hill, A. V. (1910) The possible effects of the aggregation of the molecules of haemoglobin on its dissociation curves. *Proceedings of Physiological Society 40*, iv-viii.

55. Goutelle, S., Maurin, M., Rougier, F., Barbaut, X., Bourguignon, L., Ducher, M., and Maire, P. (2008) The Hill equation: a review of its capabilities in pharmacological modelling, *Fundam. Clin. Pharmacol. 22*, 633-648.

56. Houston, C. S., Ed. (2005) Going Higher: Oxygen, Man, and Mountains. pp 5-324, Mountaineers Books, Seatle, WA.

57. Berzelius, J. J. (1806-1808) Forelesninger over Djurkemien. Vol. 1-2, Marquard, Stockholm.

58. Hoppe-Seyler, F. (1862) Uber das verhalten des blutgarbstoffes im spektrum des sonnenlichtes. *Archiv fur Pathologische Anatomie und Physiologie und fur Klinische 23*, 446.

59. Bert, P., Ed. (1878) La Pression Barometrique: Recherches de Physiolgie Ezperimentale, p 23, Masson, Paris.

60. Bohr, C. (1903) Theoretische behandlung der quantitativen verhaltnis bei der sauerstoffaufnahme des hamoglobin. *Zentralblatt fur Physiologie 17*, 682-689.

61. Christian Bohr, K. Hasselbalch, and Krogh, A. (1904) Ueber einen in biologischer beziehung wichtigen einfluss den die kohlen-sauerspannung des blutes aufdessen sauerstoffbindung ubt. *Skandinavisches Archiv fur Physiologie 15*, 401-412.

62. Tauber, H. (1934) The chemical nature of enzymes. *Chemical Reviews 15*, 99-121.

63. Sumner, J. B. (1926) The isolation and crystallization of the enzyme urease: Preliminary paper. *J. Biol.Chem. 69*, 435-441.

64. Northrop, J. H. (1930) Crystaline pepsin. I. Isolation and tests of purity. *Journal of General Physiology 13*, 739-764.

65. Crick, F. (1958) On protein synthesis. *Symposium of the Society for Experimental Biology XII*, 139-163.

66. Koshland, D. E. (1958) Application of a theory of enzyme specificity to protein synthesis. *Proc. Natl. Acad. Sci. U S A 44*, 98-104.

67. Perutz, M. F. (1953) An optical method for finding the molecular orientation in different forms of crystalline haemoglobin; changes in dichroism accompanying oxygenation and reduction. *Proceedings of the Royal Society of London 141*, 69-71.

68. Kendrew, J. C., Bodo, G., Dintzis, H. M., Parrish, R. G., Wyckoff, H., and Phillips, D. C. (1958) A three-dimensional model of the myoglobin molecule obtained by x-ray analysis, *Nature 181*, 662-666.

69. Perutz, M. F. (1960) Structure of hemoglobin. *Brookhaven Symp. Biol. 13*, 165-183.

70. Thomas, J. M. (2002) The scientific and humane legacy of Max Perutz (1914-2002). *Angewandte Chemie International Edition 41*, 3155-3166.

71. Monod, J., Cohen-Bazire, G., and Cohn, M. (1951) The biosynthesis of beta-galactosidase (lactase) in *Escherichia coli*; the specificity of induction. *Biochim. Biophys. Acta 7*, 585-599.

72. Monod, J., and Cohn, M. (1952) Biosynthesis induced by enzymes; enzymatic adaptation. *Adv. Enzymol. Relat. Subj. Biochem. 13*, 67-119.

73. Gorini, L., and Maas, W. K. (1957) The potential for the formation of a biosynthetic enzyme in *Escherichia coli*. *Biochim. Biophys. Acta 25*, 208-209.

74. Yates, R. A., and Pardee, A. B. (1957) Control by uracil of formation of enzymes required for orotate synthesis. *J. Biol. Chem. 227*, 677-692.

75. Burnett, G., and Kennedy, E. P. (1954) The enzymatic phosphorylation of proteins. *J. Biol. Chem. 211*, 969-980.

76. Fischer, E. H., and Krebs, E. G. (1955) Conversion of phosphorylase b to phosphorylase a in muscle extract. *J. Biol. Chem. 216*, 121-132.

77. Krebs, E. G., and Fischer, E. H. (1955) Phosphorylase activity of skeletal muscle extracts. *J. Biol. Chem. 216*, 113-120.

78. Krebs, E. G., and Fischer, E. H. (1956) The phosphorylase b to a converting enzyme of rabbit skeletal muscle. *Biochim. Biophys. Acta 20*, 150-157.

79. Davis, B. (1950) Studies on nutritionally deficient bacterial mutants isolated by means of penicillin. *Cellular and Molecular Life Sciences 6*, 41-50.

80. Novick, A., and Szilard, L. (1950) Experiments with the chemostat on spontaneous mutations of bacteria. *Proc. Natl. Acad. Sci. U S A 36*, 708-719.

81. Umbarger, H. E. (1956) Evidence for a negative-feedback mechanism in the biosynthesis of isoleucine. *Science 123*, 848.

82. Monod, J., and Jacob, F. (1961) Teleonomic mechanisms in cellular metabolism, growth, and differentiation. *Cold Spring Harb Symp Quant Biol 26*, 389-401.

83. Gerhart, J. C., and Pardee, A. B. (1962) The enzymology of control by feedback inhibition. *J. Biol. Chem. 237*, 891-896.

84. Changeux, J. P. (1961) The feedback control mechanisms of biosynthetic L-threonine deaminase by L-isoleucine. *Cold Spring Harb Symp Quant Biol 26*, 313-318.

85. Monod, J. (1966) From enzymatic adaptation to allosteric transitions. *Science 154*, 475-483.

86. Allen, D. W., Guthe, K. F., and Wyman, J. (1950) Further studies on the oxygen equilibrium of hemoglobin. *J. Biol. Chem. 187*, 393-410.

87. Monod, J., Wyman, J., and Changeux, J. P. (1965) On the nature of allosteric transitions: A plausible model. *J. Mol. Biol. 12*, 88-118.

88. Koshland, D. E., Jr., Nemethy, G., and Filmer, D. (1966) Comparison of experimental binding data and theoretical models in proteins containing subunits. *Biochemistry 5*, 365-385.

89. Frieden, C. (1964) Treatment of enzyme kinetic data. I. The effect of modifiers on the kinetic parameters of single substrate enzymers. *J. Biol. Chem. 239*, 3522-3531.

90. Wyman, J. (1965) The binding potential, a neglected linkage concept. *J. Mol. Biol. 11*, 631-644.

91. Wyman, J., Jr. (1964) Linked functions and reciprocal effects in hemoglobin: A second look. *Adv. Prot. Chem. 19*, 223-286.

92. Wyman, J., Jr. (1948) Heme proteins. *Adv. Prot. Chem. 4*, 407-531.

93. Wyman, J. (1967) Allosteric linkage. *J. Am. Chem. Soc. 89*, 2202-2218.

94. Weber, G. (1972) Ligand binding and internal equilibria in proteins. *Biochemistry 11*, 864-878.

95. Weber, G. (1975) Energetics of ligand binding to proteins. *Adv. Prot. Chem. 29*, 1-83.

96. Reinhart, G. D. (1983) The determination of thermodynamic allosteric parameters of an enzyme undergoing steady-state turnover. *Arch. Biochem. Biophys. 224*, 389-401.

97. Cleland, W. W. (1963) The kinetics of enzyme-catalyzed reactions with two or more substrates or products. I. Nomenclature and rate equations. *Biochim. Biophys. Acta. 67*, 104-137.

98. Reinhart, G. D. (2004) Quantitative analysis and interpretation of allosteric behavior. *Methods Enzymol. 380*, 187-203.

99. Reinhart, G. D. (1988) Linked-function origins of cooperativity in a symmetrical dimer. *Biophys. Chem. 30*, 159-172.

100. Blangy, D., Buc, H., and Monod, J. (1968) Kinetics of the allosteric interactions of phosphofructokinase from *Escherichia coli*. *J. Mol. Biol. 31*, 13-35.

101. Schirmer, T., and Evans, P. R. (1990) Structural basis of the allosteric behaviour of phosphofructokinase. *Nature 343*, 140-145.

102. Krauss, G., Ed. (2001) Biochemistry of Signal Transduction and Regulation, p 58 Wiley-VCH, New York.

103. Voet, D., Voet, J. G., and Pratt, C. W. (2008) Fundamentals of Biochemistry : Life at the Molecular Level (Fitzgerald, P., Ford, E., Dumas, S., Malinowski, S., Eds.) pp 454-455, John Wiley & Sons, Hoboken, New Jersey.

104. Kimmel, J. L., and Reinhart, G. D. (2000) Reevaluation of the accepted allosteric mechanism of phosphofructokinase from *Bacillus stearothermophilus*. *Proc. Natl. Acad. Sci. U S A 97*, 3844-3849.

105. Braxton, B. L., Tlapak-Simmons, V. L., and Reinhart, G. D. (1994) Temperature-induced inversion of allosteric phenomena. *J. Biol. Chem. 269*, 47-50.

106. Tlapak-Simmons, V. L., and Reinhart, G. D. (1994) Comparison of the inhibition by phospho(enol)pyruvate and phosphoglycolate of phosphofructokinase from *B. stearothermophilus*. *Arch. Biochem. Biophys. 308*, 226-230.

107. Cooper, A., and Dryden, D. T. (1984) Allostery without conformational change. A plausible model. *Eur. Biophys. J. 11*, 103-109.

108. Lockless, S. W., and Ranganathan, R. (1999) Evolutionarily conserved pathways of energetic connectivity in protein families. *Science 286*, 295-299.

109. K. Gunasekaran, Buyong Ma, and Ruth Nussinov. (2004) Is allostery an intrinsic property of all dynamic proteins? *Proteins: Structure, Function, and Bioinformatics 57*, 433-443.

110. Swain, J. F., and Gierasch, L. M. (2006) The changing landscape of protein allostery. *Curr. Opin. Struct. Biol. 16*, 102-108.

111. Popovych, N., Sun, S., Ebright, R. H., and Kalodimos, C. G. (2006) Dynamically driven protein allostery. *Nat. Struct. Mol. Biol. 13*, 831-838.

112. Tsai, C. J., Del Sol, A., and Nussinov, R. (2009) Protein allostery, signal transmission and dynamics: a classification scheme of allosteric mechanisms. *Mol. Biosyst. 5*, 207-216.

113. Kemp, R. G., and Foe, L. G. (1983) Allosteric regulatory properties of muscle phosphofructokinase. *Mol. Cell. Biochem. 57*, 147-154.

114. Byrnes, M., Zhu, X., Younathan, E. S., and Chang, S. H. (1994) Kinetic characteristics of phosphofructokinase from *Bacillus stearothermophilus*: MgATP nonallosterically inhibits the enzyme. *Biochemistry 33*, 3424-3431.

115. Blangy, D. (1968) Phosphofructokinase from *E. Coli*: Evidence for a tetrameric structure of the enzyme. *FEBS Lett. 2*, 109-111.

116. Le Bras, G., Deville-Bonne, D., and Garel, J. R. (1991) Purification and properties of the phosphofructokinase from *Lactobacillus bulgaricus*. A non-allosteric analog of the enzyme from *Escherichia coli*. *Eur. J. Biochem. 198*, 683-687.

117. Paricharttanakul, N. M., Ye, S., Menefee, A. L., Javid-Majd, F., Sacchettini, J. C., and Reinhart, G. D. (2005) Kinetic and structural characterization of phosphofructokinase from *Lactobacillus bulgaricus*. *Biochemistry 44*, 15280-15286.

118. Rypniewski, W. R., and Evans, P. R. (1989) Crystal structure of unliganded phosphofructokinase from *Escherichia coli. J. Mol. Biol. 207,* 805-821.

119. Shirakihara, Y., and Evans, P. R. (1988) Crystal structure of the complex of phosphofructokinase from *Escherichia coli* with its reaction products. *J. Mol. Biol. 204,* 973-994.

120. Evans, P. R., and Hudson, P. J. (1979) Structure and control of phosphofructokinase from *Bacillus stearothermophilus*. *Nature 279,* 500-504.

121. Evans, P. R., Farrants, G. W., and Hudson, P. J. (1981) Phosphofructokinase: structure and control. *Philos. Trans. R. Soc. Lond. B. Biol. Sci. 293,* 53-62.

122. Riley-Lovingshimer, M. R., Ronning, D. R., Sacchettini, J. C., and Reinhart, G. D. (2002) Reversible ligand-induced dissociation of a tryptophan-shift mutant of phosphofructokinase from *Bacillus stearothermophilus*. *Biochemistry 41,* 12967-12974.

123. French, B. A., Valdez, B. C., Younathan, E. S., and Chang, S. H. (1987) High-level expression of *Bacillus stearothermophilus* 6-phosphofructo-1-kinase in *Escherichia coli. Gene 59,* 279-283.

124. Lovingshimer, M. R., Siegele, D., and Reinhart, G. D. (2006) Construction of an inducible, pfkA and pfkB deficient strain of *Escherichia coli* for the expression and purification of phosphofructokinase from bacterial sources. *Protein Expr. Purif. 46,* 475-482.

125. Valdez, B. C., French, B. A., Younathan, E. S., and Chang, S. H. (1989) Site-directed mutagenesis in *Bacillus stearothermophilus* fructose-6-phosphate 1-

kinase. Mutation at the substrate-binding site affects allosteric behavior. *J. Biol. Chem. 264*, 131-135.

126. Riley-Lovingshimer, M. R., and Reinhart, G. D. (2001) Equilibrium binding studies of a tryptophan-shifted mutant of phosphofructokinase from *Bacillus stearothermophilus*. *Biochemistry 40*, 3002-3008.

127. Thaller, C., Weaver, L. H., Eichele, G., Wilson, E., Karlsson, R., and Jansonius, J. N. (1981) Repeated seeding technique for growing large single crystals of proteins. *J. Mol. Biol. 147*, 465-469.

128. Otwinowski, Z., Minor, W., and Charles W. Carter, Jr. (1997) Processing of X-ray diffraction data collected in oscillation mode. *Methods Enzymol.* 276, 307-326.

129. McCoy, A. J. (2007) Solving structures of protein complexes by molecular replacement with Phaser. *Acta Crystallogr. D Biol. Crystallogr. 63*, 32-41.

130. Adams, P. D., Grosse-Kunstleve, R. W., Hung, L. W., Ioerger, T. R., McCoy, A. J., Moriarty, N. W., Read, R. J., Sacchettini, J. C., Sauter, N. K., and Terwilliger, T. C. (2002) PHENIX: building new software for automated crystallographic structure determination. *Acta Crystallogr. D Biol. Crystallogr. 58*, 1948-1954.

131. Emsley, P., and Cowtan, K. (2004) Coot: model-building tools for molecular graphics. *Acta Crystallogr. D Biol. Crystallogr.60*, 2126-2132.

132. Davis, I. W., Leaver-Fay, A., Chen, V. B., Block, J. N., Kapral, G. J., Wang, X., Murray, L. W., Arendall, W. B., 3rd, Snoeyink, J., Richardson, J. S., and

Richardson, D. C. (2007) MolProbity: all-atom contacts and structure validation for proteins and nucleic acids. *Nucleic Acids Res. 35*, 375-383.

133. Quinlan, R. J., and Reinhart, G. D. (2006) Effects of protein-ligand associations on the subunit interactions of phosphofructokinase from *B. stearothermophilus*. *Biochemistry 45*, 11333-11341.

134. Ortigosa, A. D., Kimmel, J. L., and Reinhart, G. D. (2004) Disentangling the web of allosteric communication in a homotetramer: heterotropic inhibition of phosphofructokinase from *Bacillus stearothermophilus*. *Biochemistry 43*, 577-586.

135. Pflugrath, J. W. (1999) The finer things in X-ray diffraction data collection. *Acta Crystallogr. D Biol. Crystallogr. 55*, 1718-1725.

136. Selvanayagam, S., Velmurugan, D., and Yamane, T. (2006) Iterative ACORN as a high throughput tool in structural genomics. *Indian J. Biochem. Biophys. 43*, 211-216.

137. Winn, M. D., Isupov, M. N., and Murshudov, G. N. (2001) Use of TLS parameters to model anisotropic displacements in macromolecular refinement. *Acta Crystallogr. D Biol. Crystallogr. 57*, 122-133.

138. Hill, A. V. (1910) A new mathematical treatment of changes of ionic concentration in muscle and nerve under the action of electric currents, with a theory as to their mode of excitation. *J. Physiol. 40*, 190-224.

139. Johnson, J. L., and Reinhart, G. D. (1997) Failure of a two-state model to describe the influence of phospho(enol)pyruvate on phosphofructokinase from *Escherichia coli*. *Biochemistry 36*, 12814-12822.

140. Velyvis, A., Schachman, H. K., and Kay, L. E. (2009) Application of methyl-TROSY NMR to test allosteric models describing effects of nucleotide binding to Aspartate Transcarbamoylase. *J. Mol. Biol.* 387, 540-547.

141. Sprangers, R., Gribun, A., Hwang, P. M., Houry, W. A., and Kay, L. E. (2005) Quantitative NMR spectroscopy of supramolecular complexes: dynamic side pores in ClpP are important for product release. *Proc. Natl. Acad. Sci. U S A 102*, 16678-16683.

142. Sprangers, R., and Kay, L. E. (2007) Quantitative dynamics and binding studies of the 20S proteasome by NMR. *Nature 445*, 618-622.

143. Tugarinov, V., Kanelis, V., and Kay, L. E. (2006) Isotope labeling strategies for the study of high-molecular-weight proteins by solution NMR spectroscopy. *Nat. Protoc. 1*, 749-754.

144. Goto, N. K., Gardner, K. H., Mueller, G. A., Willis, R. C., and Kay, L. E. (1999) A robust and cost-effective method for the production of Val, Leu, Ile (delta 1) methyl-protonated 15N-, 13C-, 2H-labeled proteins. *J. Biomol. NMR 13*, 369-374.

145. Tugarinov, V., Hwang, P. M., Ollerenshaw, J. E., and Kay, L. E. (2003) Cross-correlated relaxation enhanced 1H[bond]13C NMR spectroscopy of methyl

groups in very high molecular weight proteins and protein complexes. *J. Am. Chem. Soc. 125*, 10420-10428.

146. Delaglio, F., Grzesiek, S., Vuister, G. W., Zhu, G., Pfeifer, J., and Bax, A. (1995) NMRPipe: a multidimensional spectral processing system based on UNIX pipes, *J. Biomol. NMR 6*, 277-293.

147. T. D. Goddard, and Kneller, D. G. Sparky 3. University of California at San Francisco, San Franciso, CA.

148. Pervushin, K., Riek, R., Wider, G., and Wuthrich, K. (1997) Attenuated T2 relaxation by mutual cancellation of dipole-dipole coupling and chemical shift anisotropy indicates an avenue to NMR structures of very large biological macromolecules in solution. *Proc. Natl. Acad. Sci. U S A 94*, 12366-12371.

149. Goto, N. K., and Kay, L. E. (2000) New developments in isotope labeling strategies for protein solution NMR spectroscopy. *Curr. Opin. Struct. Biol. 10*, 585-592.

150. Tlapak-Simmons, V. L., and Reinhart, G. D. (1998) Obfuscation of allosteric structure-function relationships by enthalpy-entropy compensation. *Biophys. J. 75*, 1010-1015.

# VITA

Rockann Elizabeth Mosser

Department of Biochemistry and Biophysics
103 Biochemistry/Biophysics Building
Texas A&M University
2128 TAMU
College Station, TX, 77843-2128

Education:

| | | |
|---|---|---|
| The University of Texas, Austin, TX | Biochemistry | B.S. 2000 |
| Texas A&M University, College Station, TX | Biochemistry | Ph.D. 2010 |

Publications:

Mosser, R.E., Reddy M., Bruning, J., Sacchettini, J.C., and Reinhart, G.D. Structure of the apo form of *Bacillus stearothermophilus* phosphofructokinase (In Preparation)

Mosser, R.E., Reddy M., Bruning, J., Sacchettini, J.C., and Reinhart, G.D. Redefining the role of the quaternary shift in *Bacillus stearothermophilus* phosphofructokinase (In Preparation)

Mosser, R.E., Igumenova, T., and Reinhart, G.D. A solution NMR study reveals evidence for an elusive ternary complex of *Bacillus stearothermophilus* phosphofructokinase (In Preparation)

Presentations:

Mosser, R.E., Reddy M., Sacchettini, J.C., and Reinhart, G.D. 2007 "Interpreting Mother Nature: The effect of modifying a completely conserved residue in the allosteric response of BsPFK." 15th Annual Biochemistry and Biophysics Research Competition, College Station, TX.

Mosser, R.E., Reddy M., Sacchettini, J.C., Igumenova, T. and Reinhart, G.D. 2009. "A solution NMR and crystallographic study of the role of the quaternary shift in the allosteric regulation of Phosphofructokinase from *B. stearothermophilus"* (1) 53rd Biophysical Society Meeting, Boston, MA.

Mosser, R.E., Reddy M., Sacchettini, J.C., Igumenova, T. and Reinhart, G.D. 2009. "A solution NMR and crystallographic study into the role of the quaternary shift in the allosteric regulation BsPFK*."* (2) 2009. 17th Annual Biochemistry and Biophysics Research Competition, College Station, TX.